STANDING BALANCE CONTROL IN PATIENTS WITH ACROMEGALY

by

Michaela Title

Submitted in partial fulfilment of the requirements
for the degree of Master of Science

at

Dalhousie University
Halifax, Nova Scotia
December 2023

Dalhousie University is located in Mi'kma'ki,
the ancestral and unceded territory of the Mi'kmaq.
We are all Treaty people.

Table of Contents

List of Tables

List of Figures

Abstract

Patients with acromegaly (PWA) experience higher rates of falls and fall-related injuries than Canadian older adults. Therefore, the aim of the present study was to determine if acromegaly influenced the control of standing balance.

Bipedal and unipedal standing balance with eyes open (EO) and eyes closed (EC) were evaluated in PWA and a control group of patients with non-functioning pituitary adenomas (PNA) using synchronized force plate and motion capture systems to measure centre of pressure (COP) and centre of mass (COM).

For bipedal stance, PWA exhibited a significantly greater increase in anteroposterior COP mean velocity with EC compared to EO ($p=0.047$) and significantly greater mediolateral mean absolute deviation of COP and COM ($p=0.005$) than PNA. Unipedal stance time was comparable between groups and to age-group norms.

Despite normal standing balance performance, PWA revealed impaired balance control for bipedal stance in the anteroposterior axis with EC and in the mediolateral axis.

List of Abbreviations Used

PWA	Patients with acromegaly
PNA	Patients with non-functioning pituitary adenoma
GH	Growth hormone
GHRH	Growth hormone releasing hormone
IGF-1	Insulin-like growth factor-1
AA	Acromegalic arthropathy
OA	Osteoarthritis
BMI	Body mass index
COM	Centre of mass
COP	Centre of pressure
COP_{net}	Total body centre of pressure
COP_L	Left foot centre of pressure
COP_R	Right foot centre of pressure
COP_x	Mediolateral (x-axis) centre of pressure
COP_y	Anteroposterior (y-axis) centre of pressure
GRF	Ground reaction force
vGRF	Vertical component of the ground reaction force
$vGRF_L$	Vertical component of the left foot ground reaction force
$vGRF_R$	Vertical component of the right foot ground reaction force
AP	Anteroposterior
ML	Mediolateral
CNS	Central nervous system
EO	Eyes open
EC	Eyes closed
3D	Three-dimensional
6DOF	Six degrees of freedom
GCS	Global coordinate system
SCS	Segment coordinate system
FPCS	Force plate coordinate system
ICC	Intraclass correlation coefficient
CV	Coefficient of variation
PEA	Prediction ellipse area
FFT	Fast Fourier transformation
MPF	Median power frequency
COP-COM	Mean absolute deviation of centre of pressure and centre of mass

Acknowledgements

I would like to thank my supervisor, Dr. Michel Ladouceur, for his mentorship and patience. I am grateful for the knowledge he has shared with me that has contributed to my growth as a researcher over the course of my master's degree.

I would like to thank my committee members, Dr. Kathleen MacLean and Dr. Syed Ali Imran, for their unwavering support and guidance. I am grateful for Dr. MacLean's voice of reason and Dr. Imran's clinical expertise. A special acknowledgment is given to Dr. MacLean for taking time out of her busy schedule to provide support throughout the final stages of thesis writing.

I would like to thank everyone on the research team who contributed to the study conceptualization and grant and ethics writing. I would like to acknowledge my research partner, Yuqi Wang, for her assistance in participant recruitment and data collection, and Lisa Tramble, for her ongoing support with recruitment from the Halifax Neuropituitary Program.

I am grateful for the camaraderie of my lab-mates as we endured the highs and lows of graduate school together. The hard days of a master's degree are a lot easier when you're not going through it alone.

I want to thank my family for their unconditional love and support along the winding road I travelled to get here. I am grateful for the support of my friends, who were always there to meet up for a tea or go for a run when I needed an escape from academic stress. My family and friends' willingness to listen to me vent about the drudgery of marker labelling did not go unnoticed. Last but definitely not least, thank you to my dog, Ava, for providing more emotional support than any human could possibly offer.

Chapter 1: Introduction

Acromegaly is a rare endocrine condition characterized by hypersecretion of growth hormone (GH), typically due to an adenoma of the anterior pituitary gland. Excess growth hormone leads to subsequent overproduction of insulin-like growth factor 1 (IGF-1), and elevated levels of these hormones result in somatic tissue overgrowth and impaired metabolic function (Melmed, 2006). Although acromegaly is of endocrine origin, it can affect all systems of the body, including cardiovascular, respiratory, nervous, and musculoskeletal systems (Abreu et al., 2016; Claessen et al., 2015; Colao et al., 2004; Melmed, 2006). Treatment of acromegaly may involve surgical removal of the adenoma, medication, and/or radiation (Katznelson et al., 2014).

Although treatment effectiveness has improved over the past few decades, some complications of acromegaly, such as structural and functional abnormalities of musculoskeletal and nervous tissues, are not resolved with successful disease control (Biermasz et al., 2005, 2012; Claessen et al., 2012, 2014, 2015; Pelsma et al., 2021; Resmini et al., 2009; Wassenaar et al., 2009b). Many patients with acromegaly (PWA) continue to experience reduced physical function and quality of life despite biochemical remission (Biermasz et al., 2005; Fatti et al., 2019; Title et al., 2023; Wassenaar et al., 2010). PWA experience falls twice as often as Canadian older adults (Title et al., 2023) and have reduced balance confidence compared to healthy controls (Atmaca et al., 2013) and patients with non-functioning (non-hormone secreting) pituitary adenomas (PNA) (Title et al., 2023). Furthermore, a few studies have revealed significant balance dysfunction in PWA using force plate measurements of centre of pressure (COP) (Haliloglu et al., 2019; Homem et al., 2017; Lopes et al., 2014).

In the current literature on acromegaly, arthropathy is commonly discussed in relation to balance dysfunction in PWA. Over 70% of PWA in remission report joint pain and/or stiffness (Biermasz et al., 2005; Wassenaar et al., 2009b), and radiological evidence of arthropathy is observed in up to 99% of PWA (Wassenaar et al., 2009b). Acromegalic arthropathy (AA) is different from other forms of arthropathy such as rheumatoid arthritis or osteoarthritis (OA) as there is no known autoimmune involvement and articular cartilage degeneration is not typically observed (Claessen et al., 2017; Prencipe et al., 2020; Wassenaar et al., 2011). Instead, AA is characterized by joint space widening due to hypertrophy of articular cartilage and periarticular soft-tissue and laxity of periarticular ligaments (Biermasz et al., 2012; Bluestone et al., 1971; Pelsma et al., 2022; Scarpa et al., 2004; Wassenaar et al., 2011) and is thought to be mediated by excess GH and IGF-1 (Biermasz et al., 2009; Colao et al., 2004).

Abnormal bone growth, including osteophytosis (outward bone growth at the articular surface) and enthesopathy (outward bone growth at ligament and tendon attachment sites), is also frequently seen in PWA despite long-term remission (Biermasz et al., 2012; Bluestone et al., 1971; Claessen et al., 2012, 2017; Ozturk Gokce et al., 2020; Pelsma et al., 2021, 2022; Podgorski et al., 1988; Rosselet et al., 1988; Wassenaar et al., 2009b, 2011). In OA, osteophytosis is proposed to develop in response to cartilage degeneration, but osteophytosis in the absence of joint space narrowing is commonly observed in AA (Wassenaar et al., 2011), which suggests that AA may have a different mechanism of osteophyte formation. GH and IGF-1 are thought to facilitate increased bone metabolism in PWA (Constantin et al., 2017). Excess IGF-1 levels have been shown to stimulate osteophyte formation in rats (Okazaki et al., 1999), and in humans, osteophytes have been

shown to express mRNA and receptors for IGF-1 (Jørgensen et al., 2023; Middleton et al., 1995). Therefore, IGF-1 may play a role in osteophyte development in PWA.

The visual, vestibular, and somatosensory systems play an imperative role in the control of balance, and the function of these systems may be impaired in PWA. Visual impairments are known to alter balance control (Bednarczuk et al., 2021; Friedrich et al., 2008; Nashner and Berthoz, 1978) and increase risk of falls and fall-related fractures (Felson et al., 1989; Freeman et al., 2007; Hong et al., 2014; Ivers et al., 1998). Mass effects of the pituitary adenoma can result in visual field defects by compressing the optic chiasm (Kan et al., 2013; Ogra et al., 2014; Rivoal et al., 2000). Many patients have improved vision post-transsphenoidal surgery, but in some, vision remains impaired or is worsened post-surgery (Butenschoen et al., 2021; Castle-Kirszbaum et al., 2022; Cohen et al., 1985; Müslüman et al., 2011; Powell, 1995).

Vestibular changes have not been documented in PWA. A few audiological studies have found overgrowth of the temporal bone or otosclerosis that may be related to hearing loss in acromegaly; however, findings are inconsistent between studies (Aydin et al., 2012; Babic et al., 2006; Baylan et al., 2011; Graham and Brackmann, 1978; Menzel, 1966; Richards, 1968; Tabur et al., 2017). Theoretically, if the inner ear structures were otosclerotic or overgrowth of the temporal bone was to impede inner ear structures, vestibular dysfunction could occur; however, this is yet to be confirmed in the literature.

There is also an absence of literature on somatosensory function in PWA. Structural changes to muscles and tendons in PWA could potentially impair the function of muscle and joint receptors (Mastaglia et al., 1970; Nagulesparen et al., 1976; Onal et al., 2016; Ozturk Gokce et al., 2020; Podgorski et al., 1988), and increased heel pad and skin thickness on the plantar surface of the foot in PWA could hypothetically impair plantar

cutaneous sensation (Gonticas et al., 1969; Kho et al., 1970; Ozturk Gokce et al., 2020; Steinbach and Russell, 1964). Furthermore, many PWA have absent knee and ankle reflexes and diminished perception of touch, temperature, pain, and vibration (Alibas et al., 2017; Jamal et al., 1987).

The transmission of signals via sensory and motor nerves also must be considered in balance control. PWA often exhibit peripheral nerve dysfunction, characterized by reduced conduction velocities and action potentials and prolonged distal latencies of sensory and motor nerves (Alibas et al., 2017; Jamal et al., 1987; Low et al., 1974; Ozata et al., 1997; Pickett et al., 1975; Sasagawa et al., 2015). Additionally, proper function of muscles and tendons is necessary for the maintenance of standing balance. PWA have reduced muscular strength and endurance (Füchtbauer et al., 2017; Guedes da Silva et al., 2013; Homem et al., 2017; Walchan et al., 2016), which may be the result of changes to the extracellular matrix of muscles and tendons (Doessing et al., 2010), tendon softening (Onal et al., 2016), and peripheral nerve dysfunction. Therefore, several mechanisms aside from AA may explain balance dysfunction in PWA.

In order to address balance through treatment interventions, the mechanism of balance impairment in PWA must be understood. Differences in standing balance control between PWA and healthy controls are most prominent in the anteroposterior (AP) direction with eyes open (EO) and the mediolateral (ML) direction with eyes closed (EC) (Haliloglu et al., 2019; Homem et al., 2017; Lopes et al., 2014). Based on known mechanisms of standing balance control in healthy populations, AP balance is primarily controlled by the ankle invertors and evertors, while loading and unloading of the lower limbs through hip abduction and adduction the is the main contributor of ML balance control (Day et al., 1993; Horak and Nashner, 1986; Winter et al., 1993, 1990). Therefore, the increase in ML

sway when the effect of vision is controlled via EC may indicate impaired frontal plane hip mechanics in PWA. This is supported by the high prevalence of hip pain and dysfunction in PWA (Biermasz et al., 2005; Title et al., 2023). Furthermore, a recent study found that increased hip disability scores predicted lower balance self-confidence in PWA (Title et al., 2023). However, two of the studies of standing balance in PWA concurrently manipulated both vision and stance width (Homem et al., 2017; Lopes et al., 2014). Narrowing the stance width requires greater contribution of the ankle invertors and evertors for ML balance control (Åberg et al., 2011; Winter et al., 1996). Therefore, the increase in ML sway in PWA with narrower stance width and EC could indicate dysfunction of ankle invertors and evertors. The difference in AP balance control in the EO but not EC condition observed in two of the previous studies suggests the possibility of vision-related changes to balance control (Haliloglu et al., 2019; Lopes et al., 2014).

Previous studies of standing balance in PWA recruited control groups of healthy participants (Haliloglu et al., 2019; Homem et al., 2017; Lopes et al., 2014; Sendur et al., 2019), which failed to control for effects of the adenoma and/or adenoma removal surgery. Furthermore, two of the studies reported remission rates of 57% and 64% in their samples of PWA, and approximately 20% of PWA did not receive surgery to remove the adenoma (Haliloglu et al., 2019; Lopes et al., 2014). Two previous studies controlled for visual field defects or uncorrected visual impairment through exclusion criteria; however, neither study specified if all patients were systematically tested for visual impairment (Haliloglu et al., 2019; Homem et al., 2017). This exclusion criteria limits the generalizability of their findings; therefore, a control group of PNA would be more suitable for controlling for visual field defects as well as other adenoma and surgery-related effects on standing balance control.

Many parameters are available to quantify balance, and thus researchers are tasked with selecting the appropriate parameters to address their research question. Prior studies of standing balance in PWA have analyzed time domain parameters of the COP signal, such as the standard deviation, range, or elliptical area of COP. While many of these time domain parameters are valid and reliable indicators of stability (Lafond et al., 2004), they cannot discern between balance control mechanisms. In contrast, frequency analysis of the COP signal allows for more insight into the neuromuscular control of balance. Furthermore, analysis of both the total body centre of mass (COM) and the COP allows for a broader understanding of the sensory and motor mechanisms that constitute the postural control system.

Reduced physical function and poor balance control are significant predictors of falls and fall-related injuries, especially in older populations and populations with neurological disorders and visual impairments (Felson et al., 1989; Freeman et al., 2007; Hong et al., 2014; Ivers et al., 1998; Nevitt, 1989; Nevitt et al., 1991; Pizzigalli et al., 2016; Quijoux et al., 2020). The relationship between falls and morbidity and mortality is well-documented (Do et al., 2015; James et al., 2020; Tinetti and Kumar, 2010), and experiencing a first fall, especially an injurious fall, is a significant predictor of subsequent falls (Nevitt, 1989; Nevitt et al., 1991; Peel, 2011). Additionally, fall-related injuries place a substantial burden on the healthcare system. Fall-related injuries in older adults result in a visit to the emergency room in more than 70% of incidences (Do et al., 2015), and those who fall incur significantly greater healthcare costs than non-fallers (Bohl et al., 2010; Burns et al., 2016; Hoffman et al., 2017; Rizzo et al., 1998; Shumway-Cook et al., 2009). Given that PWA experience twice as many falls and fall-related injuries as Canadian older adults (Title et al., 2023), it is imperative that balance dysfunction in PWA is addressed.

6

The specific of aim of the present study was to determine if acromegaly has an effect on standing balance control. This was investigated through kinematic and kinetic analysis of bipedal and unipedal standing balance with eyes open and eyes closed, using a control group of PNA. Outcome measures included time and frequency domain parameters of COP and parameters that quantified the relationship between COP and COM.

Chapter 2: Literature Review

2.1   Acromegaly

Acromegaly is a rare endocrine condition characterized by hypersecretion of GH, most often due to an adenoma of the anterior pituitary gland. Pituitary adenomas are benign tumours that are classified as functioning (secrete hormones) or non-functioning (do not secrete hormones). In acromegaly, a functioning adenoma develops due to abnormal proliferation of cells that secrete GH, which interrupts the normal function of the GH/IGF-1 axis (Figure 1) (Melmed, 2006). GH and IGF-1 are hormones that regulate the growth and metabolism of tissues throughout the body. The central nervous system (CNS) controls the secretion of GH via growth hormone releasing hormone (GHRH) and somatostatin, secreted from the hypothalamus (Frohman and Jansson, 1986; Thorner et al., 1990). Additionally, ghrelin, a growth hormone secretagogue produced primarily by endocrine cells of the gastrointestinal tract, is involved in the regulation of GH (Kojima et al., 1999). GHRH and ghrelin stimulate the synthesis and release of GH, while somatostatin inhibits GH release (Anderson et al., 2004). Downstream, GH stimulates the liver to secrete IGF-1. In normal function, a negative feedback loop prevents excess GH and IGF-1 release to carefully regulate the growth of tissues throughout the body. When GH levels are adequate, IGF-1 supresses GH secretion directly via inhibition of GH secretion from the anterior pituitary and indirectly through inhibition of GHRH secretion and activation of somatostatin secretion at the level of the hypothalamus (Niiori-Onishi et al., 1999; Sugihara et al., 1999; Yamashita and Melmed, 1987, 1986). Additionally, GH regulates its own secretion by supressing GHRH and activating somatostatin release (Berelowitz et al., 1981; Tannenbaum, 1980). In acromegaly, the GH-secreting pituitary adenoma impairs the

regulatory actions of the GH/IGF-1 axis (Figure 2) (Yamasaki et al., 1991). Therefore, excess GH signals the liver to release a surplus of IGF-1, and elevated levels of GH and IGF-1 result in somatic tissue overgrowth and metabolic dysfunction (Melmed, 2006). When acromegaly remains undiagnosed and uncontrolled, multiple systemic comorbidities tend to develop.
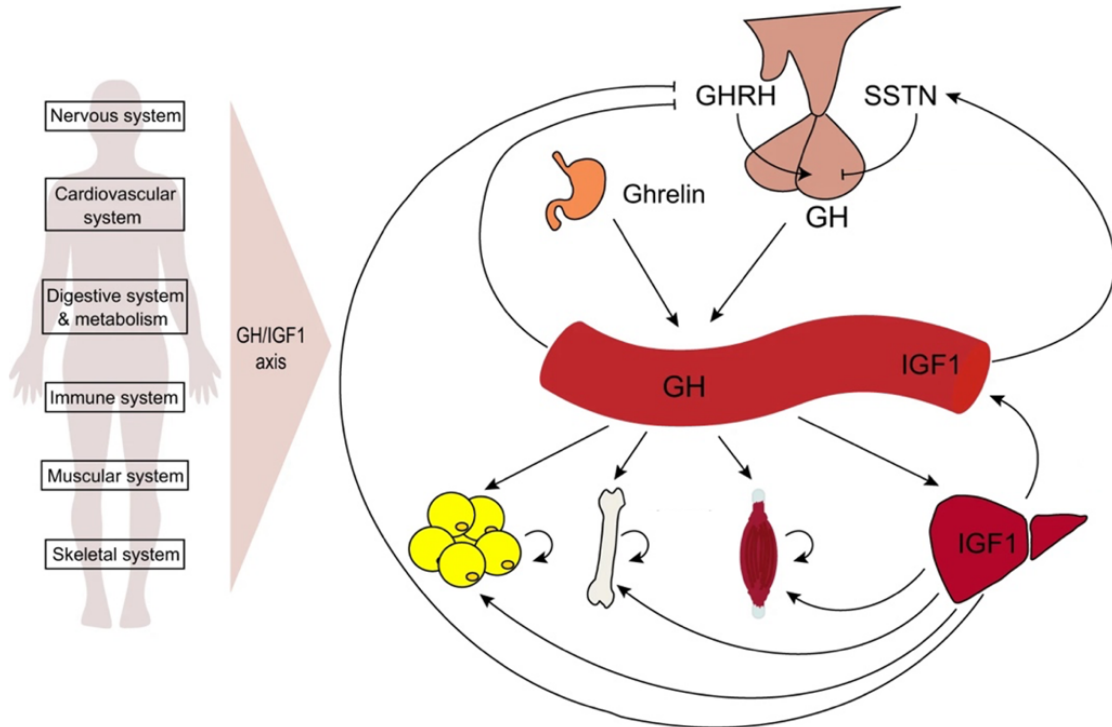
Figure 1. *Normal function of the GH/IGF-1 axis. Reproduced from Lu et al. (2019).*
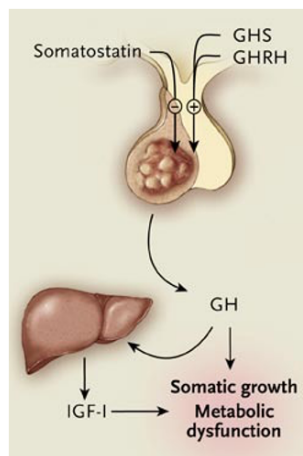
Figure 2. *The effect of a GH-secreting pituitary adenoma on the GH/IGF-1 axis. Reproduced with permission from Melmed (2006), Copyright Massachusetts Medical Society.*

2.1.1   Clinical Features of Acromegaly

The changes that develop in PWA can involve cardiovascular, respiratory, gastrointestinal, musculoskeletal, and endocrine systems (Abreu et al., 2016; Claessen et al., 2015; Colao et al., 2004; Melmed, 2006). Figure 3 lists the wide array of clinical features and comorbidities that PWA may experience due to excess GH and IGF-1 and mass effects of the tumour. Mass effects of the tumour can impair vision and lead to hypoproduction of hormones along other hypothalamic-pituitary axes (e.g., hypogonadism, hypothyroidism, hypoadrenalism) and hyperproduction of prolactin (Claessen et al., 2015; Colao et al., 2004). PWA also develop changes to their physical appearance, such as enlargement and disfigurement of the hands, feet, and face, which are associated with physical dysfunction, psychological distress, and poor body image (Imran et al., 2016; Molitch, 1992; Roerink et al., 2015; Rowles et al., 2005; Vilar et al., 2017). Symptoms and signs arise gradually and increase in severity over time as acromegaly remains uncontrolled. As shown in Figure 4, the disfiguration of facial features progresses over years (Molitch, 1992).

Despite advances in diagnostic technology for acromegaly, no reductions in time from first symptom onset to acromegaly diagnosis have been observed (Reid et al., 2010). The typical delay in diagnosis for PWA is 5-10 years (Holdaway and Rajasoorya, 1999; Reid et al., 2010).

Local tumor effects	Visceromegaly
Pituitary enlargement	Tongue
Visual-field defects	Thyroid gland
Cranial-nerve palsy	Salivary glands
Headache	Liver
Somatic systems	Spleen
Acral enlargement, including thickness of soft tissue of hands and feet	Kidney
	Prostate
Musculoskeletal system	**Endocrine and metabolic systems**
Gigantism	Reproduction
Prognathism	Menstrual abnormalities
Jaw malocclusion	Galactorrhea
Arthralgias and arthritis	Decreased libido, impotence, low levels of sex hormone–binding globulin
Carpal tunnel syndrome	
Acroparesthesia	Multiple endocrine neoplasia type 1
Proximal myopathy	Hyperparathyroidism
Hypertrophy of frontal bones	Pancreatic islet-cell tumors
Skin and gastrointestinal system	Carbohydrate
Hyperhidrosis	Impaired glucose tolerance
Oily texture	Insulin resistance and hyperinsulinemia
Skin tags	Diabetes mellitus
Colon polyps	Lipid
Cardiovascular system	Hypertriglyceridemia
Left ventricular hypertrophy	Mineral
Asymmetric septal hypertrophy	Hypercalciuria, increased levels of 25-hydroxyvitamin D_3
Cardiomyopathy	Urinary hydroxyproline
Hypertension	Electrolyte
Congestive heart failure	Low renin levels
Pulmonary system	Increased aldosterone levels
Sleep disturbances	Thyroid
Sleep apnea (central and obstructive)	Low thyroxine-binding–globulin levels
Narcolepsy	Goiter

Figure 3. *Clinical features and comorbidities of acromegaly. Reproduced with permission from Melmed (2006), Copyright Massachusetts Medical Society.*

Figure 4. *Progression of changes to facial features over 11 years in a patient with acromegaly. Reproduced from Molitch (1992).*

2.1.2 Treatment of Acromegaly

Once diagnosed, acromegaly should be treated quickly to prevent further damage from excess GH and IGF-1. The typical course of treatment for PWA is displayed in Figure 5 (Katznelson et al., 2014). The primary treatment for acromegaly is surgery to remove the pituitary adenoma (Katznelson et al., 2014; Melmed et al., 2018). In the latter half of the 20th century, this procedure became less invasive through transsphenoidal technique, which involves removing the adenoma through the nasal cavity and sphenoid sinus using an endoscope or microscope. The transsphenoidal technique has reduced complications and improved outcomes of pituitary removal surgery. Surgery success rates are greater than 85% for microadenomas and 40-50% for macroadenomas, and the 5-year post-operative recurrence of the adenoma is 2-8% (Katznelson et al., 2014). Tumours that invade the cavernous sinus are more difficult to access and typically cannot be removed via surgery. If surgery is unsuccessful or the adenoma recurs, surgery may be repeated, or other

treatments may be utilized. The next line of treatment is medical therapy for acromegaly. The main classes of medications for acromegaly include somatostatin receptor ligands, dopamine agonists (DAs), and Pegvisomant. Somatostatin receptor ligands are most commonly prescribed, and some PWA may be prescribed a combination of drug types (Fleseriu et al., 2021; Katznelson et al., 2014; Melmed et al., 2018). Finally, if no other line of treatment is effective at normalizing IGF-1 levels, the patient may receive radiation. Stereotactic radiation therapy is recommended over conventional radiation in PWA (Katznelson et al., 2014). Due to variable success rates (10-60%), higher rates of complications, and increased time to normalized GH levels compared to transsphenoidal surgery, radiation is typically the last course of treatment.
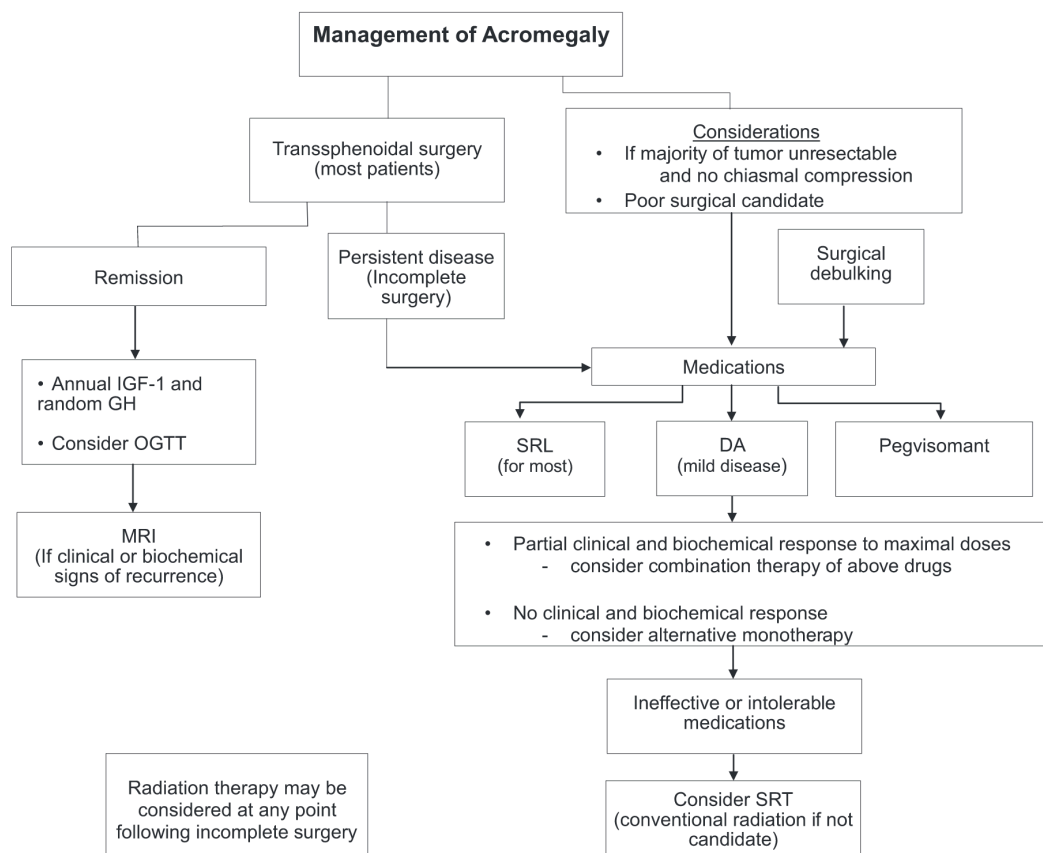
Figure 5. *Clinical practice guidelines for treatment of acromegaly. SRL, somatostatin receptor ligand; DA, dopamine agonist; SRT, stereotactic radiation therapy; OGTT, oral glucose tolerance test. Reproduced from Katznelson et al. (2014).*

2.1.3   Mortality in Acromegaly

Advances in surgical technology, radiotherapy, and medical therapies in recent decades have contributed to increased life expectancy for PWA. In meta-analyses of studies published prior to 2008, PWA had a 70-76% increased risk of mortality compared to the general population, while subgroup analyses of studies with high rates of treatment and remission showed no significant difference between mortality rates of PWA and the general population (Bolfi et al., 2018; Dekkers et al., 2008; Holdaway et al., 2008). A meta-analysis of studies published after 2008 showed no difference in mortality rates of PWA versus the general population (Bolfi et al., 2018). The standardized mortality rate was further reduced in a subgroup analysis of studies where somatostatin receptor ligands were available to PWA in addition to surgery and/or radiation; however, studies with surgery and radiation as the only treatment options had mortality rates more than double the general population. These findings highlight the positive impact of pharmaceutical innovations on life expectancy in acromegaly.

Despite reduced mortality levels for PWA who are in remission, some complications, such as arthropathy, are not reversed and continue to progress (Biermasz et al., 2005; Claessen et al., 2012, 2015; Pelsma et al., 2021). Therefore, greater emphasis is needed on reducing morbidity, improving physical function, and enhancing quality of life for PWA.

2.1.4 Physical Function in Acromegaly

In recent years, researchers have begun to explore the effects of acromegaly on physical function. Studies have used various instruments to quantify physical function in PWA including self-reported questionnaires (Claessen et al., 2014; Fatti et al., 2019; Miller et al., 2008; Pelsma et al., 2022; Title et al., 2023; Wassenaar et al., 2009b); functional tests of exercise capacity, balance, and gait (Atmaca et al., 2013; Homem et al., 2017); and laboratory assessments of balance and muscle function (Füchtbauer et al., 2017; Guedes da Silva et al., 2013; Haliloglu et al., 2019; Homem et al., 2017; Lopes et al., 2016, 2015, 2014; Omma et al., 2022; Sendur et al., 2019; Walchan et al., 2016).

Questionnaires specific to hand and/or upper limb disability have shown moderate disability in PWA compared to normative values (Pelsma et al., 2022) and significantly greater disability in PWA than PNA (Title et al., 2023). Studies have also found greater disability of the lower limb in PWA compared to general population values (Fatti et al., 2019; Pelsma et al., 2022), healthy controls (Wassenaar et al., 2009b), and PNA (Title et al., 2023). Prospective observation has shown worsening of upper extremity function in PWA, but progression of lower extremity disability was inconsistent between studies (Claessen et al., 2014; Pelsma et al., 2021).

PWA have shown reduced quadriceps and/or hamstring strength and endurance compared to healthy controls (Füchtbauer et al., 2017; Guedes da Silva et al., 2013; Homem et al., 2017; Khaleeli et al., 1984; Walchan et al., 2016). PWA exhibited a reduction in hand grip strength during active acromegaly that was normalized following remission (Füchtbauer et al., 2017); however, a long-term follow-up of muscle function in PWA found that grip strength and pinch grip strength decreased over a 2.6-year period despite remission of acromegaly (Claessen et al., 2014).

Functional tests including the Berg Balance Scale, Performance Oriented Mobility Assessment, Dynamic Gait Index, and Timed Up and Go revealed reduced balance, mobility, and gait adaptability in PWA compared to healthy controls, all of which predict an increased risk of falls (Atmaca et al., 2013; Homem et al., 2017). While time to complete a 50-meter walk test was significantly longer in older adult PWA ($\geq$ 60 years) compared to healthy older adults (Homem et al., 2017), a slightly younger cohort of PWA did not differ from healthy controls in 6-minute walk test distance (Guedes da Silva et al., 2013).

Force plate analyses have revealed significant differences in standing balance between PWA and healthy controls for bipedal (Haliloglu et al., 2019; Homem et al., 2017; Lopes et al., 2014) and unipedal stance (Haliloglu et al., 2019). In acromegaly, excess GH and IGF-1 are thought to alter the function of the nervous and musculoskeletal systems, which work collectively to control posture and balance. Balance is an important component of physical function as balance impairments are associated with an increased risk of falls and fall-related injuries, and falls are related to morbidity and premature mortality (Do et al., 2015; James et al., 2020; Tinetti and Kumar, 2010). A recent study showed that PWA were approximately twice as likely to experience a fall or fall-related injury compared to Canadian older adults (Title et al., 2023). Therefore, it is imperative to examine the mechanisms of impaired balance control in PWA.

2.2 Features of Acromegaly Proposed to Affect Balance Control

2.2.1 Arthropathy in Acromegaly

One of the most common complications of acromegaly is AA, which adversely affects physical function, psychological well-being, and quality of life in PWA (Biermasz et al., 2005; Fatti et al., 2019; Miller et al., 2008; Pelsma et al., 2022; Title et al., 2023;

Wassenaar et al., 2010). Proposed mechanisms of AA suggest that elevated levels of GH and IGF-1 induce laxity of periarticular ligaments and hypertrophy of articular cartilage and periarticular soft tissue (Colao et al., 2004).

If early intervention is successful, AA may be partially reversible (Claessen et al., 2016; Colao et al., 2003, 1999). Claessen and colleagues (2017) hypothesized that there are two components that contribute to thickened cartilage in AA: hypertrophy of cartilage (structural changes) and edema (increase in water content). They found that patients with active acromegaly had thicker cartilage and higher cartilage T2 relaxation times than patients in remission. Therefore, they suspected that cartilage hypertrophy is irreversible despite successful treatment of acromegaly, while the edema, indicated by T2 relaxation times, is resolved with successful treatment. Similarly, an earlier study found a reduction in thickness of the shoulder, wrist, and knee cartilage and heel tendon following 12 months of treatment with somatostatin receptor ligands; however, cartilage and tendon thickness did not return to normal (Colao et al., 1999).

Due to long delays in diagnosis and treatment, PWA commonly reach a stage of irreversible and progressive AA. Despite long-term biochemical control of acromegaly, joint pain and stiffness have been shown to persist in more than 70% of PWA (Biermasz et al., 2005; Wassenaar et al., 2009b), and radiographic evidence of arthropathy in at least one joint site has been observed in 99% of PWA (Wassenaar et al., 2009b). In addition to cartilage and soft-tissue hypertrophy, osteophytosis and enthesopathy have also been observed in PWA despite long-term remission (Biermasz et al., 2012; Bluestone et al., 1971; Claessen et al., 2012, 2017; Pelsma et al., 2021, 2022; Podgorski et al., 1988; Rosselet et al., 1988; Wassenaar et al., 2009b, 2011).

It is important to note that in many studies, the prevalence of clinical and radiological arthropathy may be underestimated. Many studies exploring the prevalence of AA use clinical and radiological scoring systems designed for OA, which use joint space narrowing as a criterion (Altman et al., 1991, 1990, 1986, 1995; Kellgren and Lawrence, 1957). Similarly, many scales used to quantify joint symptoms and physical disability have been validated for OA but not AA (Bellamy et al., 2002, 1988; Lyman et al., 2016a, 2016b; van der Meulen et al., 2022; Whitehouse et al., 2008).

2.2.1.1 *Acromegalic Arthropathy in Different Joint Sites*

Radiographic arthropathy is most often seen in the hip, knee, spine, and hands despite remission of acromegaly (Biermasz et al., 2012; Claessen et al., 2012, 2014; Pelsma et al., 2021, 2022; Scarpa et al., 2004; Wassenaar et al., 2009b) Similarly, joint pain and/or stiffness are most common and severe in the hip, knee, and spine in PWA (Biermasz et al., 2005; Pelsma et al., 2022; Scarpa et al., 2004; Title et al., 2023). A recent study found a significant interaction between acromegaly and body region on joint pain, with PWA experiencing more severe joint pain in the axial region (spinal joints and joints bordering the trunk) than appendicular region (joints of the upper and lower limbs) (Title et al., 2023).

2.2.1.2 *Acromegalic Arthropathy of the Spine*

Abnormal spine radiographs are present in almost 70% of PWA and are significantly more common in PWA than in healthy controls (Scarpa et al., 2004). Osteophytes, disc space narrowing, and/or wedge-shape vertebrae have been observed in 62-90% of PWA at the thoracic level and 37-40% of PWA at the lumbar level (Cellini et al., 2021; Plard et al., 2020). Ossification of spinal ligaments has also been noted in some PWA (Hoshino et al., 2022). Spinal pain and/or stiffness and decreased mobility have been

reported at significantly higher rates in PWA compared to controls, with these symptoms most common in the lumbar spine (Scarpa et al., 2004).

Abnormalities in spine and pelvis alignment in both the sagittal and frontal plane have been detected in PWA through radiographic imaging. Scoliosis has been observed in 15-35% of PWA (de Azevedo Oliveira et al., 2019; Scarpa et al., 2004). Approximately one third of PWA exhibit thoracic hyperkyphosis, while almost 50% of PWA have excessive lumbar lordosis and over 40% have posterior pelvic tilt. Thoracic hyperkyphosis and excessive pelvic tilt were significantly more common in PWA than healthy controls (Cellini et al., 2021). Frontal plane postural alignment abnormalities have not been found via photogrammetry; however, in the sagittal plane, significant differences have been observed for vertical trunk alignment, hip angle, and horizontal pelvis alignment between PWA and healthy controls (Lopes et al., 2014).

2.2.1.3   Comparison of Acromegalic Arthropathy to Osteoarthritis

AA is often referred to as a type of secondary OA; however, radiographic assessment exhibits differences between AA and primary OA (Wassenaar et al., 2011). Radiographic evidence revealed that in contrast to patients with OA who exhibit joint space narrowing due to the degeneration of articular cartilage, the majority of patients with AA have widened joint spaces and preservation or hypertrophy of articular cartilage (Biermasz et al., 2012; Claessen et al., 2012, 2017; Detenbeck et al., 1973; Pelsma et al., 2021, 2022; Scarpa et al., 2004; Tagliafico et al., 2011; Tornero et al., 1990; Wassenaar et al., 2009b, 2011). PWA have been shown to have 31% thicker joint cartilage and higher cartilage T2 relaxation times compared to patients with primary OA, suggesting that PWA have greater cartilage water content and structural abnormalities (Claessen et al., 2017). Prevalence of

osteophytosis has been shown to be similar or higher in AA compared to OA, with comparable severity between the two conditions (Claessen et al., 2017; Wassenaar et al., 2011). In OA, osteophyte formation is thought to be secondary to articular cartilage degeneration; however, the majority of PWA have osteophytes in the absence of joint space narrowing (Wassenaar et al., 2011). Therefore, it appears that the pathogenesis of osteophytosis in AA may be different than OA.

Some researchers propose that osteophytosis may be the result of altered joint geometry due to abnormal cartilage and bone growth and increased mobility due to ligament laxity (Bluestone et al., 1971; Killinger et al., 2010). In rodent studies, elevated IGF-1 levels were shown to stimulate osteophyte formation (Okazaki et al., 1999), while osteophytes did not develop in cases of GH and IGF-1 deficiency despite cartilage degeneration (Ekenstedt et al., 2006). Human osteophytes contain osteoblasts and osteoclasts that express mRNA for IGF-1 and type I IGF receptors (Jørgensen et al., 2023; Middleton et al., 1995). However, the literature is inconclusive regarding the relationship between GH and/or IGF-1 concentrations and general OA (Denko et al., 1990, 1996; Dixit et al., 2021; Hochberg et al., 1994; Lloyd et al., 1996; McAlindon et al., 1993; Schouten et al., 1993). In PWA, higher pre-treatment serum IGF-1 levels appear to be associated with a greater risk of AA (Biermasz et al., 2009). Therefore, further investigation of the role of IGF-1 in osteophyte formation is necessary in PWA.

2.2.1.4   *Treatment of Acromegalic Arthropathy*

Despite the debilitating and progressive nature of AA and its high prevalence in patients with acromegaly, treatment of AA has been neglected in the literature. The absence of specific treatment guidelines for AA means that clinicians often resort to treatments

designed for OA to manage AA despite notable differences between the two conditions (Claessen et al., 2016; Pelsma et al., 2021). Hip and knee pain and dysfunction are common in PWA (Biermasz et al., 2005; Title et al., 2023), yet PWA receive significantly fewer hip and knee replacements compared to patients with hip OA, suggesting that AA may be undertreated (Wassenaar et al., 2011). However, hip replacements are significantly more frequent in PWA compared to PNA (Title et al., 2023). While those with joint surgery typically see improvements in pain and physical function (Akkaya et al., 2022; Rosselet et al., 1988), joint pain, stiffness, and functional disability remain elevated in PWA despite higher rates of joint surgery (Title et al., 2023). Additionally, the frequency of medication use for joint pain does not appear to be different between PWA and PNA albeit significantly higher joint pain levels in PWA (Title et al., 2023; van der Klaauw et al., 2008). This further supports that symptoms of AA are often poorly managed. There is limited discussion of non-surgical and non-pharmacological approaches to managing AA in the literature.

In recent years, a few studies have explored the effect of rehabilitation exercise programs on quality of life and functional outcomes in PWA. The results of these studies have shown efficacy of structured exercise programs for improvement of quality of life, aerobic capacity, dynamic balance, quadriceps muscle strength, flexibility, lower extremity disability, fatigue, and body image in PWA (Haliloglu et al., 2019; Hatipoglu et al., 2015, 2014; Lima et al., 2019, 2019). Outcomes such as handgrip and hamstring strength did not significantly increase with the exercise intervention (Hatipoglu et al., 2015; Lima et al., 2019), and changes in static balance were inconsistent between studies (Haliloglu et al., 2019; Lima et al., 2019). After a one-month washout period following the structured exercise program, most progress from the intervention was lost; however, lower extremity disability and static balance improvements were maintained a month later (Lima et al.,

2019). Higher body mass index (BMI) was found to be a significant predictor of worse functional outcomes of arthropathy (Kropf et al., 2013); therefore, exercise programs could also help with weight management. However, body composition outcomes in PWA following the exercise intervention varied by study (Hatipoglu et al., 2015; Lima et al., 2019).

Although these findings reveal several benefits of physical rehabilitation programs in PWA, the studies were limited by small sample sizes. Additionally, assignment to the intervention and control group was through self-selection (Haliloglu et al., 2019; Hatipoglu et al., 2015, 2014), and one study failed to include a control group (Lima et al., 2019). Therefore, large-scale randomized, controlled trials are warranted.

2.2.1.5   Possible Phenotypes of Acromegalic Arthropathy

Some researchers have looked to genetic factors to explain why certain patients have unresolved arthropathy following long-term remission of acromegaly. In humans, there is polymorphism of GH receptors, meaning that there are different genetic expressions or phenotypes. A common GH receptor polymorphism, genomic deletion of exon 3, can increase the responsiveness of GH receptors via amplified signal transduction (Dos Santos et al., 2004; Pantel et al., 2000; Sobrier et al., 1993). Wassenaar and colleagues (2009a) found that those with exon 3 deletion had significantly higher prevalence of radiographic arthropathy of the hip, while another study revealed a trend towards increased frequency of arthropathy in PWA with exon 3 deletion (Mercado et al., 2008). When examining a subgroup of PWA with higher pre-treatment GH levels, those with the exon 3 deletion had greater arthropathy of the knee and distal interphalangeal joint (Wassenaar et al., 2009a).

However, the effect of exon 3 deletion on post-treatment arthropathy-related outcomes requires further exploration.

In a small number of cases, approximately 10-15%, PWA reach a stage of degenerative joint disease (Claessen et al., 2013; Rosselet et al., 1988). Researchers have not yet determined whether the development of subchondral cysts and joint space narrowing in PWA is end-stage AA or a separate phenotype of AA. Early researchers have proposed that degeneration may be due to abnormal hyaline cartilage growth (Bluestone et al., 1971; Rosselet et al., 1988). Histological findings revealed that cartilage cells proliferate nonuniformly in PWA, producing excess cartilage matrix in the middle and basal layers (Bluestone et al., 1971). This creates greater stress in the inter-territorial regions and can result in cartilage ulcers. In OA, fibrocartilage is laid down over damaged hyaline cartilage; however, in PWA, fibrocartilage is deposited in excessive volumes in response to cartilage damage. Fibrocartilage creates greater friction in the joint and is prone to more wear than hyaline cartilage, leading to further degeneration and eventually the exposure of subchondral bone. Subchondral sclerosis and cysts then result. Subchondral sclerosis, the depositing of dense bone in locations of eroded subchondral bone, occurs in excess in acromegaly. A cross-sectional study showed a relationship between higher age, female sex, and higher BMI and joint space narrowing in PWA, which are all predictors of OA in the general population (Claessen et al., 2013). Knee joint space narrowing was associated with past knee trauma and surgery but not any variables related to acromegaly, suggesting that PWA who developed knee joint space narrowing may have also been predisposed to OA. However, hip joint space narrowing was related to higher pre-treatment GH and IGF-1 concentrations, longer duration of exposure to excess GH, and delayed or unsuccessful surgical cure of acromegaly. Furthermore, hip joint space narrowing was more

prevalent in PWA treated with somatostatin receptor ligands compared to those who were not. Considering these associations were not found for other joint sites and the hip is one of the most common and severe sites of AA, the relationship between hip joint space narrowing and acromegaly clinical characteristics should be further explored.

2.2.2   Peripheral Neuropathy in Acromegaly

Peripheral neuropathy has been observed in several studies of PWA (Alibas et al., 2017; Dinn and Dinn, 1985; Jamal et al., 1987; Koçak, 2015; Low et al., 1974; Ozata et al., 1997; Pickett et al., 1975; Sasagawa et al., 2015). Although much of the focus is on carpal tunnel syndrome and neuropathy of the median nerve, a small number of studies have also examined peripheral nerves in the lower extremity (Alibas et al., 2017; Dinn and Dinn, 1985; Jamal et al., 1987; Low et al., 1974; Ozata et al., 1997; Stewart, 1966).

A few studies performed biopsies of the common peroneal nerve or sural nerve in a small sample or single case of PWA (Dinn and Dinn, 1985; Low et al., 1974; Stewart, 1966). Nerve enlargement due to hypertrophy of perineural and endoneural tissue was often observed alongside segmental demyelination and a reduction in the number of myelinated fibres. In two studies, hypertrophic onion bulb formations were noted, in which abnormal proliferation of Schwann cell processes and collagen result in a bulb-like formation surrounding the axon following repeated demyelination and remyelination (Dinn and Dinn, 1985; Low et al., 1974).

Regarding the function of peripheral nerves of the lower extremity, Jamal et al., (1987) observed decreased motor nerve conduction velocities and increased distal latencies of the common peroneal nerve in half of their sample of PWA. This observation was further supported by the findings of two other studies, which revealed significantly reduced

conduction velocities and compound motor action potentials and increased F latencies of the common peroneal nerve in PWA compared to healthy controls (Low et al., 1974; Ozata et al., 1997). In contrast, Alibas et al. (2017) found no significant differences between PWA and healthy controls for common peroneal nerve conduction tests; however, they did find significantly smaller compound motor action potentials and significantly prolonged distal latencies and F latencies for the tibial nerve in PWA. While only 14% of PWA in Jamal and colleagues' (1987) study revealed abnormalities of sural nerve sensory action potentials and latencies, other studies found significantly lower conduction velocities and action potentials of the sural nerve and/or superficial peroneal nerve in PWA compared to healthy controls (Alibas et al., 2017; Ozata et al., 1997).

Ozata et al., (1997) found longer response latencies following somatosensory evoked potentials of the tibial nerve in PWA compared to healthy controls, suggesting potential somatosensory dysfunction of the lower extremity. Somatosensory dysfunction could also be indicated by observations made by Jamal et al. (1987), who found absent ankle reflexes and absent or diminished knee reflexes in all PWA and abnormal perception of thermal and vibration stimuli in 62% and 37% of PWA, respectively. Similarly, another study found impaired sensation of pain/thermal, touch, and vibration stimuli in 60%, 15%, and 42% of PWA, respectively; however, they only observed diminished deep tendon reflexes in 19% of PWA (Alibas et al., 2017).

Studies of lower extremity peripheral neuropathy have mostly examined PWA with biochemically active disease or a mixed sample of controlled and active disease. Therefore, the results of previous studies may not be generalizable to PWA in biochemical remission. Alibas et al. (2017) had the largest proportion of PWA with controlled disease (71%) of all previously mentioned studies, and all PWA in their study underwent transsphenoidal

surgery and somatostatin receptor ligand therapy. They found that polyneuropathy (neuropathy of at least two nerves in additional to the median nerve) was significantly more common in PWA who had biochemically active disease than controlled disease, while no differences in the rate of carpal tunnel syndrome or neuropathy symptoms and signs were found between PWA with biochemically controlled and active disease. In contrast, another study found significantly greater median nerve thickness in PWA with active disease than controlled disease (Koçak, 2015). Peripheral nerve enlargement has been found to be only partially reversible in PWA after one year of biochemical disease control, in which the median and ulnar nerves of PWA were significantly smaller at the one-year follow-up but remained significantly larger in size than healthy controls (Resmini et al., 2009). Pickett et al. (1975) found that the majority of PWA with carpal tunnel syndrome had an absence of symptoms but still had abnormal median nerve conduction tests 12-21 months after surgical removal of the pituitary adenoma. Although it appears that nerve function may not fully be restored with treatment of acromegaly, the study by Pickett et al. (1975) was conducted close to a half-century ago and acromegaly treatments have since improved. Additionally, the latter three studies only examined the peripheral nerves of the upper extremity. Therefore, further investigation of the effects of biochemical remission on the structure and function of lower extremity peripheral nerves is necessary.

2.2.3   Changes to Muscles and Tendons in Acromegaly

Muscle and tendon structural and functional abnormalities have been noted in several studies of PWA. Muscle biopsies of PWA revealed evidence of myopathy, but the specific findings differed by study. Two studies found a higher frequency of hypertrophy in type I muscle fibres, while type II muscle fibres were more commonly atrophied (Khaleeli et al.,

1984; Nagulesparen et al., 1976). In contrast, another study found that mean fibre diameters were higher in PWA than healthy controls for both type I and type II muscle fibres (Mastaglia et al., 1970). Hypertrophy was observed alongside reduced muscle strength; therefore, it was suggested that GH-mediated muscle hypertrophy may reduce muscle contractile strength as seen in rodent studies (Bigland and Jehring, 1952). An ultrasonographic study did not reveal significant increases in overall muscle size of the quadriceps, gastrocnemius, or soleus in PWA; however, muscle fibre pennation angle of the vastus medialis and vastus lateralis were significantly smaller in PWA than healthy controls, suggesting abnormal muscle structure and lower force production capabilities of pennate muscles in PWA (Aagaard et al., 2001; Ozturk Gokce et al., 2020).

Abnormal tendon structure has also been shown in PWA. Several studies have found sonographic evidence of significantly increased Achilles tendon thickness in PWA compared to healthy controls (Colao et al., 1998; Koçak, 2015; Onal et al., 2016; Ozturk Gokce et al., 2020). While Koçak (2015) found no significant differences in Achilles tendon thickness between PWA with active and controlled disease, other studies found that PWA with active disease had significantly higher Achilles tendon thickness than PWA with controlled disease (Colao et al., 1998; Onal et al., 2016). Therefore, there is limited consensus on whether Achilles tendon thickness is normalized with biochemical remission of acromegaly, and longitudinal studies evaluating tendon thickness from acromegaly diagnosis to long-term biochemical remission are warranted. In addition to identifying increased Achilles tendon thickness, Onal et al. (2016) found significantly softened Achilles tendons in PWA using sonoelastography. This increase in softness of the Achilles could potentially indicate impaired passive and active stiffness of the plantar flexor muscles in PWA.

Studies of muscle function in PWA have shown reduced quadriceps and hamstring strength and endurance (Füchtbauer et al., 2017; Guedes da Silva et al., 2013; Homem et al., 2017; Walchan et al., 2016). An earlier study reported quadriceps action potentials of significantly shorter duration in PWA than healthy controls (Mastaglia et al., 1970). Due to the presence of myopathy, arthropathy, and peripheral neuropathy in PWA, the mechanism of reduced muscle function is unclear. Lopes (2016) found that increased GH levels, female sex, and older age were predictors of decreased muscle strength and endurance in PWA.

GH and IGF-1 have been proposed to be responsible for structural muscle and tendon changes in PWA due to their role in the regulation of collagen in the extracellular matrix of muscles and tendons. To examine the relationship between GH and IGF-1 and musculotendinous collagen production, Doessing et al., (2010) compared collagen mRNA expression and the rate of collagen and myofibrillar protein synthesis between PWA and patients with GH deficiency. They found that PWA had greater expression of collagen and IGF-1 mRNA in their skeletal muscles than patients with GH deficiency and that collagen mRNA and IGF-1 mRNA expression were significantly correlated in PWA. The rate of collagen and myofibril synthesis in muscle and tendon were not found to significantly differ between PWA and patients with GH deficiency; however, there was a trend towards greater collagen synthesis rates in PWA. These findings suggest that IGF-1 plays a role in regulation of collagen in the extracellular matrix of muscles and tendons in PWA, and the absence of relationship between GH/IGF-1 levels and myofibril synthesis rates suggests that synthesis of contractile tissue is not affected by GH/IGF-1. Therefore, this may explain the paradox of muscle and tendon hypertrophy in conjunction with reduced muscle strength; however, larger studies are necessary to further examine this theory.

2.3   *Neuromuscular Control of Standing Balance*

Maintenance of quiet upright stance is a form of static postural equilibrium in which the body's COM is maintained within the base of support, defined by the boundaries of the body segments in contact with the support surface (e.g., the boundaries of the feet in bipedal upright stance) (Horak and Macpherson, 1996). Based on anthropometric models which divide the body into segments at moveable joints, the COM of the body is the three-dimensional (3D) position determined by the weighted average of the COM of each body segment and is the point of application of the resultant force acting on the body (Horak and Macpherson, 1996; Winter, 1995). To achieve static equilibrium, a force must oppose gravity with equal magnitude, and in quiet upright stance, this opposing force is called the ground reaction force (GRF).

Standing is a task that often feels effortless for an able-bodied, healthy individual. However, standing demands constant neuromuscular control due to the force of gravity and internal physiological disturbances (Forbes et al., 2018). Furthermore, upright bipedal stance in humans is relatively unstable compared to quadrupedal stance in other species due to the smaller area of the base of support and greater height of the body's COM (Horak and Macpherson, 1996). With a smaller base of support, there is less surface area in which the COM can travel without loss of static equilibrium. The greater height of the COM with respect to the base of support in humans results in increased gravitational torque of the body about its base of support and requires higher magnitudes of muscle torque to oppose the gravitational torque and maintain upright stance.

The complexity of standing balance control becomes more apparent when key components of the balance control system are impaired due to factors such as older age, illness, or injury. The effects of balance impairment can be deleterious. Impaired balance

due to older age, physical limitations, and/or sensory impairment greatly increases one's risk of falls, and falls are significant predictors of morbidity and mortality (Ivers et al., 1998; Nevitt, 1989; Nevitt et al., 1991; Peel, 2011; Shumway-Cook et al., 2009).

2.3.1 Postural Control System

Posture can be defined by the position and alignment of body segments at a given point in time and is expressed relative to the line of the gravitational force (Horak and Macpherson, 1996; Winter, 1995). Each individual has a unique alignment of body segments that characterizes their postural orientation. Although an individual's postural orientation is typically considered to be stable, it can face gradual alterations as biomechanical or neural constraints change with aging, injury, or in the rare case of prolonged space flight (Horak and Macpherson, 1996; Lestienne and Gurfinkel, 1988)

Postural strategies are high-level plans that are developed and executed by complex sensorimotor processes (Horak and Macpherson, 1996). The overarching goal of a postural strategy is maintaining postural equilibrium by ensuring the COM stays within the bounds of the base of support; however, several underlying postural goals also exist such as orientating the trunk or head to a specific reference frame or minimizing energy expenditure. There are numerous combinations of movement patterns and muscle synergies that can achieve the same postural outcome; therefore, postural strategies will vary depending on the task, environmental conditions, and which of the underlying goals are prioritized. The coordination of many body systems is necessary to implement a postural strategy. These systems include the sensory and motor components of the peripheral nervous system, the CNS, and the musculoskeletal system. Thus, complex modelling is required to better understand postural control.

Early models of postural control were static and focused on only the sagittal plane of motion (Gordon et al., 1986; Nashner and McCollum, 1985). The models contained a limited selection of muscle synergies that could restore the COM. However, when compared to prior experimental force plate and EMG data, these models only accounted for the muscle activations observed in approximately half of the participants (Nashner, 1976). Due to the numerous combinations of muscle activations capable of producing the same motion, modelling a limited number of muscle synergies is not generalizable. The difficulty of modelling all possible muscle combinations can be evaded by studying control of posture at the level of joint moments instead of the level of muscular synergies since the joint moment accounts for the net muscle activity about a joint (Yang et al., 1990).

As shown in Figure 6, changes in posture due to internal or external forces are detected by three main types of sensory receptors: visual, vestibular, and somatosensory (proprioceptive) (Winter et al., 1990). The information from these sensory receptors is integrated in the CNS, and information regarding the required muscle tone to stabilize the COM is sent via motor neurons to the muscles. Postural adjustments also consider the underlying task goal. This process repeats as the sensory system continuously monitors postural changes and the musculoskeletal system continuously adapts to these changes to maintain the COM within the base of support.

Although this review will predominantly focus on the control of unperturbed stance, postural strategies following external perturbations may be discussed if relevant to the understanding of standing balance control.
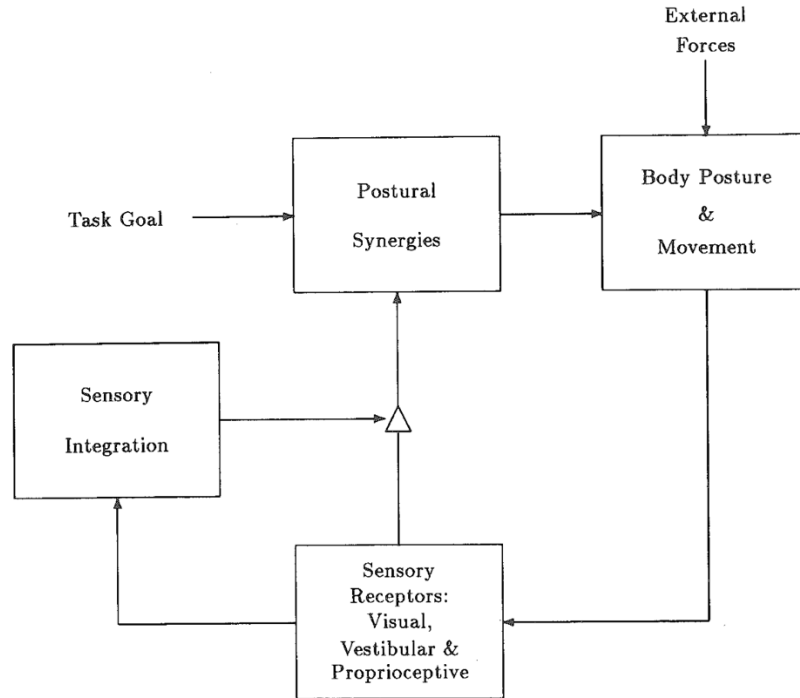
Figure 6. *Schematic of the postural control system. Reproduced from Winter et al. (1990).*

2.3.2   Sensory Control of Standing Balance

The sensory control of standing balance involves the vestibular, visual, and somatosensory systems, which each provide a different mode of information (Horak and Macpherson, 1996; Winter et al., 1990). The vestibular system is comprised of the otolith organs and semi-circular canals located in the inner ear, which detect linear and angular motion, respectively. Vestibular afferents provide information about head orientation relative to the gravitational line. The somatosensory system allows for perception of various types of stimuli external and internal to the body through different receptor types located inside the body and on its outer surface. The proprioceptive receptors located in the muscles and joints detect the length and force production of muscles and orientation of body segments with respect to each other. Skin receptors aid in perception of the external environment by detecting touch, temperature, noxious stimuli, and pressure. The visual

system provides information about the external environment through two different types of photoreceptors located in the retina, rods and cones, that provide night vision and colour vision, respectively. Visual afferents indicate the orientation of the head with respect to the environment.

Each sensory system does not provide complete information on its own; therefore, integration of information from different sensory modalities is necessary for meaningful interpretation of body orientation (Horak and Macpherson, 1996). For example, visual afferents can indicate that the visual scene is moving with respect to the environment, but vision alone cannot determine whether the body itself is moving or whether the environment is moving around the body. Integration with somatosensory and/or vestibular afferents can help to resolve this discrepancy. Sensory integration involves identifying conflicting information, determining which signals are relevant, and weighting the sensory information according to importance in the specific environmental context.

The contribution and interaction of each sensory system in postural control has been studied by controlling inputs from one or more sensory systems. Although integration of multiple sensory modalities increases the precision of self-perceived body orientation, redundancy of sensory information allows postural equilibrium to be achieved even if some sources of sensory input are absent or impaired. Nashner (1971) developed a platform that rotated forward and backward at the same frequency as postural sway to prevent angular motion about the ankle joint, which would typically occur during quiet stance due to gravitational torque. Through the platform rotations, proprioceptive cues from the ankle joint, the main controller of AP postural control, provided inaccurate information about the ankle angle and orientation of the body relative to the support surface. An additional component was later added to control visual inputs, which obstructed the participant's

visual field with a box that could move in synchronization with the displacement of the head during postural sway (Nashner and Berthoz, 1978). Using these devices, those with functioning sensory systems only had slight increases in body sway when inaccurate visual or proprioceptive afferents were provided, but inaccurate information from both sensory systems increased postural sway by 50% (Black et al., 1988). In those with impaired or absent vestibular function, loss of balance occurred when both visual and somatosensory inputs were inaccurate; however, when only one of the two sensory systems was manipulated, upright stance was maintained despite increased sway. When both visual and proprioceptive cues were accurate, those with vestibular dysfunction had close to normal postural sway values. This suggests that only one functional sensory system is required to maintain upright stance; however, sway increases with an increase in the number of impaired sensory systems.

In those with reduced vestibular function or with unilateral vestibular loss, conflicting information from somatosensory and visual afferents resulted in loss of balance, thus Nashner (1982) argued that the vestibular system is located at the top of the hierarchy for postural control. He suggested that sensory integration is a weighted sum of vestibular, somatosensory, and visual information, where body orientation determined by the vestibular system is the reference to which somatosensory and visually derived orientation is compared. Thus, an inaccurate vestibular reference would result in a flawed interpretation of body orientation in the context of conflicting somatosensory and visual information. Jeka et al. (2004) proposed that the velocity of the body's COM is the most accurate information detected by the sensory system, and that the increased postural sway observed when information from certain sensory modalities is absent or inaccurate is due to a loss of COM velocity information.

There is also evidence of changes to sensory organization in those with impaired sensory systems and with aging. For example, in individuals with visual impairments, less postural sway is observed than in individuals with normal vision when standing on a compliant surface with EC, suggesting an adaptation of enhanced somatosensory and vestibular function in those with visual impairments (Friedrich et al., 2008). Similarly, it has been proposed that there is re-weighting of sensory information in order adults, who often experience a reduction in sensory function (Horak et al., 1989; Pasma et al., 2015; Woollacott et al., 1986). This has been experimentally demonstrated by increasing somatosensory sensory stimuli through the use of textured firm and compliant insoles, which decreased postural sway in older adults but not in young adults (Qiu et al., 2012).

2.3.3 Muscular Control of Standing Balance

Despite the stationary appearance of quiet stance, its postural control is dynamic in nature (Horak and Macpherson, 1996). Small continuous movements of the COM occur during quiet stance, reflecting the body sway caused by gravity and internal body vibrations from physiological processes (e.g., breathing). Muscle activation must occur to counteract this passive sway and restore static equilibrium. Muscle forces produce joint torques and lead to subsequent forces applied to the support surface that accelerate the body and help to restore the position of the COM. Since the GRF must be equal and opposite to the gravitational force in order to maintain static equilibrium, muscle activation shifts the origin of the GRF, which subsequently restores the COM (i.e., the point of origin of the gravitational force). The point of origin of the GRF is termed the COP, and its position changes as a result of the muscular forces that accelerate the body.

2.4   *Inverted Pendulum Model of Standing Balance*

The inverted pendulum model of human balance describes the control of standing balance in relation to the trajectories of COM and COP. It is based on the theory that the COM oscillates during stance due to the gravitational force and physiological vibrations (e.g., breathing), while COP displacement results from muscle torque that attempts to restore the COM position (Winter et al., 1998). Therefore, COM is often considered as the controlled variable, whereas COP is the controlling variable. The inverted pendulum model has guided researchers' understanding of the muscular mechanisms for the control of upright stance.

In the sagittal plane, an ankle strategy is described for control of quiet upright stance in which the ankle plantar flexors/dorsiflexors are activated in response to AP changes in COM, resulting in a moment at the ankle which translates the COP anterior or posterior to the COM (Horak and Nashner, 1986; Mori, 1973; Nashner, 1970; Winter, 1995). As the base of support becomes narrower, such as in tandem stance, an ankle strategy no longer dominates AP balance control and a hip strategy takes over (Winter et al., 1996). Similarly, a hip strategy involving rapid hip flexion or extension is observed in the AP direction when the COM is close to the limits of the base of support and an anterior or posterior perturbation is applied in the same direction that the person is leaning (Horak and Moore, 1993).

Day and colleagues (1993) studied motor mechanisms responsible for the control of upright stance in the ML direction. They proposed that the hip abductors/adductors and ankle invertors/evertors were primary involved in the ML fluctuations in COP. Winter et al. (1996, 1993) researched ML control of quiet stance with similar findings. By measuring left and right foot COP (COP_L and COP_R) separately using two adjoining force plates, they

observed synchronization between COP_L and COP_R in the AP direction and determined

that total body COP (COP_{net}) was simply the mean of COP_L and COP_R; however, in the

ML direction, changes in COP_L and COP_R were antiphase and had no relation to COP_{net}.

Through analysis of the left and right foot vertical GRF ($vGRF_L$ and $vGRF_R$), they found

that in the ML direction, $vGRF_L$ and $vGRF_R$ were strongly related to COP_{net}, indicating a

loading and unloading mechanism at the hip.

2.4.1   Control of Standing Balance in the Sagittal Plane

Figure 7 displays the ankle strategy of postural control in a person standing

quietly on a single force platform at five points in time, while Equation 1 describes the

relationship between the variables noted in Figure 7.
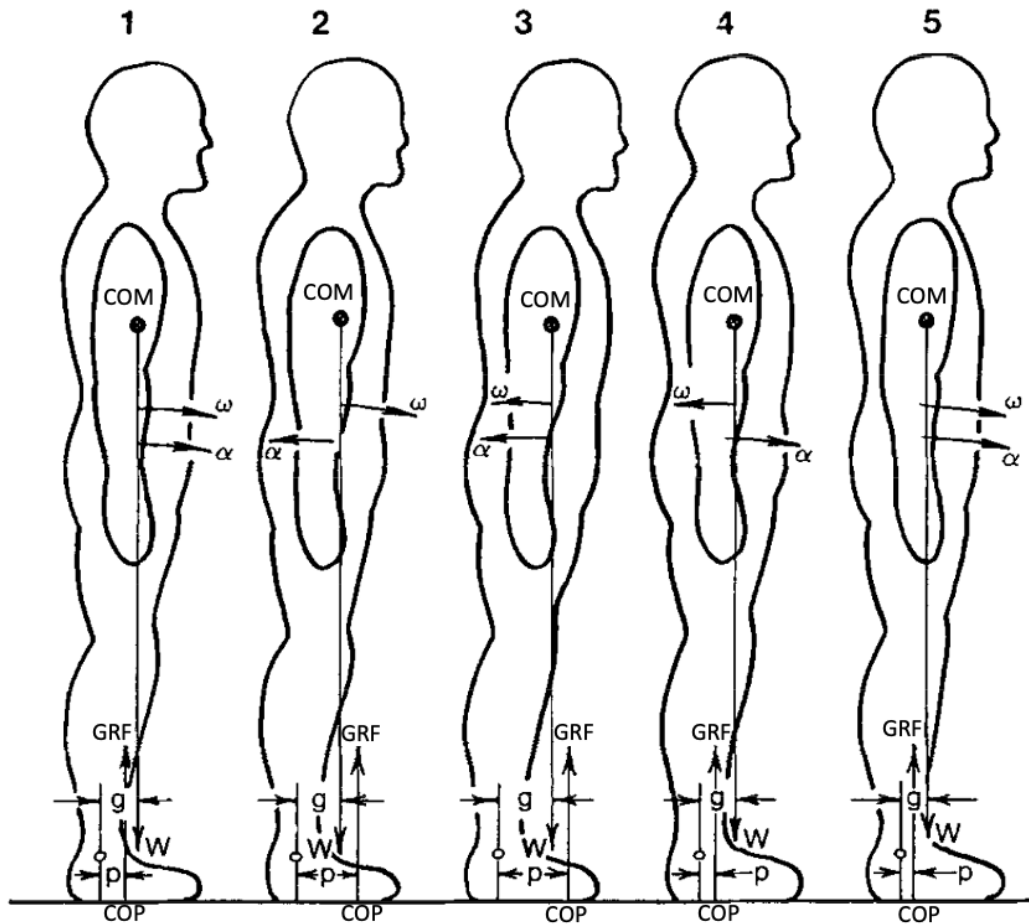
Figure 7. Schematic of the ankle strategy of postural control. Subject is swaying back and forth on a force platform at five different points in time. Variables noted are the locations of the centre of mass (COM) and centre of pressure (COP); gravitational force (W) and ground reaction force (GRF), which originate at the COM and COP, respectively; perpendicular distances between W and ankle joint (g) and GRF and ankle joint (p); and angular acceleration (α) and angular velocity (ω) about the ankle joint. Reproduced from Winter (1995).

The ankle strategy shown in Figure 7 and Equation 1 assumes an inverted pendulum rotating about the ankle in the AP direction with symmetric muscular contributions from the left and right limbs. The GRF and gravitational force (W) are equal and opposite forces that are assumed to remain constant during quiet stance. The product of the perpendicular distance between the line of action of these forces and the centre of the ankle joint (p and g) determines the moment of these forces. Applying this to Newton's second law for

38

angular motion, the difference between the moments of the GRF (M_{GRF}) and gravitation

force (M_W) is equivalent to the product of the moment of inertia of the total body about the

ankle joint (I) and the angular acceleration of the body about the ankle joint (α):

$$\Sigma M = I\alpha$$

$$M_{GRF} - M_W = I\alpha$$

$$GRF\ p - Wg = I\alpha \qquad (1)$$

Therefore, the direction of the acceleration and net moment at the ankle can be determined

by monitoring the COM and COP trajectories. Furthermore, the activation of muscle groups

at the ankle can be predicted. For example, in Figure 7 at Time 1, anterior sway of the body

shifted the position of the COM anterior to the COP; therefore, the moment of the GRF is

less than the gravitational torque, resulting in clockwise angular acceleration and a

clockwise net moment about the ankle (Winter, 1995). In order to restore the COM, the

ankle plantar flexors must be activated, which translate the COP anteriorly. This muscle

activation leads to the position observed at Time 2, where the COP is anterior to the COM,

the moment of the GRF is greater than the gravitational torque, and a counter clockwise

angular acceleration is produced. Once Time 3 is reached, the counter clockwise angular

acceleration reverses the direction of the angular velocity, and the body begins to sway

posteriorly. The posterior shift of the COM results in decreased plantar flexor activation

and increased dorsiflexor activation, which translates the COP posteriorly and produces a

clockwise angular acceleration as seen at Time 4. At Time 5, the clockwise angular

acceleration reverses the direction of the angular velocity and the cycle of the inverted

pendulum repeats.

From Equation 1, the difference between COP and COM can be estimated. Applying the knowledge that the tangential acceleration of a point mass constrained to a circular path is proportional to its angular acceleration by a factor of the circle radius, the angular acceleration about the ankle is equivalent to the horizontal acceleration of the COM (a_x) divided by the distance from the centre of the ankle joint to the COM (d). It is also known that in quiet stance, the magnitude of the GRF and gravitational force are equal. Finally, if the global origin is located at the ankle, then COP is equivalent to p and COM is equivalent to g. Therefore, Equation 1 can be rearranged to define the difference between the COM and COP in the AP direction.

$$\alpha = \frac{a_x}{d}, \qquad \therefore GRF\ p - Wg = I\frac{a_x}{d}$$

$$GRF = W, \qquad \therefore W\ (p - g) = I\frac{a_x}{d}$$

$$p - g = \frac{Ia_x}{Wd}$$

$$COP = p;\ COM = g, \qquad \therefore COP - COM = \frac{Ia_x}{Wd}$$

$$COP - COM = \frac{I}{Wd}a_x = ka_x \qquad \qquad (2)$$

Equation 2 shows that the difference between the COP and COM is proportional to the horizontal acceleration of the COM, which Winter (1995) described as the error in the balance control system. When measured experimentally over a 120 second duration of quiet stance, a high negative correlation (r=-0.91 to r=-0.94) was found between the difference between COP and COM and the horizontal COM acceleration, providing evidence of

validity of the inverted pendulum model (Gage et al., 2004; Winter et al., 1998). A comparison of the COP and COM signals in the sagittal plane over the course of 7 seconds is shown in Figure 8. The COP signal has both a higher amplitude and frequency than the COM, which is consistent with the theory that the COP is the controlling variable and COM is the controlled variable and that COP must travel anterior or posterior to the COM to reverse the direction of the COM acceleration.
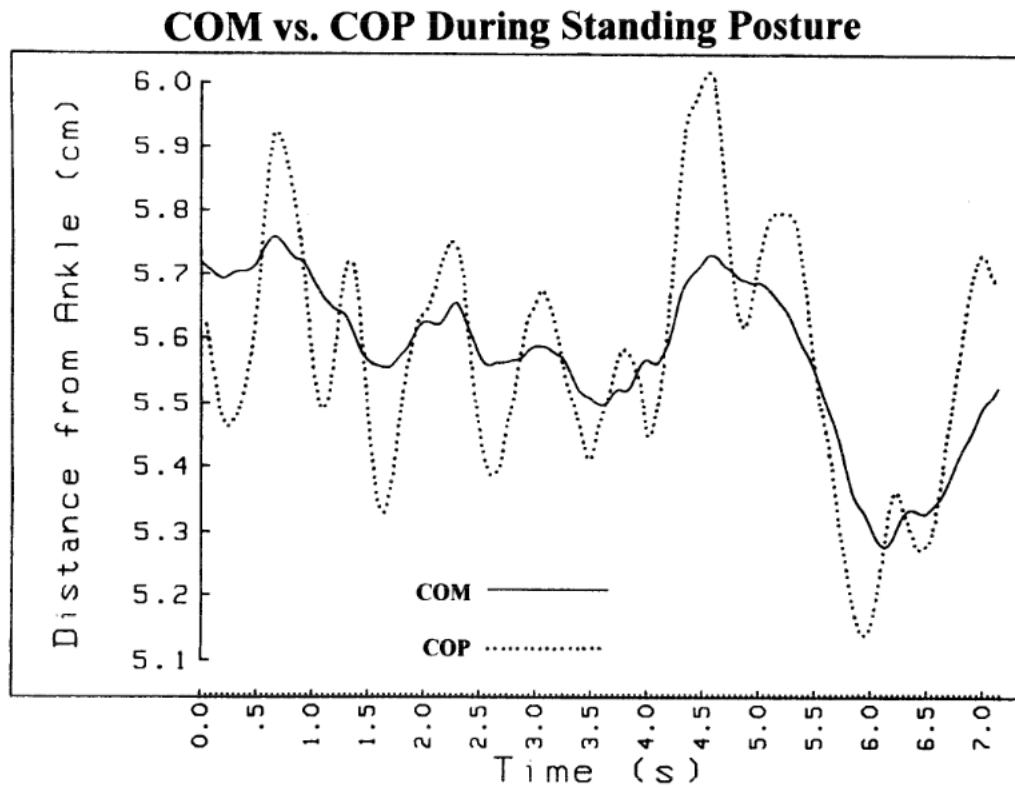
Figure 8. *Comparison of COP and COM in the AP direction with respect to the ankle joint during quiet upright stance. Reproduced from Winter (1995).*

2.4.2   Application to Frontal Plane and Asymmetric Loading

The ankle strategy previously described assumes a whole body COP measured from a single force platform with symmetrical control from the left and right ankles, which is not generalizable to frontal plane mechanics or individuals with limb dominance or unilateral pathologies (Winter, 1995). The mechanism for control of upright stance in the

ML direction is different from the ankle control strategy defined for the AP direction and requires separate analysis of the COP_L and COP_R using two contiguous force plates due to the hip load-unload mechanism (Winter et al., 1996, 1993). Equation 3 describes the relationship between COP_{net} and COP_L and COP_R in either AP or ML directions

$$COP_{net} = COP_L \frac{vGRF_L}{(vGRF_L + vGRF_R)} + COP_R \frac{vGRF_R}{(vGRF_L + vGRF_R)} \qquad (3)$$

where $vGRF_L$ and $vGRF_R$ are the vertical GRF acting on the left and right feet, respectively.

In Equation 3, COP_L and COP_R represent the muscular control at the ankle, while $vGRF_L/(vGRF_L+vGRF_R)$ and $vGRF_R/(vGRF_L+vGRF_R)$ represent the proportion of total body weight loaded under the left and right feet. Therefore, COP_{net} is a weighted average of COP_L and COP_R. In the AP direction with the assumption of symmetric load bearing and muscle activity between limbs, COP_{net} is simply the mean of COP_L and COP_R since $vGRF_L$ and $vGRF_R$ are assumed to be equal in magnitude. In the ML direction, COP_L and COP_R are controlled by the ankle invertors and evertors. However, previous studies have shown that changes in load bearing between limbs are anti-phase in the ML direction, meaning that as one limb increases its load, the other limb decreases its load by the same proportion of body weight. This loading and unloading mechanism, represented by $vGRF_L/(vGRF_L+vGRF_R)$ and $vGRF_R/(vGRF_L+vGRF_R)$, is controlled by the hip abductors and adductors and thus modifies the amount of weight given to COP_L and COP_R when determining COP_{net}. For example, activation of the right abductors or left adductors would increase $vGRF_R$ and subsequently decrease $vGRF_L$ by the same magnitude, increasing the contribution of COP_R and decreasing the contribution of COP_L to COP_{net}.

The waveforms of COP_L, COP_R, and COP_{net} in the AP direction reveal that all three signals change in phase with one another (Figure 9) (Winter et al., 1993). COP_{net} lies almost

directly between COP_L and COP_R, which is consistent with the theory that COP_{net} is the mean of COP_L and COP_R in the AP direction. In contrast, COP_L and COP_R changes in the ML direction are anti-phase and have no relationship to COP_{net} (Figure 10). However, the waveforms of $vGRF_L$ and $vGRF_R$ (Figure 11), which are also anti-phase, change in amplitude at approximately the same time points as the changes in amplitude of the COP_{net} waveform in the ML direction (Figure 10). Since there is a stronger relationship between $vGRF_L$, $vGRF_R$, and COP_{net} than COP_L, COP_R, and COP_{net} in the ML direction, this implies a greater contribution of the hip ab/adductors than the ankle evertors/invertors to the control of COP_{net} in the ML direction during quiet stance.
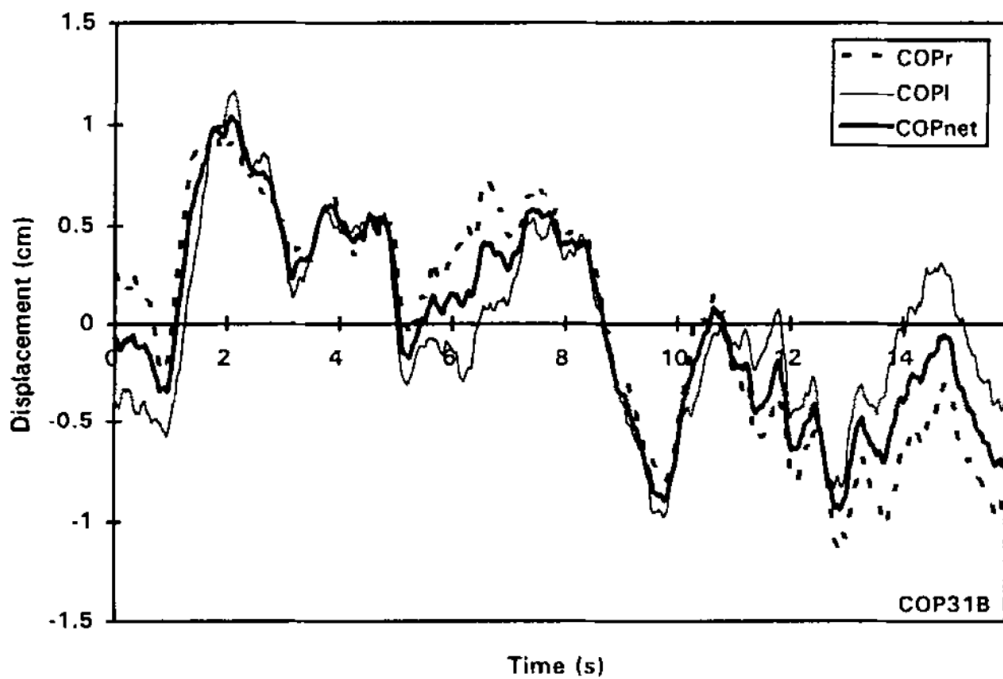
Figure 9. *Left, right, and net COP displacement in the AP direction during bipedal stance. Reproduced from Winter (1995).*

43
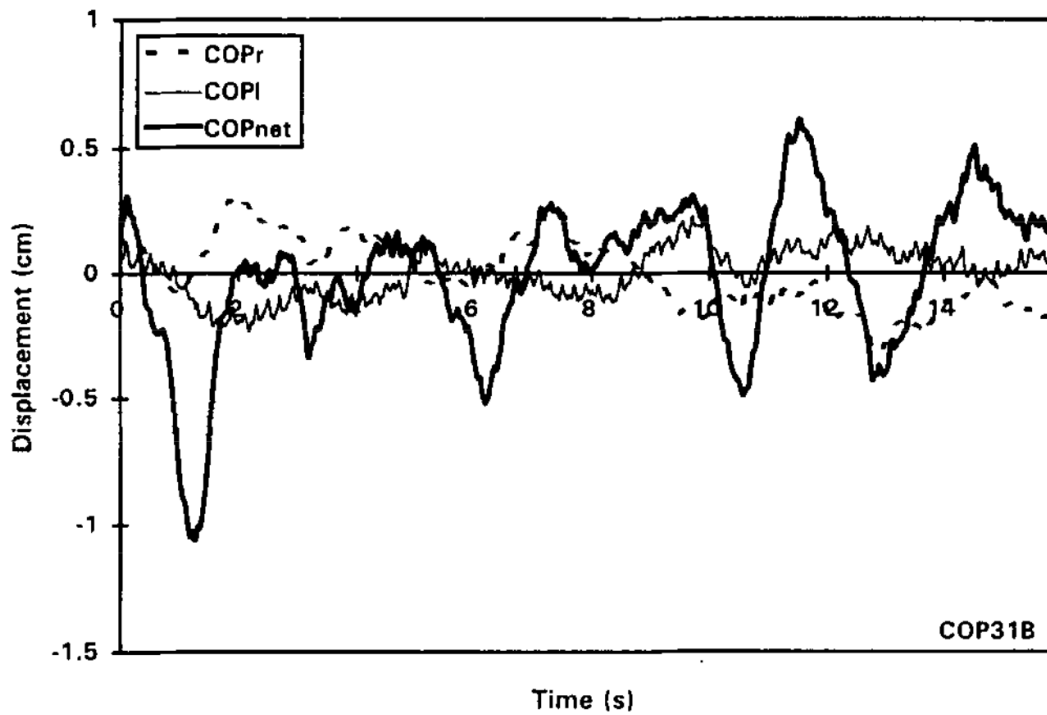
Figure 10. Left, right, and net COP displacement in the ML direction during bipedal stance. Reproduced from Winter (1995).
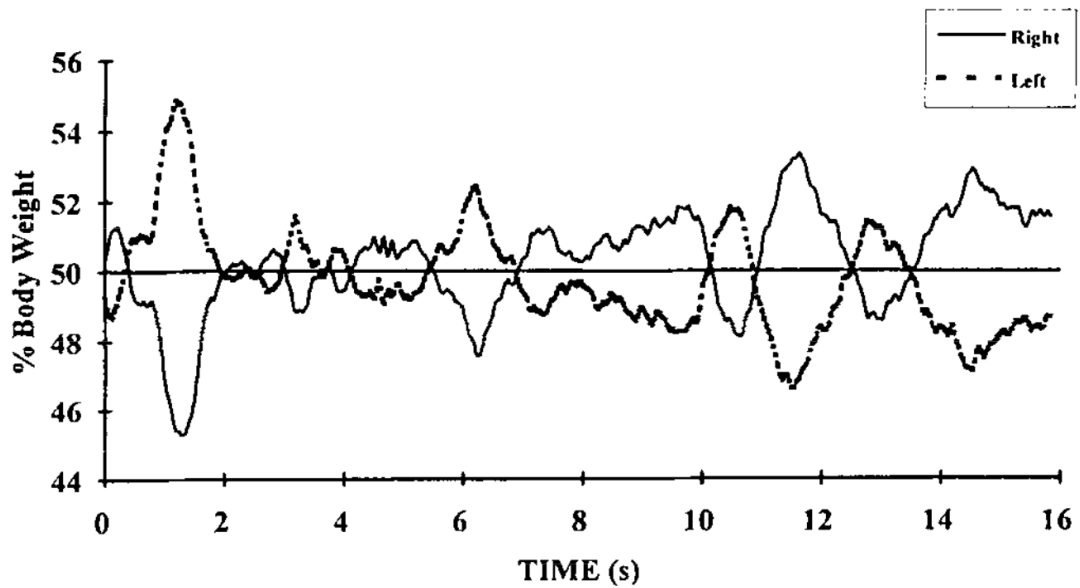
Figure 11. Left and right vertical GRF as a percentage of total body weight during bipedal stance. Reproduced from Winter (1995).

Similar to the AP direction, modifying the stance width changes the relative contributions of ankle and hip muscles to ML control of standing balance. There is increased contribution of the ankle evertors/invertors to ML balance control in narrow or single leg stance, while stances wider than hip distance show improved coupling between the ankle and hip muscles, creating greater passive stiffness and improved effectiveness of COM restoration via the moment generated about the hip (Åberg et al., 2011; Bingham et al., 2011; Day et al., 1993; Goodworth and Peterka, 2010; Winter et al., 1996).

2.4.3   Open Loop versus Closed Loop Control of Quiet Stance

Based on the trajectories of the COP and COM, researchers sought to investigate whether muscular control of quiet upright stance entailed an open loop system involving passive muscle stiffness or a closed loop system involving reactive feedback control. This question has been explored through modelling and experimental studies.

Winter and colleagues (1998) experimentally measured a 4 ms lag of the COP behind the COM. They proposed a passive stiffness model rather than reactive muscular control as the latency of sensory feedback and reactive muscular activation is known to be upwards of 100 ms (Horak and Nashner, 1986; Rietdyk et al., 1999; Winter et al., 2001). Moreover, Winter et al. (1998) negated the involvement of visual feedback in quiet stance as they saw no difference in sway patterns between EO and EC conditions, and they ruled out involvement of the vestibular system and proprioceptive joint receptors as the small displacements and accelerations in quiet stance do not reach these receptors' activation thresholds.

This was challenged by researchers who suggested that the inverted pendulum of the human body could not be stabilized solely by passive muscle stiffness as the estimates

45

of passive ankle stiffness are not sufficient to counteract gravitational body sway (Casadio et al., 2005; Loram and Lakie, 2002a; Morasso and Sanguineti, 2002; Morasso and Schieppati, 1999). Morasso and colleagues (1999) argued that the zero-phase delay between COP and COM is related to the inherent instability of the inverted pendulum system and, therefore, that the zero-lag does not justify a theory of passive stiffness.

Collins and De Luca (1993) proposed a novel method of balance assessment that related human control of quiet stance to Brownian motion theory and was based upon the experimental measurement of ~1 s unidirectional movements in the AP axis during quiet stance that were unaffected by the absence of visual feedback. They proposed the involvement of both open and closed loop feedback controllers in quiet stance, where the open loop process controlled the sway occurring over a ~ 1 s time scale and the closed loop process controlled the sway happening over longer time scales. The theory of a hybrid controller in quiet stance has been adopted in models by other researchers (Lakie et al., 2003; Loram et al., 2005; Loram and Lakie, 2002b; Morasso and Sanguineti, 2002; Morasso and Schieppati, 1999; Peterka, 2000). Winter et al. (2003, 2001) argued that Morasso and Schieppati's (1999) hybrid model disregarded the latencies of afferent and efferent signals, and thus, the muscular control variable in their model would have a delay of at least 50-70 ms behind the COM, which contradicts Winter's experimentally measured lag of 4 ms.

The theory of feedforward control suggests that postural strategies are not selected in response to individual changes in the COM position but are predetermined based on knowledge from prior sensory feedback and previous motor responses to various types of COM perturbations and sensory conditions (Gatev et al., 1999; Horak and Nashner, 1986; Macpherson et al., 1989; Moore et al., 1986; Nashner, 1976). This theory is in agreement

with both Winter's (1998) theory of passive ankle stiffness and studies that have shown increased sway in those with sensory dysfunction. Therefore, in accordance with Winter's (1998) passive stiffness theory, the amount of passive muscle stiffness required to maintain upright stance in a given sensory environment would be pre-set based on predictions made from prior sensory information.

Regardless of the explanation for the minimal phase lag between the COP and COM, it is clear from experimental studies that the sensory system is involved in maintaining quiet stance.

2.5   Measurement of Standing Balance

2.5.1   Measurement of Centre of Pressure

Force platforms are considered the gold standard instrumentation for COP measurement. Force plates which contain strain gage load cells are ideal for standing balance assessment due to their ability to accurately measure static forces that are sustained over a long duration (Robertson et al., 2013). Strain gages are a type of resistive sensor, and in the case of a force plate, produce electrical signals which are proportional to the applied force (Winter, 2009). Strain gages function according to the stress-strain relationship. Stress is defined as the amount of force per unit area of force application, while strain is the amount of deformation or change in length of a material caused by the applied force. The slope of the elastic region of a stress-strain curve is based on a material's elastic modulus, a coefficient representing the ratio of stress to strain, and allows for the applied force to be predicted based on the amount of deformation of the material. When an external force is applied to the force plate, a fine wire inside the strain gage changes in length and experiences a proportional change in its electrical resistance (Webster, 2009).

Since the strain does not exceed the wire's elastic limit, the wire returns to its normal length when the external load is removed.

In a force plate load cell, four strain gages are arranged in type of circuit called a Wheatstone bridge, which contains four active resistive arms (R_1, R_2, R_3, and R_4) (Figure 12). A Wheatstone bridge can be considered as two parallel voltage dividers, with R_1 and R_2 comprising one voltage divider and R_3 and R_4 comprising the other. A signal conditioner supplies an excitation voltage to the strain gage unit. Zeroing the signal conditioner balances the bridge, meaning the ratio of the resistances in each voltage divider are equal ($R_1/R_2=R_3/R_4$) and the output voltage is zero. When the wire in a strain gage undergoes deformation due to an external load, a change in the wire's electrical resistance occurs. This results in a difference in electrical potential between the two sides of the bridge; therefore, an output voltage is produced. The relationship between the output voltage and the resistance of each wire is defined by

$$V_{out} = V_{in} \left(\frac{R_3}{R_3 + R_4} - \frac{R_2}{R_1 + R_2} \right) \tag{4}$$

where R_1, R_2, R_3, and R_4 are the resistance of wires, V_{in} is the excitation voltage, and V_{out} is the output voltage.

The output voltage is amplified by the signal conditioner, and the analog signals are digitized by an analog to digital converter. A calibration matrix provided by the force plate manufacturer allows for conversion of the output voltage into force (N) and moment of force (Nm) units based on known properties of the strain gage load cells.
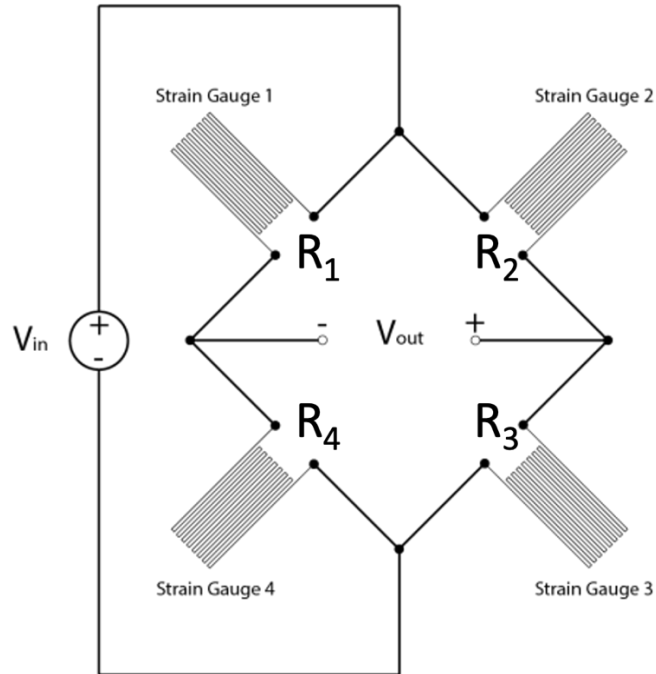
Figure 12. *Four strain gages arranged in a Wheatstone bridge. V_{in} is the excitation voltage supplied by the signal conditioner, V_{out} represents the difference in electrical potential between the two sides of the bridge, and R_1, R_2, R_3, and R_4 are the resistance of each .strain gage.*

Force plates can contain four load cells, one in each corner of the force plate, or one load cell in the centre of the force plate (Robertson et al., 2013; Winter, 2009). Modern force plates typically contain four load cells due to greater accuracy in measuring forces that are applied further from the center of the plate. The remainder of this paper will reference a four load cell force plate that outputs the ground reaction force and moment of the ground reaction force in the x, y, and z axes, with the force plate origin located below the centre of the force plate surface by a known vertical offset, d_z. This type of force plate outputs the GRF and the moment of the GRF in the x, y, and z axes (Figure 13).
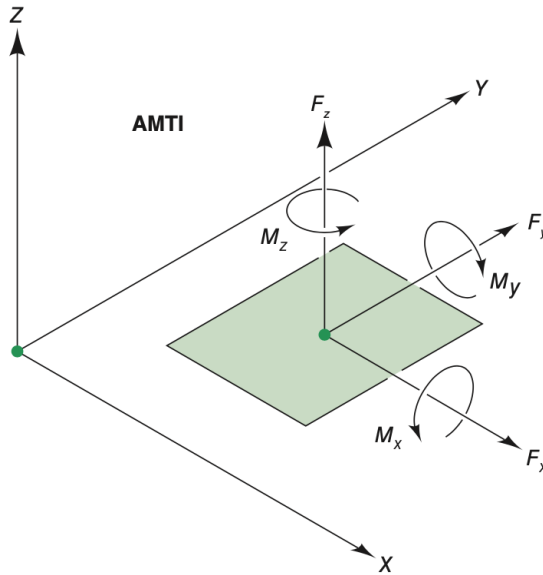
Figure 13. *An AMTI strain gage force plate that measures the GRF and moment of the GRF in the x, y, and z axes. Reproduced from Robertson et al. (2013).*

The COP is the average position of pressure distributed over the surface area in contact with the support surface, which is the intersection of the GRF vector with the support surface (Robertson et al., 2013; Winter, 2009). The COP position is typically expressed with respect to the centre of the top surface of the force plate; therefore, only the x and y coordinates are calculated, and the vertical component of COP is assumed to be zero. However, in experiments that use synchronized force plate and motion capture data, the COP may be expressed with respect to the global coordinate system (GCS) or the projection of the ankle joint centre on the support surface. The equations for calculating COP can be found in section 4.8.4.

COP signals can be analyzed in both the time domain and frequency domain. Common time domain parameters of COP include root mean square amplitude, AP or ML range, 95% PEA, and mean velocity. In the frequency domain, median power frequency (MPF), mean power frequency, total power, and fractal dimension of the COP are often

used. Time domain parameters are commonly reported as they are easiest to calculate and provide a reliable indication of stability during quiet stance (Lafond et al., 2004; Ruhe et al., 2010). Frequency domain parameters require transformation of the time-varying COP signal to the frequency domain using transformations such as a fast Fourier transformation (FFT) or wavelet transformation. Despite the more complex analysis, frequency domain COP parameters provide more insight into the sensory control of balance.

Frequency analysis of the COP signal allows for insight into the relative contributions of the three sensory systems in the control of balance. Each of the sensory systems are proposed to operate within specific frequency ranges; however, these ranges have not been explicitly confirmed in the literature. Changes in COP position in response to visual feedback are thought to occur at frequencies below 0.1 Hz (Dichgans and Brandt, 1978; Horak and Macpherson, 1996). A frequency range of 0.03-0.1 Hz for visual control of balance was experimentally determined using Fourier transform of the COP signal in eight different frequency windows and comparing the difference between adjacent frequency windows between participants with visual impairments and normal vision (Friedrich et al., 2008). Similarly, higher mean and median power frequencies have been observed in EC compared to EO conditions, suggesting that visual control operates at lower frequencies than other sensory systems (Davis et al., 2009; Sozzi et al., 2021). Lestienne et al. (1977) experimentally derived a frequency range of 0.02-0.2 Hz representing postural readjustments in response to a moving visual scene. They also observed sharp peaks at higher frequencies of approximately 0.15-0.5 in response to the moving visual scene; therefore, there may be a second frequency range representing visual feedback that is slightly higher in frequency. Frequencies above 0.1 Hz have been linked to vestibular function during postural control; however, the otoliths may only provide accurate

information at sway frequencies below 0.5 Hz as higher sway frequencies may prevent the otoliths from differentiating between tangential acceleration of the head versus tilting of the head (Nashner, 1971, 1972; Nashner et al., 1989). Medium to high frequencies of approximately 0.5-1 Hz are linked to somatosensory and lower extremity muscular control (Diener et al., 1984; Nashner et al., 1982; Oppenheim et al., 1999). High frequency bursts during stance that are greater than 1 Hz are thought to be provoked by CNS dysfunction.

COP parameters typically increase in reliability with longer test durations. Test durations of 90 to 120 seconds are recommended to achieve an ICC $\geq$ 0.75 for most COP parameters (Carpenter et al., 2001; Ruhe et al., 2010). Additionally, averaging multiple trials over a single day or multiple days increases reliability (Lafond et al., 2004; Santos et al., 2008). The data acquisition settings can influence the reliability and validity of COP measures. A sampling frequency of at least 100 Hz is recommended, while recommended lowpass filter cut-off frequencies range from 3-10 Hz (Gage et al., 2004; Ruhe et al., 2010).

2.5.2   Measurement of Centre of Mass

Three-dimensional motion capture systems are the gold-standard for kinematic analysis of human movement. Passive optical motion capture systems use multiple cameras that emit and capture infrared light and retroreflective markers that are placed on specific anatomical landmarks on the subject being measured. The cameras are arranged around the periphery of the capture volume so that each camera has a unique viewpoint, and each marker is visible by two or more cameras (Figure 14). The infrared light emitted from each camera is reflected off the markers, and 2D marker positions in the camera's coordinate system are determined by capturing the reflected infrared light (Robertson et al., 2013; Winter, 2009). Direct linear transformation of the 2D marker coordinates from two or more

synchronized cameras allows for the output of 3D marker coordinates in the GCS using the assumption that a marker's 2D coordinates in two or more different camera coordinate systems are linearly related to the marker's 3D position in the GCS (Adbel-Aziz and Karara, 1971).
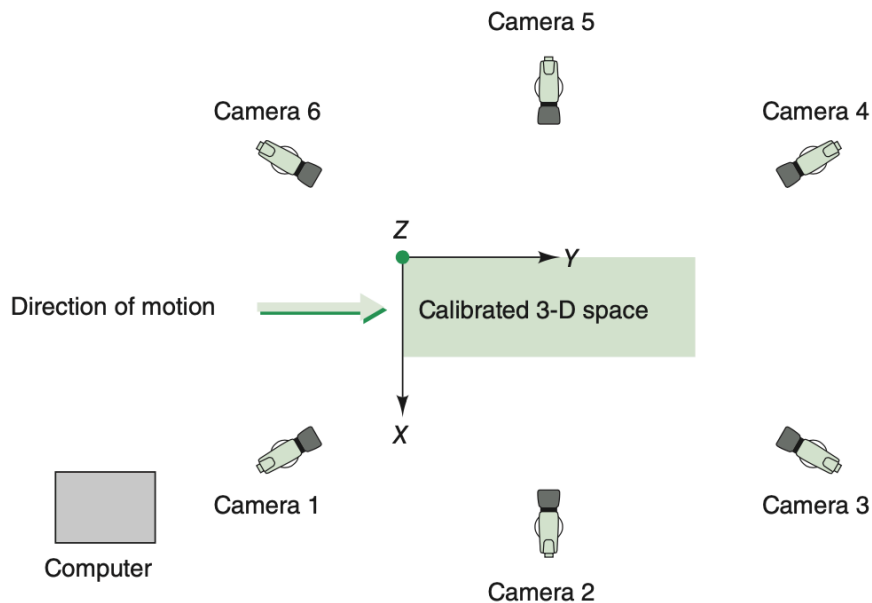
Figure 14. *An arrangement of six motion capture cameras around the periphery of the capture volume. Reproduced from Robertson et al. (2013).*

Although several methods have been proposed to estimate the total body COM from a force plate to reduce the cost and time associated with data collection and processing, these methods only allow for estimation of COM in one dimension (Lafond et al., 2004). In contrast, the segmentation technique, which is based upon the definition of COM, uses motion capture analysis to allow for COM estimation in 3D (Winter, 2009). Time-series position data collected during motion capture analysis can be paired with anthropometric models and measurements to estimate total body COM using the segmentation method. The equation for calculating COM is shown in section 4.7.4.

The mean absolute error in the anthropometric measurements required for the segmentation method were shown to range from 1.9-7.4 mm (Hasan et al., 1996a). Accurate marker placement on anatomical landmarks and validity of the anthropometric model(s) for the study population are important factors in the accuracy of the segmentation method (Lafond et al., 2004). Motion capture sampling rates are typically greater than 20 Hz for analysis of quiet stance, and recommended low-pass filter cut-off frequencies range from 1.5-5 Hz based on residual analysis (Corriveau et al., 2000; Gage et al., 2004; Hasan et al., 1996b, 1996a).

2.6   Balance in Acromegaly

2.6.1   Balance Confidence and Falls

Balance confidence scales are valid and reliable measures of fear of falling, which can predict fall risk in various populations (Menezes et al., 2020; Peretz et al., 2006; Schepens et al., 2010; Tsang et al., 2022). Previous studies have shown significantly reduced balance confidence in PWA compared to PNA (Title et al., 2023) and healthy controls (Atmaca et al., 2013). In contrast, a study of older adult PWA ($\geq$ 60 years) found no decrease in balance self-confidence compared to healthy older adults; however, this may partially be explained by a smaller sample size compared to the previously mentioned studies (Homem et al., 2017).

In PWA, hip functional disability predicted low balance confidence, while older age, female sex, and poor foot and ankle function were predictors of reduced balance confidence in both PWA and PNA (Title et al., 2023). Additionally, lower balance confidence was a predictor of poorer performance on the Berg balance scale, which is a functional balance test that predicts fall risk (Atmaca et al., 2013). Higher age, more falls

in the past year, increased depression and anxiety scores, longer 50-meter walk duration, and shorter one-leg stance duration were also correlated with reduced balance confidence in PWA. These findings suggest relationships between balance self-confidence, physical function, balance performance, and falls in PWA.

Although there was no difference in the number of falls between PWA and PNA (Title et al., 2023) or healthy controls (Atmaca et al., 2013), PWA experienced twice as many falls as Canadian older adults (Title et al., 2023). Additionally, it is possible that falls may not have occurred yet as balance confidence scales have been shown to predict future falls (Tsang et al., 2022).

2.6.2 Laboratory Assessment of Standing Balance Control

Few studies have performed laboratory assessment of balance control in PWA (Haliloglu et al., 2019; Homem et al., 2017; Lopes et al., 2014; Sendur et al., 2019). Lopes and colleagues (2014) found significant differences between PWA and healthy controls of similar age, sex, and BMI in the EO, feet apart condition. These differences were found in both AP and ML axes for the SD and range of COP displacement and in scalar measurements of COP mean speed, COP length, and elliptical and rectangular areas of COP. However, in the EC, feet together condition, the COP length, speed, and AP displacement parameters were no longer significantly different between groups.

When examining an older adult cohort of PWA and healthy controls, Homem et al. (2017) found differences in ML COP range between groups, and these differences were apparent in both EO, feet apart and EC, feet together conditions. No differences between groups in AP balance measures were indicated for either condition.

Haliloglu and colleagues (2019) compared several COP parameters between PWA and healthy controls in bipedal stance with EO and EC and unipedal stance with EO. Unlike previously mentioned studies, stance width was not narrowed in the bipedal EC condition. The significant variables found during bipedal stance were AP COP displacement in the EO condition and ML COP mean velocity in the EC condition. In unipedal stance, AP COP displacement was significantly different between groups for the left foot, while a significant difference between groups in ML COP displacement was found for the right foot.

In contrast with all other studies, Sendur et al. (2019) found no difference in COP displacement between PWA and healthy controls; however, their study was limited by the use of pressure sensing insoles, which have been shown to have poor agreement with force plate measurements of COP, especially in the ML direction (Chesnin et al., 2000; Chevalier et al., 2010; DeBerardinis et al., 2020; Oerbekke et al., 2017). Furthermore, the mean vGRF measured from static analysis in this study appears to be inaccurate based on the reported mean body weight of participants. It is not possible for the vGRF to be greater than 1.3 times body weight during a static measurement; therefore, this study likely contains methodological flaws.

2.6.3   Potential Mechanisms of Balance Impairment in Acromegaly

Several complications of acromegaly may be involved in balance control. Features of arthropathy such as joint pain and widened joint spaces have often been the focus of balance control studies in PWA. In other clinical populations such as chronic low back pain and OA, pain is associated with abnormal balance control in both young and older adults and in both bipedal and unipedal stance (Caffaro et al., 2014; Da Silva et al., 2018, 2016; Della Volpe et al., 2006; Hassan, 2001; Hirata et al., 2019; Lafond et al., 2009). More

difficult sensory conditions, such as compliant surfaces and closing the eyes, have been shown to increase stiffness and decrease sway in patients with symptomatic knee OA (Hirata et al., 2019). In patients with chronic low back pain, prolonged standing for 30 minutes increased postural sway compared to healthy controls, while a shorter stance duration of 60 seconds revealed reduced sway compared to controls (Lafond et al., 2009). Researchers have attributed decreased lumbar proprioception and increased activation of low back muscles to an impaired hip loading mechanism and greater stiffness in patients with low back pain (Mok et al., 2004). Therefore, the joint pain experienced by PWA may contribute to impaired balance control. Additionally, PWA often undergo joint surgeries, including hip and knee replacements (Title et al., 2023). Hip joint surgery has been shown to alter balance control, with total hip arthroplasty possibly relating to an impaired hip loading and unloading mechanism (Rougier et al., 2008).

Peripheral nerve dysfunction is common in PWA and has been shown to delay nerve conduction and reduce action potential amplitudes of sensory and motor nerves that supply the lower extremities (Alibas et al., 2017; Jamal et al., 1987; Low et al., 1974; Ozata et al., 1997). Somatosensory function of the foot and ankle may be impaired as PWA have been found to present with absent ankle reflexes and impaired thermal and vibration sensation at the ankle and tarsal bone (Jamal et al., 1987). Furthermore, plantar cutaneous sensation could be affected by increased skin and heel pad thickness on the plantar surface of the foot (Gonticas et al., 1969; Kho et al., 1970; Ozturk Gokce et al., 2020; Steinbach and Russell, 1964). Therefore, diminished or delayed sensory feedback and muscular responses related to peripheral neuropathy in PWA could contribute to impaired balance control.

Standing balance may also be affected by the reduction in quadriceps and hamstring strength and endurance in PWA (Guedes da Silva et al., 2013; Homem et al., 2017; Khaleeli

et al., 1984; Walchan et al., 2016), which may be partially related to peripheral neuropathy, but also could be influenced by the changes to muscle size and structure (Mastaglia et al., 1970; Nagulesparen et al., 1976); joint pain (Biermasz et al., 2005; Pelsma et al., 2022; Scarpa et al., 2004; Title et al., 2023; Wassenaar et al., 2010); and enthesopathy (Bluestone et al., 1971; Podgorski et al., 1988).

Visual field defects often occur in PWA due to the adenoma compressing the optic chiasm (Kan et al., 2013; Ogra et al., 2014; Rivoal et al., 2000). Although visual field defects are often resolved following transsphenoidal surgery, in some cases they may persist or worsen (Butenschoen et al., 2021; Castle-Kirszbaum et al., 2022; Cohen et al., 1985; Müslüman et al., 2011; Powell, 1995). Vision plays a significant role in the sensory control of standing balance (Bednarczuk et al., 2021; Friedrich et al., 2008; Horak and Macpherson, 1996; Nashner and Berthoz, 1978), and visual field defects are associated with increased risk of falls (Freeman et al., 2007; Hong et al., 2014; Ivers et al., 1998).

Additionally, PWA may take nonsteroidal anti-inflammatory drugs or opioids to manage joint pain and may be prescribed anti-hypertensive medication due to elevated rates of hypertension in PWA (Katznelson et al., 2014; Mosca et al., 2013). Opioids, anti-inflammatory drugs, and anti-hypertensive medications, such as calcium channel blockers, have been shown to increase risk of falls (Juraschek et al., 2019; Kosk et al., 1996; Virnes et al., 2022; Woolcott, 2009). Finally, obstructive sleep apnea is a common comorbidity in PWA (Parolin et al., 2020; Wennberg et al., 2019). Obstructive sleep apnea increases the risk of falls (Stevens et al., 2020), and a few studies have shown impaired balance control in patients with obstructive sleep apnea (Degache et al., 2016; Micarelli et al., 2017; Yilmaz Gokmen et al., 2021).

The significant difference in ML COP measures but not in AP COP measures between PWA and healthy controls during EC conditions suggests that the absence of vision may highlight impairments in ML balance control in PWA. As ML standing balance is primarily controlled by the muscles of the hip (Day et al., 1993; Winter et al., 1996, 1993) and evidence of pathology, symptomology, and functional impairments of the hip are well-established in PWA (Johanson et al., 1983; Title et al., 2023; Wassenaar et al., 2009b), it is probable that changes to hip joint structure and function in PWA may contribute to impaired ML control of balance. Furthermore, hip function has been shown to be a significant predictor of balance confidence in PWA (Title et al., 2023). Sagittal plane postural abnormalities in PWA, including thoracic kyphosis, lumbar lordosis, and pelvic tilt (Bluestone et al., 1971; Cellini et al., 2021; de Azevedo Oliveira et al., 2019; Lopes et al., 2014; Podgorski et al., 1988; Scarpa et al., 2004), could contribute to altered hip mechanics during stance.

However, in two of the previously mentioned studies, stance width was simultaneously manipulated with vision (Homem et al., 2017; Lopes et al., 2014). A narrower stance width would be expected to require greater contribution of the hip flexors and extensors in the AP axis and ankle evertors and inverters in ML axis (Åberg et al., 2011; Winter et al., 1996); therefore, the increased ML sway in PWA in the narrow stance EC condition may be explained by ankle invertor/evertor dysfunction in PWA. Dysfunction of the ankle invertors and evertors could be related to decreased motor nerve conduction velocities and action potentials of the common peroneal nerve as well as reduced sensory nerve conduction and action potentials of the sural nerve in PWA (Jamal et al., 1987; Ozata et al., 1997).

AP COP displacement and COP speed appear similar between PWA and healthy controls for the EO condition in studies that controlled for visual impairment through exclusion criteria (Haliloglu et al., 2019; Homem et al., 2017) and in the EC condition in all three studies (Haliloglu et al., 2019; Homem et al., 2017; Lopes et al., 2014), which suggests a potential influence of vision on balance control in PWA. To further explore the effect of vision on balance control in PWA, stance width should be kept constant between EO and EC conditions.

Based on these findings, PWA have impaired standing balance control compared to healthy participants, especially in the ML direction, which could indicate a mechanism related to impaired frontal plane hip or ankle mechanics. When vision is controlled, AP balance appears to be similar between PWA and healthy controls, suggesting the possibility of a visual mechanism. However, the methodologies of previous studies failed to control for the effects of the adenoma and provided limited insight into the mechanisms of balance impairment in PWA.

Chapter 3: Specific Aim

3.1   Specific Aim

PWA experience balance dysfunction and low balance confidence; however, potential mechanisms of balance dysfunction in PWA have not been examined. Clinical evidence of radiographic and symptomatic arthropathy, abnormal muscle structure and function, peripheral nerve dysfunction, and bone overgrowth are well-documented in PWA and have the potential to influence balance control. While many of these changes to musculoskeletal and nervous tissue are proposed to be mediated by excess GH- and IGF-1 during the time of active acromegaly, mass effects of the pituitary adenoma or pituitary adenoma removal surgery have not been ruled out as a mechanism of balance impairment. For example, compression effects of the pituitary adenoma may result in visual field defects, which are often but not always resolved post-adenoma removal surgery.

Poor standing balance control and low balance confidence are associated with increased risk of falls and fall-related injuries. While PWA have been shown to have reduced balance confidence compared to PNA, previous studies that identified standing balance impairments in PWA have used healthy controls and, thus, have failed to control for effects of the pituitary adenoma and adenoma removal surgery. **Therefore, the specific aim of the present study was to establish if acromegaly modifies standing balance control.** To control for the adenoma-related effects and, therefore, isolate the effects specific to acromegaly, a sample of PNA were selected for the control group.

3.2   Hypotheses

To address the specific aim, the present study manipulated the effect of vision and controlled for the effects of the pituitary adenoma through a control group of PNA, while

selecting outcome variables that provided insight into different aspects of standing balance performance and control (see Table 1, Section 4.9).

Regarding balance performance outcome measures, it was hypothesized that there would be a significant interaction effect of acromegaly and vision on standing balance, such that PWA would have a greater increase in COP 95% PEA and a greater decrease in unipedal stance time than PNA in EC compared to EO. Significant main effects of group and vision were hypothesized such that PWA would exhibit a larger COP 95% PEA and shorter unipedal stance time than PNA and that the EC condition would reveal a larger COP 95% PEA and shorter unipedal stance time than the EO condition.

For uniaxial balance performance, it was hypothesized that PWA would have a greater increase in both AP and ML COP range than PNA in EC compared to EO. COP range was hypothesized to be larger in PWA than PNA and in EC compared to EO in both the AP and ML axes.

It was hypothesized that there would be a significant interaction effect of acromegaly and vision on outcome measures of balance control. AP and ML COP mean velocity; COP MPF; and the cross-correlation, time lag, and mean absolute deviation of COP and COM were all hypothesized to increase to a greater extent for PWA than PNA with EC compared to EO. It was also hypothesized that PWA would exhibit worse balance control (larger outcome measures) than PNA and that the balance control outcome measures would increase in the EC condition compared to the EO condition.

Chapter 4: Methods

4.1 Ethics

The study protocol received approval from the Nova Scotia Health Authority and Western Ontario University Health Sciences Research Ethics Boards (NSHA REB ROMEO, File no. 1025532; UWO HSREB, File no. 119246). All participants provided written informed consent prior to data collection. The consent form is located in Appendix A.

4.2 Participants

4.2.1 Recruitment

Participants were recruited from the Halifax Neuropituitary Program for a two-part study. While completing the survey portion of the project (Part 1), participants had the option to consent to participate in the biomechanical laboratory assessment (Part 2). Twelve PWA and 11 PNA (control group) who provided consent were selected to participate in Part 2 of the study. The participants were selected based on the inclusion and exclusion criteria outlined in section 4.2.2, residence in Nova Scotia, ability to travel to Halifax for data collection, and similar ranges of age, sex, and BMI within each group.

4.2.2 Inclusion and Exclusion Criteria

The inclusion criteria for the study were a diagnosis of either acromegaly (PWA group) or a non-functioning pituitary adenoma (PNA group). Participants were excluded if they had inflammatory arthritis, neurological or vestibular disorders, significant orthostasis, drug or alcohol abuse, amputations, weight change greater than 5% of their body weight over the past 12 months, or inability to ambulate.

4.3 Research Design

The present study used a quasi-experimental design to assess the interaction effect of acromegaly and vision on standing balance. For the between-subjects factor, participants were assigned to the PWA or PNA group based on a prior diagnosis of acromegaly or non-functioning pituitary adenoma. The within-subjects factor, vision, was manipulated via repetition of each trial with EO and EC. The interaction effect of acromegaly and vision on the balance outcomes was analyzed. Task difficulty was also manipulated through the use of bipedal and unipedal stance trials; however, this factor could not be included in the statistical model due to low sample sizes for unipedal stance, especially for the EC trial.

The original proposed study planned to match PWA and PNA by age, sex, and BMI, allowing for the use of a repeated measures model. The repeated measures model would have increased statistical power; however, recruiting an adequate sample size of matched pairs was not possible. Additionally, a missing data point for one participant meant that the matched participant also had to be excluded from the analysis. Therefore, the decision was made to no longer match the groups and instead recruit participants with similar age, sex, and BMI across groups to allow for a larger sample size. The larger sample helped to counterbalance the loss of power from switching to a mixed model.

4.4 Experimental Protocol

Each participant visited the laboratory on one occasion for data collection. The experimental procedure described in this section includes the first and third steps of the procedure for the larger study (Figure 15).
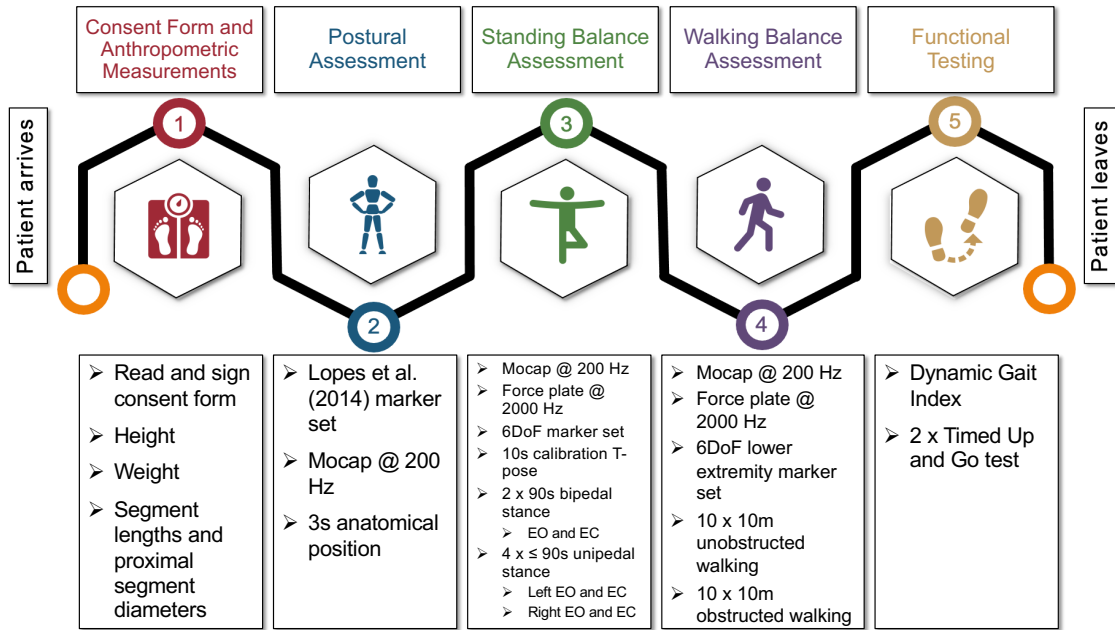
Figure 15. Experimental procedure of the larger study. Steps 1 and 3 are relevant to the proposed study.

Upon arrival, participants reviewed and signed the consent form. Participants were asked to wear tight clothing, preferably shorts and a sleeveless shirt, to enable accurate marker placement.

The participants' weight and height were recorded without shoes, while wearing the same clothing worn during the balance assessment. Lower extremity segment lengths and proximal segment diameters were also collected (see data collection sheet in Appendix B for list of anthropometric measurements).

Retroreflective markers were placed on the participants according to the six degrees of freedom (6DOF) marker set for the lower body, and additional markers were placed to define the segments of the upper body. Ten rigid bodies, each containing four non-collinear markers, were placed on the posterior head, posterior trunk, and lateral portion of the left and right thigh, shank, upper arm, and forearm. Thirty-six retroreflective markers were placed on the following anatomical landmarks on the left and right sides: temporal process,

acromion process, lateral and medial humeral epicondyles, radial and ulnar styloid processes, second and fifth metacarpal heads, anterior and posterior superior iliac spines, lateral and medial femoral epicondyles, lateral and medial malleoli, calcaneal tuberosity, first and fifth metatarsal heads, and distal hallux (Figure 16 and 17).
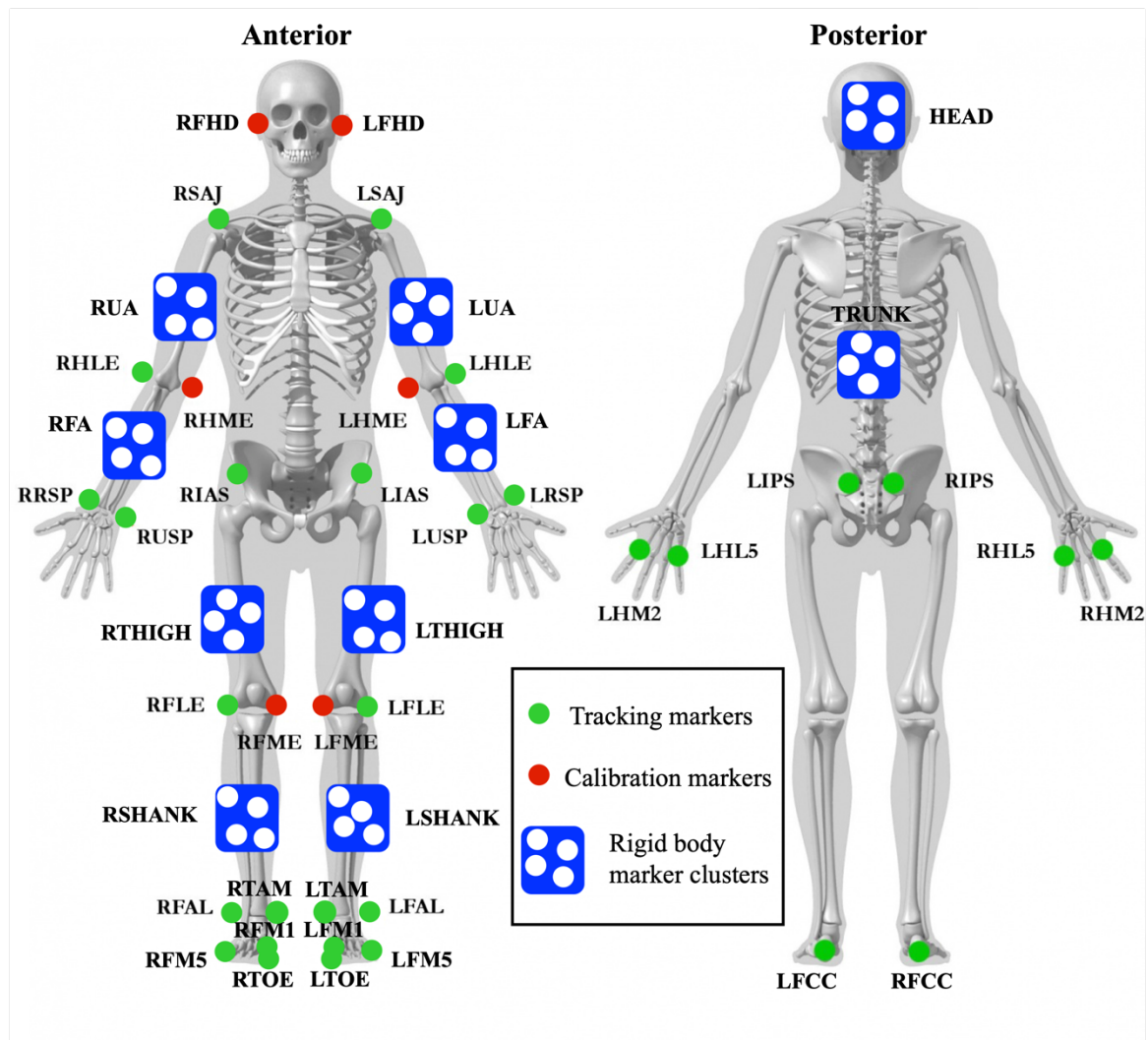
*Figure 16. Diagram of 6DOF marker set. **Anterior view from superior to inferior:** RFHD/LFHD, Right/left temporal process; RSAJ/LSAJ, Right/left acromion process; R/LUA, Right/left upper arm rigid body marker cluster; TRUNK, Trunk rigid body marker cluster; R/LHLE, Right/left humeral lateral epicondyle; R/LHME, Right/left humeral medial epicondyle; R/LFA, Right/left forearm rigid body marker cluster; R/LIAS, Right/left anterior superior iliac spine; R/LRSP, Right/left radial styloid process; R/LUSP, Right/left ulnar styloid process; R/LTHIGH, Right/left thigh rigid body marker cluster; R/LFLE, Right/left femoral lateral epicondyle; R/LFME, Right/left femoral medial epicondyle; R/LSHANK, Right/left shank rigid body marker cluster; R/LFAL, Right/left lateral*

*malleolus; R/LTAM, Right/left medial malleolus; R/LFM5, Right/left 5th metatarsal head; R/LFM1, Right/left 1st metatarsal head; R/LTOE, Right/left distal hallux. **Posterior view from superior to inferior:** HEAD, Head rigid body marker cluster; R/LIPS, Right/left posterior superior iliac spine; R/LHM5, Right/left 5th metacarpal head; R/LHM2, Right/left 2nd metacarpal head; R/LFC, Right/left aspect of Achilles tendon insertion on calcaneus.*

Anterior	**Posterior**	**Lateral**
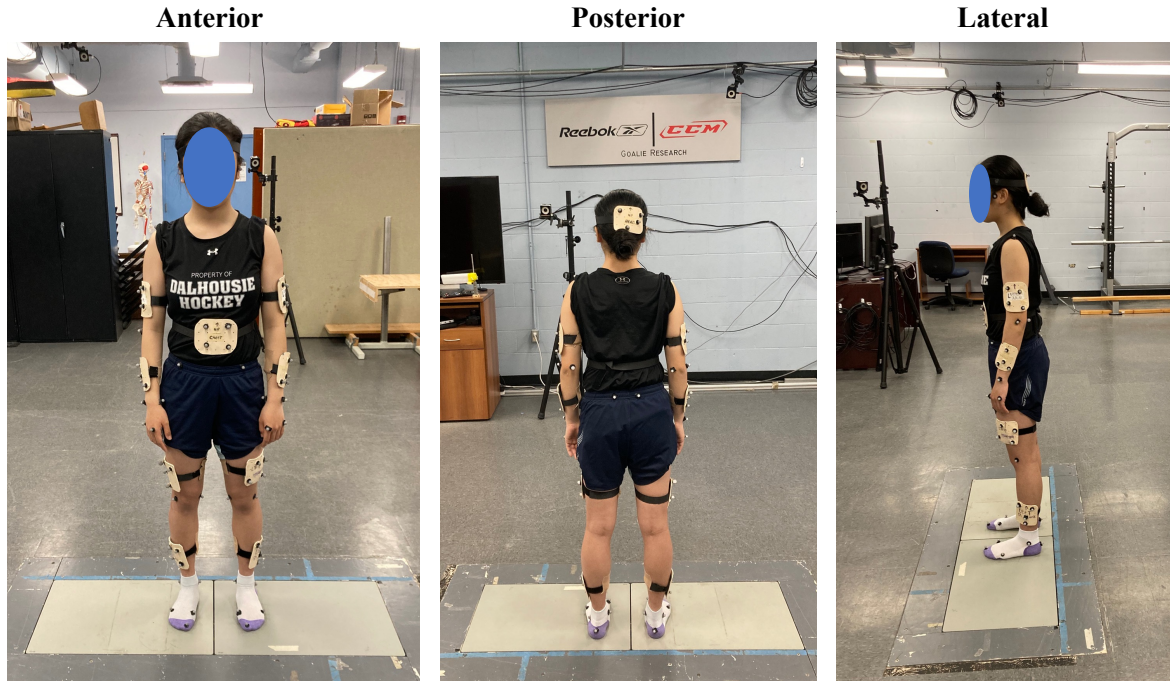
Figure 17. *Markers and rigid bodies according to the 6DOF marker set.*

The following experimental procedure is shown in Figure 18. A calibration trial was carried out for 10 seconds in T-pose with both the tracking markers and rigid bodies (Figure 16: green markers and blue rigid bodies) and the calibration markers (Figure 16: red markers). For the balance trials, all calibration markers were removed.

Six different balance conditions were tested: bipedal stance EO, bipedal stance EC, unipedal stance EO (left and right sides), and unipedal stance EC (left and right sides). Each bipedal trial had a 90-second duration, while unipedal trials had a maximum duration of 90 seconds and were terminated prior to 90 seconds if the participant touched their non-

supporting foot down to the floor or placed their hand on a support surface positioned at hand-height in front of the participant.

For the bipedal stance trials, the participants were instructed to stand with one foot on each force plate, with feet parallel and hip width apart. Their arms were placed by their side to emulate their natural stance. The participant was instructed to stand as still as possible for 90 seconds, with EO for the first trial and EC for the second trial. The participant was provided a countdown to initiate the start of each trial.

For the unipedal trials, the participant began with both feet on the ground (one foot on each force plate) and arms positioned by their side. At the end of the countdown, they were asked to lift the non-supporting leg off the force plate. Participants were allowed to move their arms during the unipedal stance trials to help maintain balance. If the participant felt as though they were going to lose balance, they were instructed to place their non-supporting foot on the force place and/or hand on the support surface in front of them. The first unipedal trial was performed with EO and the left foot supporting their body mass. The second unipedal EO trial switched to the right foot as the supporting limb. The third and fourth unipedal trials were performed with EC, first with the left foot and then the right foot as the supporting limb. Any trials with a duration of less than 5 seconds were excluded from the analysis.
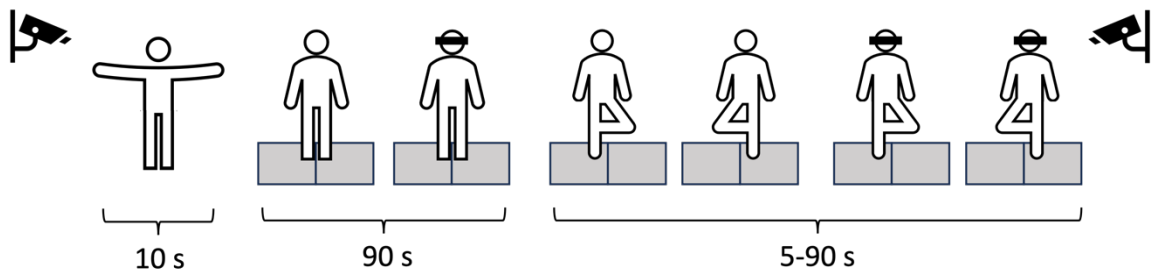
Figure 18. Experimental procedure for the standing balance assessment

4.5   Instrumentation

4.5.1   Motion Capture System

Kinematic analysis of standing balance was performed using a 14-camera OptiTrack motion capture system (OptiTrack, NaturalPoint, Inc., OR, USA) at a sampling frequency of 200 Hz. One camera from the motion capture system was used to capture video, while the remaining 13 cameras collected marker position data. Motive software (version 2.1.1, NaturalPoint, Inc., OR, USA) was used for both data acquisition and post-collection marker labelling.

4.5.2   Force Plate System

Two AMTI multi-axis strain gauge force plates (OR6-5-2000, Advanced Mechanical Technology, Inc., MA, USA) were used to collect kinetic data at a sampling frequency of 2000 Hz. The two force plates were contiguous and built into the floor, located at approximately the centre of the motion capture volume (Figure 19). Mr. Kick data acquisition software was used to acquire the force plate signals and export raw force plate signals as a MATLAB data file. Force plate acquisition was switched to custom MATLAB software for later participants. The two force plate amplifiers (MiniAmp MSA-6, Advanced Mechanical Technology, Inc., MA, USA) provided ± 10 V excitation voltage to the force plates and 1000x gain to each force plate channel.

69

Figure 19. *Location of the two force places within the motion capture volume*

4.5.3   Motion Capture and Force Plate Synchronization

The analog signals from each force plate were synchronized with the motion capture system using the eSync 2 (NaturalPoint, Inc., OR, USA) synchronization hub. The 12 analog force plate channels (six channels per force plate) were connected to a BNC connector box (BNC-2090A, National Instruments Corporation, TX, USA), which was wired to a PCIe DAQ device (PCIe-6321, National Instruments Corporation, TX, USA) that was interfaced with the motherboard of the computer that contained the Mr. Kick data acquisition software. The PCIe device contained a 16-bit analog-to-digital converter (ADC), which digitized the analog force plate signals. The BNC connector box was connected to the 'Isolated Sync In' port on the eSync 2 synchronization hub, while the motion capture cameras were connected to the ethernet switch, from which an ethernet cable was connected to the eSync 2 device. To connect the cameras to the computer that contains Motive software, another ethernet cable extended from the ethernet switch to the computer. Figure 20 displays the motion capture and force plate synchronization set-up. For later data collections, the BNC connector box and PCIe DAQ device were replaced with two 16-bit ADCs (USB-6341, National Instruments Corporation, TX, USA) that were connected to the computer containing the custom MATLAB force plate acquisition software (Figure 21).
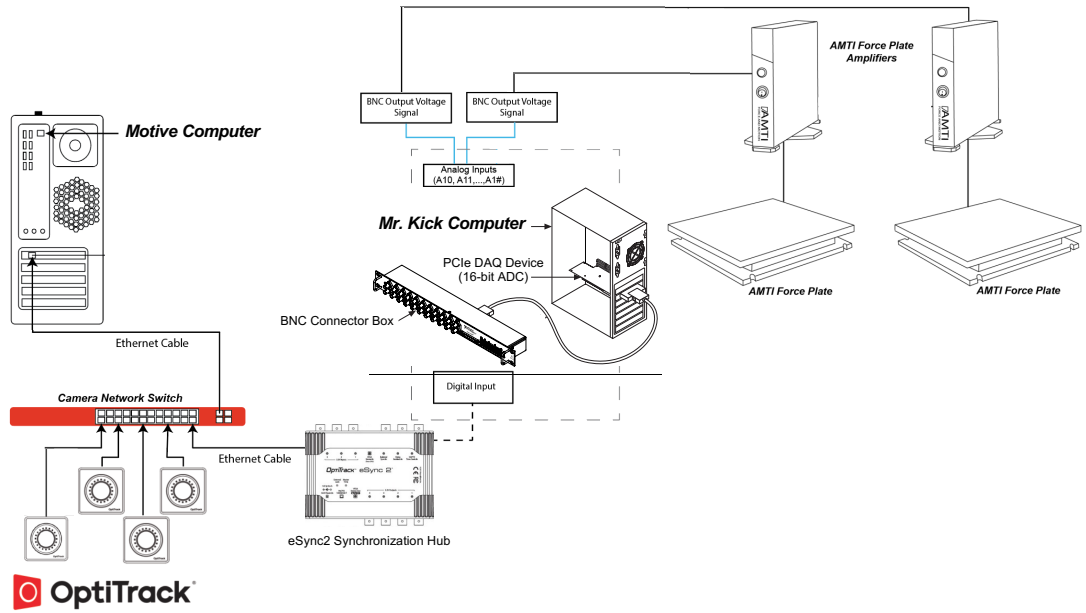
Figure 20. *Schematic of the original motion capture and force plate synchronization set-up. Adapted from OptiTrack Documentation (NaturalPoint, Inc., OR, USA)*
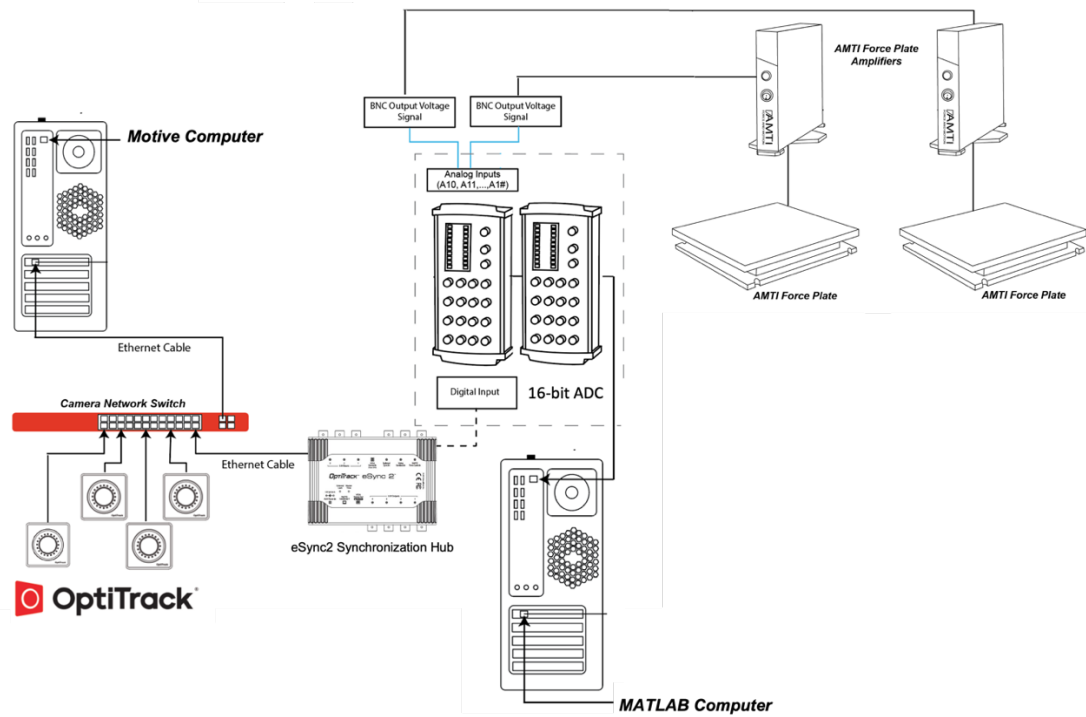
Figure 21. *Schematic of the modified motion capture and force plate synchronization set-up. Adapted from OptiTrack Documentation (NaturalPoint, Inc., OR, USA)*

71

4.6   Anthropometry

The participants' height, weight, and lower extremity segment lengths and proximal diameters were collected at the beginning of the data collection session and were used in conjunction with anthropometric models to estimate the inertial properties of the body segments (see data collection sheet in Appendix B). Dempster's (1955) regression equations were used to estimate the mass of each segment. The 3D position of each segment COM was estimated using Hanavan's (1964) geometric model.

4.7   Kinematic Data Processing

4.7.1   Signal Processing of Kinematic Data

Missing data points in the marker trajectories were interpolated via cubic spline. The marker trajectories were then filtered using a 4th order, 6 Hz, zero-phase lag, low-pass Butterworth filter to attenuate noise at frequencies above 6 Hz.

4.7.2   Six Degrees of Freedom Model

The 6DOF marker set was selected to allow independent tracking of each segment and 6DOF at each joint. The principle of 6DOF is that the pose of each segment is defined by six variables, three coordinates that describe the segment origin and three vectors that describe its rotation about the axes of the segment coordinate system (SCS). The 6DOF marker set includes calibration markers that are placed on bony landmarks during the static trial but removed during the movement trials and rigid body marker clusters placed on each segment for segment tracking during movement trials. As seen in Figure 16, the green markers and blue rigid body marker clusters were used for both segment definition and tracking, while the red markers were used only for segment definition during the calibration trial. In the present study, each rigid body marker cluster contained four non-collinear

markers as recommended by Cappozzo et al. (1997). Segment tracking requires a minimum of three tracking markers; therefore, a 4-marker rigid body allows for segment tracking even if one marker on the rigid body becomes occluded. Since rigid body marker clusters can be placed anywhere on the segment, they can be placed on the lateral portion of the segment to prevent marker occlusion that typically occurs with medially placed tracking markers (Żuk and Pezowicz, 2015). Additionally, rigid body markers can be placed in locations that experience less soft-tissue artifact (i.e., tracking markers can be placed where there is less skin movement relative to the underlying bone), which is typically the distal portion of the limb segments (Cappozzo et al., 1996; Manal et al., 2000). Studies have shown comparable accuracy of the 6DOF marker set when compared to the conventional gait model marker set and high reliability of the 6DOF marker set (Collins et al., 2009; Żuk and Pezowicz, 2015). Additionally, construct validity is greater in the 6DOF marker set compared to the conventional gait model due to independence of segments and the absence of joint constraints (Collins et al., 2009).

4.7.3 Defining Segment Coordinate Systems

Kinematic data analysis began by defining the segment coordinate system (SCS) for the head and neck, trunk, pelvis, and the left and right upper arm, forearm, hand, thigh, shank, and foot. The calibration trial marker positions were used to calculate the origin and rotation matrix for each segment, which are required to transform marker positions from the GCS to the SCS. The origin of each segment was defined at the proximal end of the segment at the joint centre. For the trunk, the proximal segment end was defined by its attachment with the pelvis. The SCS for the pelvis and right thigh, shank, and foot were defined according to the equations outlined by Robertson and colleagues (2013). The left-

sided calculations were performed similarly to the right-sided equations; however, the direction of unit vector $\hat{v}$ was reversed by subtracting the markers in the opposite order. The pelvis segment was modeled as the CODA pelvis, and the hip joint centre was first calculated relative to the pelvis SCS using the regression equations derived by Bell et al. (1989). To define the proximal end of the trunk, the left and right iliac crest landmarks were estimated using equations derived from anthropometric data in the Terry Database (Kepple et al., 1997; Rab et al., 2002). The shoulder joint centre was estimated relative to the acromion marker as a fraction of the distance between left and right acromion markers (Rab et al., 2002). Sample calculations for defining the origins and rotation matrices of the pelvis and right thigh SCS can be found in Appendix C.

4.7.4 Pose Estimation using Segment Optimization Method

A segment optimization procedure was used for pose estimation. Segment optimization, also termed the 6DOF method, estimates the pose of a segment using at least three non-collinear tracking markers that are assumed to be located rigidly on the segment at a fixed position in the SCS (Lu and O'Connor, 1999; Spoor and Veldpaus, 1980). It is termed the 6DOF method as it defines the pose of the segment through six variables which include the three coordinates that describe its origin (translation from GCS to SCS) and the three vectors that describe its rotation about the axes of the SCS. Segment optimization is often preferred over direct methods of pose estimation as segment optimization tracks each segment independently, while direct methods model the segment based on the joint centre locations estimated from markers at the proximal joint. Therefore, when using direct methods of pose estimation, errors at proximal segments can propagate down the chain as each distal SCS is computed (Buczek et al., 2010; Schmitz et al., 2016; Stagni et al., 2000).

Segment optimization does not place any constraints on the joints that connect adjacent segments and thus segments can move independently of one another based on the joint motion detected in the motion capture collection. Although global optimization procedures that use joint constraints may reduce soft-tissue artifacts and other sources of error to a greater extent than segment optimization in healthy populations, the joint constraints used in global optimization may mask pathological joint motion. Therefore, due to known joint pathology including widened joint spaces, hypertrophied cartilage, osteophytosis, and increased ligament laxity in PWA, segment optimization was selected over global optimization for this study.

Segment optimization uses the least squares approach to estimate the pose of a segment (Robertson et al., 2013; Spoor and Veldpaus, 1980). The known parameters in the least squares model include the location of the three or more tracking markers in the SCS determined from calibration trial marker positions (see section 4.7.3 and Appendix C) and the position of the tracking markers in the GCS measured by the motion capture system during the balance trials. Therefore, for each frame captured by the motion capture system, the origin (translational vector) and rotation matrix defining the orientation of the SCS in the GCS must be solved for. The goal of the optimization procedure is to minimize the sum of squares error expression to diminish the effect of noise or artifact on pose estimation. Additionally, the vectors in the 3x3 rotation matrix must be orthogonal; therefore, an orthonormal constraint is applied to the problem. This constrained optimization problem has infinite solutions for the origin and rotation matrix; therefore, the Lagrange multiplier technique is used to obtain a unique solution.

4.7.5   Centre of Mass

The 3D position of total body COM was determined by the segmentation method, which is the weighted average of the COM location of 14 body segments (head, trunk, and left and right upper arm, forearm, hand, thigh, shank, and foot). The mass of each segment was determined by Dempster's (1955) segment mass ratios. The position of each segment's COM was determined using anatomical landmark positions and equations from Hanavan's (1964) geometric model of the human body. The x and y coordinates of the COM position were determined by the sum of the products of each segment's COM position and mass divided by total body mass:

$$\text{COM}(x) = \frac{1}{M}\sum_{i=1}^{14}\text{COM}_i(x)m_i \tag{5}$$

$$\text{COM}(y) = \frac{1}{M}\sum_{i=1}^{14}\text{COM}_i(y)m_i$$

where M is the total body mass, COM_i is the position of the ith segment, and m_i is the mass of the ith segment.

4.7.6   Error Detection and Correction within the Centre of Mass Signals

All further reduction of kinematic data was performed in MATLAB.

Despite efforts to correct marker label assignment errors using the labelling functions within the motion capture software, some instances of extreme spikes were observed when plotting the time-series COM signals. Therefore, a code was written in MATLAB to detect any frames in the signal where the marker jumped more than 5 mm from the position in the previous frame (velocity > 1 m/s). If the previous frame had a missing value, the position in the current frame was compared to the position up to 10

frames prior (velocity > 0.1 m/s). If the value was determined to exceed these thresholds, the frame was deleted. Any missing frames were then interpolated using a cubic spline.

4.7.7 Translation of Centre of Mass

The COM trajectory was translated from the GCS to the origin defined by the projection of the ankle position vector onto the support surface. The ankle position vector was defined as the position vector from the GCS to the midpoint of the two ankle joint centres for bipedal trials, the left ankle joint centre for left foot unipedal trials, and the right ankle joint centre for right foot unipedal trials. The projection of the ankle position vector onto the support surface was calculated by taking the difference between the ankle position vector and the projection of the ankle position vector onto the support surface normal vector:

$$proj_{SS}(\vec{a}) = \vec{a} - proj_{\vec{n}}(\vec{a}) = \vec{a} - (\vec{a} \cdot \hat{n})\hat{n} = \vec{a} - a_z\hat{n} \qquad (6)$$

where $proj_{SS}(\vec{a})$ is the projection of the ankle position vector onto the support surface, $proj_{\vec{n}}(\vec{a})$ is the projection of the ankle position vector onto the support surface normal vector, $\vec{a}$ is the ankle position vector, and $\hat{n}$ is the unit vector of the support surface normal vector.

The projection of the ankle position vector onto the support surface normal vector describes a vector parallel to the support surface normal vector, with a magnitude and directional sign given by the dot product of the ankle position vector and the unit vector of the support surface normal vector. Since the support surface is located within the x,y-plane of the GCS, the unit vector of the support surface normal vector is the GCS z-axis unit vector, $\hat{k}$=(0,0,1), and the dot product of the ankle position vector and z-axis unit vector is equal to the z-component of the ankle position vector. Therefore, the projection of the ankle

position vector onto the support surface is the difference between the ankle position vector and the product of the GCS z-axis unit vector and the z-component of the ankle position vector (Figure 22).
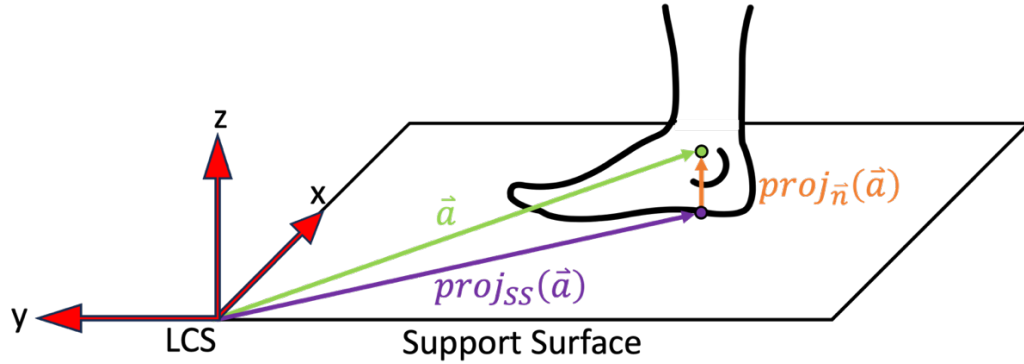
Figure 22. *The projection of the ankle position vector onto the support surface, $proj_{SS}(\vec{a})$, is the difference between the ankle position vector, $\vec{a}$, and projection of the ankle position vector onto the support surface normal vector, $proj_{\vec{n}}(\vec{a})$*

The translation of the COM position vector from the GCS to the origin located at the projection of the ankle position vector onto the support surface was calculated by subtracting the average position vector of the new origin in the GCS from the trajectory of the COM position vector in the GCS:

$$COM_{proj_{SS}(\vec{a})} = COM_{GCS} - \overline{proj_{SS}(\vec{a})_{GCS}} \qquad (7)$$

where $COM_{proj_{SS}(\vec{a})}$ is the COM position vector relative the projection of the ankle position vector onto the support surface, COM_{GCS} is the COM position vector in the GCS, and $\overline{proj_{SS}(\vec{a})_{GCS}}$ is the average position of the projection of the ankle position vector onto the support surface in the GCS.

4.8 Kinetic Data Processing

4.8.1 Zeroing the Kinetic Data

The first 1000 samples were averaged from a trial when the force plate was empty. This value was subtracted from the 12 raw force plate signals for each of the six balance trials to zero the data.

4.8.2 Signal Processing of Kinetic Data

The 12 force plate signals (six from each force plate) were filtered using a 4th order, 6Hz, zero-phase lag, low-pass Butterworth filter. Each force plate signal was down sampled by a factor of 10 from 2000 Hz to 200 Hz to match the sampling frequency of the motion capture data.

4.8.3 Force Plate Signal Conversion

The force plate data was exported from Mr. Kick and imported in Visual 3D. The force plate signals required conversion from mV to N or Nm as well as scaling to adjust for the excitation voltage and amplifier gain. The calibration matrix and true origin (offset) of the force plates were obtained from the manufacturer calibration. The six signals from each of the two force plates were converted from mV to V, multiplied by the transpose of the calibration matrix, and divided by the product of the excitation voltage and the channel gain of the ADC. This process converted the first three channels of each force plate to N (GRF) and the latter three channels of each force plate to Nm (moment of the GRF).

4.8.4 Centre of Pressure Calculation

The COP was calculated for both force plates. To calculate the COP with respect to the centre of the top surface of the force plate, the true origin (offset from the centre of the top surface of the force plate) was obtained from the manufacturer calibration. The z-

coordinate of the COP was assumed to be zero. The x- and y-components of the COP were calculated using the following equations:

$$COP_x = \frac{F_x d_z - M_y}{F_z} \tag{8}$$

$$COP_y = \frac{F_y d_z + M_x}{F_z}$$

where F_x and F_y are the x- and y-components of the GRF with respect to the true origin, M_x and M_y are the x- and y-components of the moment of the GRF about the true origin, and d_z is the vertical offset of the true origin of the force plate.

Since the COP is located on the surface of the force plate, the z-component of the COP was assumed as zero.

4.8.5 Transformation to the Global Coordinate System

The GRF and COP must be transformed from the FPCS to the GCS in order to pair the kinematic and kinetic data. The positions of the four corners of each force plate in the GCS were used to determine the origin and rotation matrix that define each force plate in the GCS. The origin of the force plate in the GCS ($FPOrigin_{GCS}$) was calculated by taking the average position of the four corners of the force plate (C_1, C_2, C_3, and C_4).

$$FPOrigin_{GCS} = 0.25 * (C_1 + C_2 + C_3 + C_4) \tag{9}$$

The rotation matrix was composed of the three orthogonal unit vectors that define the rotation from the GCS to the FPCS. The unit vector $\hat{\imath}$, directed anteriorly across the surface of the force plate, was determined by finding the directional vector from the 3rd to the 4th corner of the force plate and then dividing the vector by its norm.

$$\hat{i} = \frac{(C_4 - C_3)}{|C_4 - C_3|} \tag{10}$$

A unit vector along the surface of the force plate in the lateral direction was calculated by determining the vector from the 3rd to 2nd force plate corners and dividing the vector by its norm.

$$\hat{v} = \frac{(C_2 - C_3)}{|C_2 - C_3|} \tag{11}$$

Next, the cross product of unit vectors $\hat{i}$ and $\hat{v}$ was used to define unit vector $\hat{k}$, which is directed superior and normal to the surface of the force plate.

$$\hat{k} = \hat{i} \times \hat{v} \tag{12}$$

A unit vector, $\hat{j}$, that is orthogonal to unit vectors $\hat{i}$ and $\hat{k}$ and completes the right-handed coordinate system defining the orientation of the force plate was determined by.

$$\hat{j} = \hat{k} \times \hat{i} \tag{13}$$

The unit vectors $\hat{i}$, $\hat{j}$, and $\hat{k}$ were horizontally concatenated to form the matrix R_{FP}, defining the rotation from the GCS to the FPCS.

$$R_{FP} = \begin{bmatrix} \hat{i}_x & \hat{i}_y & \hat{i}_z \\ \hat{j}_x & \hat{j}_y & \hat{j}_z \\ \hat{k}_x & \hat{k}_y & \hat{k}_z \end{bmatrix} \tag{14}$$

The force plate origin in the GCS and transpose of the rotation matrix were used to transform the GRF and COP from the FPCS to the GCS using the following equations, which were performed for each force plate and each trial.

$$GRF_{GCS} = R'_{FP} * GRF_{FPCS} \tag{15}$$

$$COP_{GCS} = R'_{FP} * COP_{FPCS} + FPOrigin_{GCS} \tag{16}$$

81

4.8.6   Calculating Net Centre of Pressure for Bipedal Stance

Measuring bipedal balance using two separate force plates allows for assessment of asymmetries in limb loading. Since asymmetries in balance control were suspected in PWA, a weighted average was used to determine COP_{net} from COP_L and COP_R for both AP and ML directions (Winter et al., 1996, 1993):

$$COP_{net} = COP_L \frac{vGRF_L}{(vGRF_L + vGRF_R)} + COP_R \frac{vGRF_R}{(vGRF_L + vGRF_R)} \tag{3}$$

where $vGRF_L$ and $vGRF_R$ are the vertical GRF acting on the left and right feet, respectively.

4.8.7   Translation of Centre of Pressure

All force plate data reduction beyond this point was performed in MATLAB.

The COP trajectory was translated from the GCS to the coordinate system defined by the projection of the ankle position vector onto the support surface. This was achieved using the same procedure described in section 4.7.7 for the COM trajectory.

4.8.8   Determining Start and End of Unipedal Stance

Many participants were not able to hold unipedal stance for 90 seconds. Therefore, the unipedal stance trials were truncated at the points in time when the foot was lifted off the force plate and when the foot touched back down on the force plate. The video recordings for each trial were scanned frame by frame to visually determine the approximate frame when foot lift-off and foot touchdown (or hand touchdown on a raised surface in front of the participant) occurred. For participants whose hand touched down first or whose foot touched down off the force plate, the visual estimation was used to determine foot touchdown. For all other participants, visual estimation was used only as a reference value.

The vGRF was used to determine foot lift-off and touchdown. Foot lift-off was determined by the first sample when the vGRF was equal to zero, while foot touchdown was defined by the first sample after foot lift-off when the vGRF was greater than zero. All MATLAB derived lift-off and touchdown points were verified with the visually derived points prior to proceeding.

Once these points were determined and verified, the onset of loss of balance was estimated. The following protocol to determine loss of balance was a modified version of the algorithm proposed by Hasan and colleagues (1990). The reference value for balance control in each participant was determined by the interquartile range of the vGRF of the supporting leg over the first half of the duration from foot lift-off to touchdown or the first five seconds if unipedal stance duration was greater than 10 seconds. All samples in the second half of the unipedal stance trial were scanned for the first instance in which the vGRF was greater than the sum or less than the difference of the median vGRF and 1.5 times the interquartile range of the vGRF. Once the onset of loss of balance was determined, the signal was truncated at the point of foot lift-off and the onset of loss of balance, if a loss of balance occurred.

4.9 Primary Outcome Measures

Table 1. Outcome measures

	Characterization of Balance Performance	Characterization of Uniaxial Balance Performance	Characterization of Balance Control
COP time domain	95% prediction ellipse area (cm²)	AP and ML range (cm)	AP and ML mean velocity (cm/s)
COP frequency domain			AP and ML median power frequency (cm)
Relationship between COP and COM			AP and ML mean absolute deviation (cm)
			AP and ML cross-correlation
			AP and ML time lag (ms)
Temporal measure	Unipedal stance time (s)		

4.9.1 Centre of Pressure 95% Prediction Ellipse Area

The COP 95% prediction ellipse area (PEA) is a measure of sway and indicates the variability of the COP position over the course of a balance trial. A larger COP 95% PEA indicates a larger spread of the COP position and thus greater sway during balance.

Several previous studies that calculated COP ellipse area have mistaken a confidence ellipse for a prediction ellipse or used the terms interchangeably; however, these two measures have different computations and interpretations. Schubert and Kirchner (2014) outlined the differences in the calculation and interpretation of the confidence ellipse and prediction ellipse. Although the confidence ellipse and prediction ellipse are both centred at the sample mean, the confidence ellipse contains the true population mean with $100(1-\alpha)$% probability, while the prediction ellipse contains a future observation with

100(1-α)% probability. The calculation of the confidence ellipse area differs from the PEA by a factor of 1/n, meaning that the confidence ellipse is smaller than the prediction ellipse and the confidence ellipse decreases as sample size increases. Since the present study had a sampling frequency of 200 Hz and trial durations of up to 90 seconds, the confidence ellipse would be smaller than the prediction ellipse by a factor of 1/18000 for 90-second trials. Furthermore, the confidence ellipse area would not be appropriate for comparison between trials of different duration, which occurred in the present study since the duration of unipedal stance trials varied depending on how long the participant could maintain unipedal stance. Therefore, the prediction ellipse is most suitable for quantifying the covariation of the AP and ML COP position in the present study.

The 95% PEA was calculated using the methods outlined by Schubert and Kirchner (2014). Principal component analysis was used to obtain the eigenvalues and eigenvectors of the variance-covariance matrix of AP and ML COP time-series data, which indicated the magnitude and direction of the orthogonal axes of the ellipse that best fit the COP data points in the transverse (x,y) plane. The 95% prediction ellipse was approximated using the critical value of the inverse chi-square cumulative distribution function with two degrees of freedom for α=0.05 ($\chi^2_{0.95,2} \approx 5.99$). The length of the semi-major and semi-minor axes of the 95% prediction ellipse were defined as the square root of the product of the chi-square critical value and eigenvalue. The area of an ellipse is calculated by

$$A = \pi a b$$

where a is the length of the semi-major axis and b is the length of the semi-minor axis. The length of the axes in a 95% prediction ellipse are approximated by

$$a \approx \sqrt{\chi^2_{0.95,2} \lambda_1}$$

$$b \approx \sqrt{\chi_{0.95,2}^2 \lambda_2}$$

and therefore, the approximation for the 95% PEA is

$$PEA_{0.95} \approx \pi \sqrt{\chi_{0.95,2}^2 \lambda_1} \sqrt{\chi_{0.95,2}^2 \lambda_2} = \chi_{0.95,2}^2 \pi \sqrt{\lambda_1 \lambda_2} \approx 5.99\pi \sqrt{\lambda_1 \lambda_2} \qquad (17)$$

where $\chi_{0.95,2}^2$ is the critical value of the inverse chi-square cumulative distribution function with two degrees of freedom for $\alpha=0.05$, and λ_1 and λ_2 are the eigen values from the variance-covariance matrix of AP and ML COP.

The COP 95% PEA was shown to have poor test-retest reliability in EO conditions for participants with musculoskeletal disorders, with an intraclass correlation coefficient (ICC) of 0.33; however, the ICC almost doubled in the EC condition (ICC=0.64) (Salavati et al., 2009). The coefficient of variation (CV) indicated a large amount of error between trials for both visual conditions (EO, CV=27.4%; EC, CV=24.4%).

4.9.2 Centre of Pressure Range

The COP range is a commonly used parameter to quantify the sway of the COP in the AP or ML axis. As the control of standing balance involves different mechanisms in the AP versus ML axes, analyzing the COP sway uniaxially may allow for better insights into the mechanisms of balance control for PWA. The COP range along the AP and ML axes were calculated by taking the difference between the maximum and minimum AP components of COP and the maximum and minimum ML components of COP.

Low to moderate ICCs were observed for the intersession reliability of COP range in the AP and ML axes (Lafond et al., 2004). The ICCs increased as the trial duration increased from 30 s (AP, ICC=0.29; ML, ICC=0.44) to 60 s (AP, ICC=0.38; ML, ICC=0.57) to 120 s (AP, ICC=0.52; ML, ICC=0.62). Another study found that COP range

had moderate intersession reliability for trials of 10-second duration, with ICCs of 0.43 with EO and 0.65 with EC in the AP axis and 0.71 with EO and 0.51 with EC in the ML axis (Doyle et al., 2005). Despite the moderate ICCs, the CV indicated a large amount of error between measurements (AP EO, CV=38.9%; AP EC, CV=24.1%; ML EO, CV=32.2%; ML EC, CV=37.4%).

4.9.3 Centre of Pressure Mean Velocity

COP mean velocity was selected as an outcome variable due to its ability to distinguish between fallers and non-fallers (Pizzigalli et al., 2016; Quijoux et al., 2020) and its excellent re-test reliability, with ICCs higher than other COP parameters for the average of two 120-second trials in bipedal stance (AP, ICC=0.83; ML, ICC=0.94) (Lafond et al., 2004) and the average of three 30-second trials in unipedal stance (AP, ICC=0.85; ML, ICC=0.82) (da Silva et al., 2013). COP mean velocity has also been shown to discriminate between visual conditions better than other COP parameters (Baig et al., 2012).

COP velocity was calculated in both the AP and ML directions using the central difference approximation of the derivative of COP displacement:

$$v_{x_i} = \frac{x_{i+1} - x_{i+1}}{2\Delta t} \tag{18}$$

$$v_{y_i} = \frac{y_{i+1} - y_{i+1}}{2\Delta t}$$

where v_{x_i} and v_{y_i} are the velocity of COP in the ML and AP directions at time sample i, x_{i+1} and y_{i+1} are the ML and AP COP positions at time sample $i + 1$, x_{i-1} and y_{i-1} are the ML and AP COP positions at time sample $i - 1$, and $2\Delta t$ is the change in time between sample $i + 1$ and $i - 1$, which is equivalent to the duration of two sampling periods.

The mean COP velocity in the AP and ML axes was determined by calculating the mean of the absolute value of the COP velocity at each time sample

$$\bar{v}_x = \frac{1}{n}\sum_{i=1}^{n}|v_{x_i}| \tag{19}$$

$$\bar{v}_y = \frac{1}{n}\sum_{i=1}^{n}|v_{y_i}|$$

where $\bar{v}_x$ and $\bar{v}_y$ are the sample mean of COP velocity in the ML and AP directions, $|v_{x_i}|$ and $|v_{y_i}|$ are the absolute value of the COP velocity in the ML and AP directions at time sample i, and n is the number of samples.

4.9.4 Cross-correlation of Centre of Pressure and Centre of Mass

Time-series data is often reduced to a single data point for further analysis, which although effective at answering certain research questions, tends to lead researchers to overlook important information contained in the time-series signal. Cross-correlation is a method that is used to measure association between time-series signals without the need to reduce the signals to a discrete data point (Derrick and Thomas, 2004). The cross-correlation is calculated like the Pearson product moment correlation, where the covariance of the two signals is divided by the product of each signal's standard deviation; however, the correlation coefficient is expressed as a function of the signal lag. In the present study, the cross-correlation of COP and COM in the AP axis and ML axis were calculated using the following equation (shown only for the ML axis)

$$\rho_{COP_xCOM_x}(\ell) = \frac{\sum_{i=0}^{n-1}(COP_{x_{i+\ell}} - \overline{COP_x})(COM_{x_i} - \overline{COM_x})}{\sqrt{\sum_{i=0}^{n-1}(COP_{x_{i+\ell}} - \overline{COP_x})^2}\sqrt{\sum_{i=0}^{n-1}(COM_{x_i} - \overline{COM_x})^2}} \tag{20}$$

where $\rho_{COP_xCOM_x}(\ell)$ is the cross-correlation of the ML components of COP and COM as a function of lag, ℓ; COM_{x_i} is COM_x at time sample i for $0 \leq i \leq$ n-1; $COP_{x_{i+\ell}}$ is COP_x at time sample $i + \ell$ for $0 \leq i \leq$ n-1 and -(n-1)$\leq \ell \leq$ n-1; and $\overline{COP_x}$ and $\overline{COM_x}$ are the sample mean

of COP_x and COM_x, and n is the number of samples in the trial. The same method was used to calculate the cross-correlation of COP and COM in the AP axis.

The output of the cross-correlation analysis was a set of correlations of the two signals for a series of time lags. The time lag between the COP and COM has been referenced in several theories of the motor control of standing balance (see section 2.4.3). In the present study, the time lag corresponding to the highest correlation coefficient was determined as the time lag between COP and COM. If the time lag was positive, COP was said to lead ahead of COM, while a negative time lag indicated that COP lagged behind the COM.

4.9.5   Mean Absolute Deviation of Centre of Pressure and Centre of Mass

Winter (1998) proposed that the difference between COP and COM during quiet stance represents the error in the balance control system and showed a strong negative correlation (r = -0.91 to -0.94) between the difference between COP and COM and the horizontal acceleration of the COM.

In healthy older adults, the difference between COP and COM has moderate to excellent intra-session reliability, with ICCs from a 30-second trial of 0.79 and 0.69 for the AP and ML directions, respectively (Corriveau et al., 2000). The average of four 30-second trials increased ICCs to 0.94 in the AP direction and .90 in the ML direction. The standard error for a single trial was estimated to be 0.10 mm for the AP direction and 0.17 mm for the ML direction, and the 95% confidence interval representing the minimal metrically detectable change was ±0.19 mm and ±0.28 mm for the AP and ML directions, respectively.

The mean absolute deviation of the COP and COM (COP-COM) was calculated in both the AP and ML directions as follows (equation shown for ML axis):

$$COP_x - COM_x = \frac{1}{n}\sum_{i=1}^{n}\left|COP_{x_i} - COM_{x_i}\right| \qquad (21)$$

where $COP_x - COM_x$ is the mean absolute deviation of the ML components of the COP and COM, COP_{x_i} is the ML component of the COP position at time sample i, COM_{x_i} is the ML component of the COM position at time sample i, and n is the number of samples in the trial.

4.9.6 Median Power Frequency of Centre of Pressure

The COP MPF was selected as an outcome measure for the present study due to its ability to detect changes in sensory control mechanisms (see section 2.5.1).

The AP and ML COP signals were transformed from the time domain to the frequency domain using an FFT. Sample power spectral density plots derived from the FFT can be found in Appendix D. The power spectral densities were trimmed at an upper limit of 2 Hz based on the findings by Sozzi et al. (2021), which found that only 0.7% the COP 95% PEA remained after applying a high-pass filter at a cut-off frequency of 2 Hz. The power spectral densities had frequency resolutions of 0.006 Hz for the bipedal trials and 0.006-0.195 Hz for the unipedal trials depending on unipedal stance duration. The MPF (Hz) was defined as the frequency below which 50% of the total power distribution lies (Figure 23).
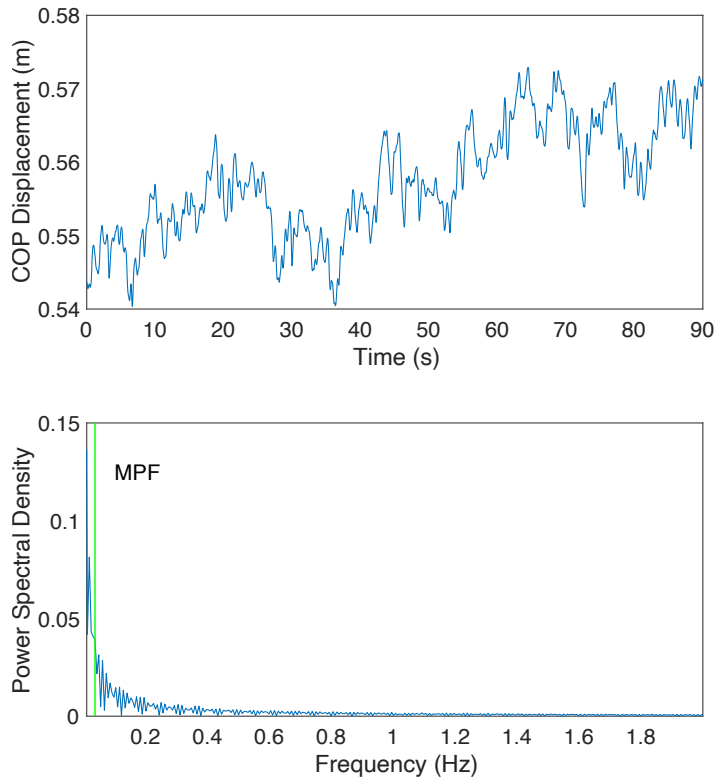
Figure 23. *Example of a time-varying signal (top) converted to a power spectral density (bottom) via fast Fourier transformation. The median power frequency (MPF; Hz) is indicated by the green vertical line on the power spectral density plot.*

Figure 23 displays the heavy-tailed distribution of a COP power spectral density plot; therefore, the MPF provides a more accurate representation of central tendency than the mean power frequency.

In healthy older adults, the MPF calculated from a single 120-second trial had an intrasession reliability defined by ICCs of 0.34 and 0.47 in AP and ML directions, respectively, while to achieve an ICC greater than 0.9, averaging 18 120-second trials in the AP direction and 10 120-second trials in the ML direction were necessary (Lafond et al., 2004). Decreasing the trial duration to 30 seconds had similar ICCs of 0.32 and 0.41 for AP and ML directions, respectively. However, when intersession reliability was assessed using a different method of reliability analysis that partitioned systematic and random error, the MPF in the AP and ML directions only required six and three 60-second

91

trials, respectively, to achieve an index of dependability (same interpretation as ICC) greater than 0.75 (Santos et al., 2008). In an EC condition, only four trials were needed in both AP and ML directions to achieve the same reliability index. The standard error of measurement, expressed as a percentage of the grand mean across days (same interpretation as CV), was 9.3% (AP) and 10.9% (ML) for EO and 10.2% (AP) and 11.5% (ML) for EC.

4.9.7   Unipedal Stance Time

Unipedal stance time was selected as an outcome measure due to its ease of measurement and excellent test-retest reliability in both young (ICC=0.75) and older adults (ICC=0.87) (da Silva et al., 2013). Unipedal stance time was calculated from foot lift off to foot touchdown of the non-supporting leg for both EO and EC trials.

4.10 Statistical Analysis

Normality was assessed via histograms, QQ-plots, and Shapiro-Wilks test, and homoscedasticity was examined using Levene's test. Residual analysis was performed to assess model fit.

For the analysis of participant characteristics, PWA and PNA were compared using Welch's t-tests for normally distributed continuous variables, Wilcoxon rank sum tests for ordinal or non-normally distributed variables, and Fisher exact tests for nominal variables.

Two-way [2 Group (PWA/PNA) x 2 Vision (EO/EC)] mixed non-parametric ANOVA-type tests were used to explore the interaction effect between acromegaly and vision on the COP 95% PEA, COP range, COP mean velocity, COP MPF, cross-correlation of COP and COM, time lag between COP and COM, and COP-COM during bipedal stance. The tests were performed for each outcome measure apart from the COP 95% PEA in both

the AP and ML axes. Significant interaction effects were further explored via data visualization.

All unipedal balance trials with a duration of less than five seconds were excluded, and the average was taken from the left and right sides for each visual condition. Welch's t-tests were used to examine the effect of acromegaly on COP 95% PEA, COP range, COP mean velocity, and COP MPF during unipedal stance with EO. Due to small sample sizes (PWA, n=3; PNA, n=1), inferential statistics were not conducted for unipedal stance with EC. Each outcome measure was analyzed in the AP and ML axes, except for the COP 95% PEA. The interaction between acromegaly and vision on unipedal stance time was assessed using a two-way [2 Group (PWA/PNA) x 2 Vision (EO/EC)] mixed ANOVA.

R statistical software (R Foundation for Statistical Computing, Vienna, Austria) was used for all statistical analyses. The nparLD package in R was used to compute non-parametric ANOVA-type statistics (Noguchi et al., 2012). Significance was set at α=0.05.

Chapter 5: Results

5.1 Group Characteristics

Data were collected on 12 PWA and 11 PNA. Table 2 and Table 3 display characteristics for each group. Both groups had similar proportions of female participants (PWA, 42% female; PNA, 45% female; $p=1$, $OR=0.863$) and similar distributions of age (PWA, $M=54.9$y, $SD=12.2$y; PNA, $M=56.1$y, $SD=10.3$y; $t(20.87)=-0.25$, $p=0.804$, $d=-0.10$) and BMI (PWA, $M=33.3$kg/m^2, $SD=5.5$kg/m^2; PNA, $M=31.63$kg/m^2, $SD=6.83$kg/m^2; $t(19.31)=0.65$, $p=0.526$, $d=0.27$).

Both groups were similar in age at diagnosis (PWA, $M=42.8$y, $SD=14.9$y; PNA, $M=49.4$y, $SD=9.4$y; $t(18.70)=1.76$, $p=0.220$, $d=-0.52$), and at the time of the study, the mean duration since diagnosis was greater for PWA than PNA, although not significant (PWA, $M=12.1$y, $SD=10.1$y; PNA, $M=6.7$y, $SD=2.8$y; $t(12.80)=1.76$, $p=0.103$, $d=0.72$). All participants underwent surgery to remove the pituitary adenoma. Pituitary radiotherapy was received by 33% of PWA and 0% of PNA ($p=0.093$, $OR=$Inf). Medical therapy for acromegaly was utilized by 25% of PWA (n=3), of which 67% (n=2) used somatostatin receptor ligands. At the time of the study, all PWA were in remission based on most recent IGF-1 levels, with a mean duration in remission of 8.5 years ($SD=5.9$y). Of PWA with available bloodwork records (GH, n=8; IGF-1, n=9), mean pre-treatment GH and IGF-1 levels expressed as a percent of the upper limit of normal were 147.8% ($SD=229.3\%$) and 221.3% ($SD=66.8\%$), respectively.

There were no differences between groups in rates of secondary hypoadrenalism, hypothyroidism, or hypogonadism, and all participants with these diagnoses received hormone replacement therapy. PWA and PNA had no significant differences in use of anti-

hypertensive, sleep, or analgesic medication. PWA had significantly higher rates of obstructive sleep apnea compared to PNA (PWA, 66.7%; PNA, 0%; p=0.001, OR=Inf), and all patients with obstructive sleep apnea were treated.

Rates of joint surgery were similar between groups (PWA, 33.3%; PNA, 36.4%; p=1, OR=0.88). There were no significant differences between groups for joint surgery of any body-region or type of surgery. In PWA, one participant had a total knee replacement, and one had a total hip replacement, whereas no PNA had joint replacement surgery.

Table 2. *Group characteristics (continuous variables)*

	PWA [*M* (*SD*)]	PNA [*M* (*SD*)]	*t*-stat	*df*	*p*-value	*d*
Age (years)	54.9 (12.2)	56.1 (10.3)	-0.25	20.87	0.804	-0.10
BMI (kg/m^2)	33.3 (5.5)	31.6 (6.8)	0.65	19.31	0.526	0.27
Height (m)	1.7 (0.1)	1.7 (0.1)	0.10	20.91	0.917	0.04
Weight (kg)	97.0 (18.9)	92.1 (22.0)	0.57	19.85	0.575	0.24
Age at Dx (years)	42.8 (14.9)	49.4 (9.4)	-1.27	18.70	0.220	-0.52
Duration since Dx (years)	12.1 (10.1)	6.7 (2.8)	1.76	12.80	0.103	0.72
Duration in Remission (years)	8.5 (5.9)					
GH at Dx (%ULN)	147.8 (229.3)					
IGF-1 at Dx (%ULN)	221.2 (66.8)					

Table 3. *Group characteristics (categorical variables)*

	PWA [n (%)]	PNA [n (%)]	p-value	OR
Sex (Female)	5 (41.7)	5 (45.5)	1	0.86
Pituitary Surgery	12 (100.0)	11 (100.0)	1	0
Pituitary Radiation	4 (33.3)	0 (0.0)	0.093	Inf
Acromegaly Remission	12 (100.0)			
Acromegaly Medication	3 (25.0)			
SRL	2 (16.7)			
DA	0 (0.0)			
Pegvisomant	0 (0.0)			
SHA	1 (8.3)	1 (9.1)	1	0.91
Adrenal HRT	1 (8.3)	1 (9.1)	1	0.91
SHT	4 (33.3)	5 (45.5)	0.68	0.61
Thyroid HRT	4 (33.3)	5 (45.5)	0.68	0.61
SHG	3 (25.0)	3 (27.3)	1	0.89
Gonadal HRT	3 (25.0)	3 (27.3)	1	0.89
Anti-hypertensive Medication	5 (41.7)	3 (27.3)	0.667	1.85
OSA	8 (66.7)	0 (0.0)	**0.001**	Inf
OSA Therapy	8 (66.7)	0 (0.0)	**0.001**	Inf
Sleep Medication	0 (0.0)	0 (0.0)	1	0
Analgesic Medication	5 (41.7)	4 (36.4)	1	1.24
Joint Surgery	4 (33.3)	4 (36.4)	1	0.88
Hip	1 (8.3)	1 (9.1)	1	0.91
Knee	1 (8.3)	1 (9.1)	1	0.91
Ankle/Foot	0 (0.0)	1 (9.1)	0.478	0
Back	0 (0.0)	0 (0.0)	1	0
Neck	0 (0.0)	0 (0.0)	1	0
Shoulder	0 (0.0)	0 (0.0)	1	0
Elbow	0 (0.0)	0 (0.0)	1	0
Hand/Wrist	4 (33.3)	3 (27.3)	1	1.32
Arthroscopy	0 (0.0)	1 (9.1)	0.478	0
Bone	1 (8.3)	3 (27.3)	0.317	0.26
Carpal Tunnel	4 (33.3)	1 (9.1)	0.317	4.68
THR	1 (8.3)	0 (0.0)	1	Inf
TKR	1 (8.3)	0 (0.0)	1	Inf
Soft-tissue	4 (33.3)	3 (27.3)	1	1.32

SRL, somatostatin receptor ligand; DA, dopamine agonist; SHA, secondary hypoadrenalism; SHT, secondary hypothyroidism; SHG, secondary hypogonadism; HRT, hormone replacement therapy; OSA, obstructive sleep apnea; THR, total hip replacement; TKR, total knee replacement.

Table 4 displays the group comparison of joint pain scores measured on a visual analog scale. PWA had significantly higher joint pain scores than PNA for the back (PWA, *Mdn*=50, *IQR*=50.2; PNA, *Mdn*=0, *IQR*=12; *W*=114, *p*=0.003, *r*=0.63), hip (PWA, *Mdn*=33.8, *IQR*=41.9; PNA, *Mdn*=0, *IQR*=1; *W*=106.5, *p*=0.010, *r*=0.54), and knee (PWA, *Mdn*=39.2, *IQR*=29.5; PNA, *Mdn*=0, *IQR*=25.2; *W*=105.5, *p*=0.015, *r*=0.51). There were no significant differences in pain scores between groups for the ankle/foot, elbow, hand/wrist, or neck.

Table 4. *Group comparison of joint pain scores measured on a visual analog scale*

	PWA [*Mdn* (*IQR*)]	PNA [*Mdn* (*IQR*)]	*W*-stat	*p*-value	*r*
Ankle/Foot	10.5 (25.1)	0.0 (8.8)	89.0	0.153	0.30
Back	50.0 (50.2)	0.0 (12.0)	114.0	**0.003**	0.63
Elbow	0.0 (4.5)	0.0 (3.5)	68.5	0.889	0.04
Hand/Wrist	11.2 (39.9)	0.0 (5.2)	96.0	0.058	0.40
Hip	33.8 (41.9)	0.0 (1.0)	106.5	**0.010**	0.54
Knee	39.2 (29.5)	0.0 (25.2)	105.5	**0.015**	0.51
Neck	17.5 (25.2)	0.0 (34.0)	87.0	0.193	0.28
Shoulder	13.2 (38.4)	0.0 (3.8)	94.0	0.077	0.38

The group comparison of functional ability questionnaire scores is shown in Table 5. PWA had significantly greater functional ability of the upper limb (QuickDASH) than PNA (PWA, *Mdn*=79.5, *IQR*=21; PNA, *Mdn*=97.9, *IQR*=4.8; *W*=24, *p*=0.010, *r*=0.54). No significant differences were found between groups for balance confidence (ABC-6), foot and ankle functional ability (Quick-FAAM), hip functional ability (HOOS, JR), and knee functional ability (KOOS, JR); however, there was a trend towards greater knee and hip functional disability in PWA compared to PNA. There was no difference in number of falls in the past 12 months between groups.

Table 5. Group comparison of functional ability scores

	PWA [*Mdn* (*IQR*)]	PNA [*Mdn* (*IQR*)]	*W*-stat	*p*-value	*r*
ABC-6	77.5 (50.8)	95.0 (19.2)	46.5	0.236	0.25
QuickDASH	79.5 (21.0)	97.7 (4.8)	24.0	**0.010**	0.54
Quick-FAAM	87.5 (30.2)	100.0 (18.2)	36.0	0.103	0.36
HOOS, JR	73.6 (39.0)	100.0 (22.2)	37.0	0.070	0.38
KOOS, JR	70.8 (15.9)	100.0 (29.2)	35.5	0.059	0.40
Falls in past 12 months	0.0 (2.5)	0.0 (0.0)	87.5	0.094	0.36

ABC-6, 6-item Activities-specific Balance Confidence scale; QuickDASH, 11-item Disabilities of the Arm, Shoulder, and Hand outcome measure; Quick-FAAM, 12-item Foot and Ankle Mobility measure; HOOS, JR, 6-item Hip dysfunction and Osteoarthritis Outcome Score for Joint Replacement; KOOS, JR, 7-item Knee injury and Osteoarthritis Outcome Score for Joint Replacement.

5.2 Bipedal Standing Balance

5.2.1 Centre of Pressure 95% Prediction Ellipse Area

The COP 95% prediction ellipse for a representative participant can be found in Appendix E (Figure 41A and 41B).

There was no significant interaction effect between group and vision or main effect of group on the COP 95% PEA (Table 6). However, there was a trend towards a main effect of vision (*ATS*(1)=3.60, *p*=0.058). In Figure 24, the COP 95% PEA increased marginally for both groups with EC compared to EO, with a slightly greater increase for PWA than PNA.

Table 6. Two-way [2 group (PWA/PNA) x 2 vision (EO/EC)] non-parametric mixed ANOVA-type test of COP 95% prediction ellipse area (cm^2) during 90-second bipedal stance

	ATS	*df1*	*df2*	*p*-value
Group	0.26	1	20.14	0.615
Vision	3.60	1		0.058
Group:Vision	0.21	1		0.644
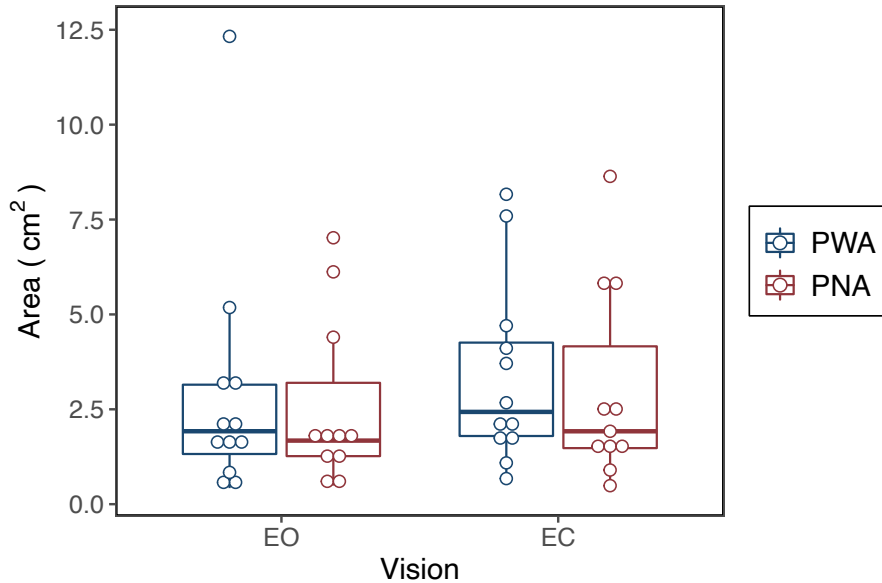
Figure 24. *COP 95% prediction ellipse area (cm²) during 90-second bipedal stance with eyes open (EO) and eyes closed (EC)*

5.2.2 Centre of Pressure Range

There was no significant interaction of group and vision on the COP AP range, and neither of the main effects were significant (Table 7). Figure 25 shows a small increase in the COP AP range for PWA but a minimal change for PNA when going from EO to EC.

Table 7. *Two-way [2 group (PWA/PNA) x 2 vision (EO/EC)] non-parametric mixed ANOVA-type test of COP range (cm) in the AP axis during 90-second bipedal stance*

	ATS	*df1*	*df2*	*p*-value
Group	0.23	1	20.66	0.635
Vision	2.63	1		0.105
Group:Vision	1.68	1		0.195

No significant interaction of group and vision on the COP ML range was found (Table 8). A main effect of vision was detected for COP ML range (ATS(1)=5.20, p=0.023), but there was no main effect of group. In accordance with the main effect of vision, Figure

25 reveals that COP ML range increased for both groups when going from EO to EC, with a slightly higher COP ML range in both visual conditions for PWA than PNA.

Table 8. Two-way [2 group (PWA/PNA) x 2 vision (EO/EC)] non-parametric mixed ANOVA-type test of COP range (cm) in the ML axis during 90-second bipedal stance

	ATS	*df1*	*df2*	*p*-value
Group	0.29	1	20.89	0.595
Vision	5.20	1		**0.023**
Group:Vision	0.01	1		0.935
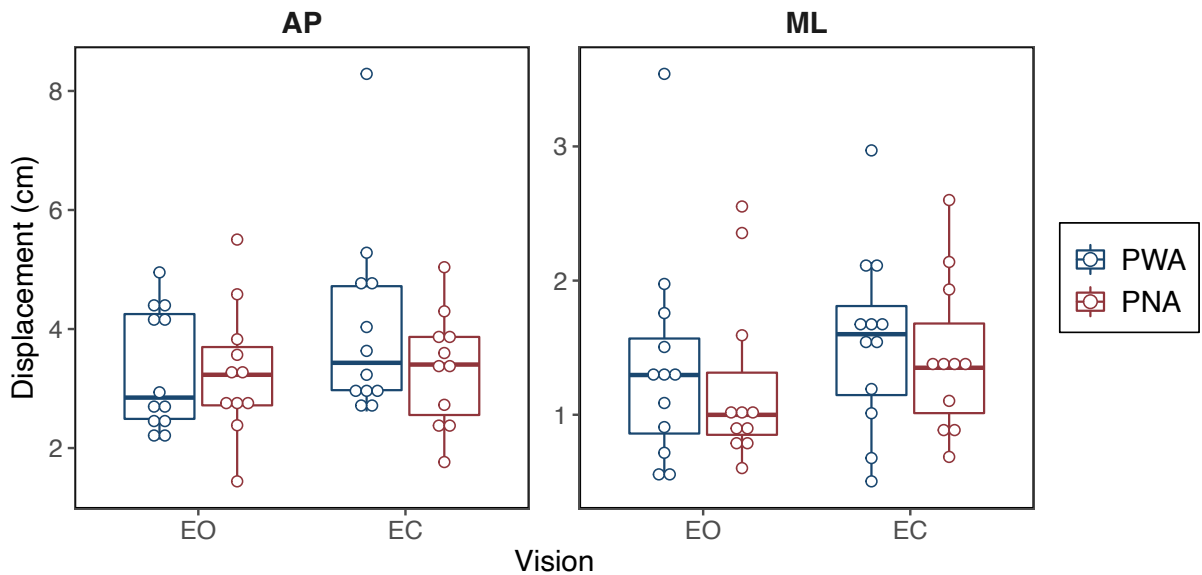
Figure 25. COP range (cm) in the anteroposterior (AP) and mediolateral (ML) axes during 90-second bipedal stance with eyes open (EO) and eyes closed (EC)

5.2.3 Centre of Pressure Mean Velocity

There was a significant interaction of group and vision ($ATS(1)$=3.95, p=0.047) and a significant main effect of vision ($ATS(1)$=77.94, p=<0.001) on the COP mean velocity in the AP axis (Table 9). There was no significant main effect of group. Although both groups revealed an increase in AP COP mean velocity in the EC compared to EO condition, this increase occurred to a greater extend in PWA than PNA (Figure 26).

Table 9. *Two-way [2 group (PWA/PNA) x 2 vision (EO/EC)] non-parametric mixed ANOVA-type test of COP mean velocity (cm/s) in the AP axis during 90-second bipedal stance*

	ATS	df1	df2	p-value
Group	0.19	1	18.58	0.669
Vision	77.94	1		**<0.001**
Group:Vision	3.95	1		**0.047**

No significant interaction of group and vision was found for COP mean velocity in the ML axis (Table 10). There was a main effect of vision ($ATS(1)=14.17$, $p=<0.001$) but no main effect of group on ML COP mean velocity. Figure 26 shows a trend towards lower ML COP mean velocity in PWA compared to PNA.

Table 10. *Two-way [2 group (PWA/PNA) x 2 vision (EO/EC)] non-parametric mixed ANOVA-type test of COP mean velocity (cm/s) in the ML axis during 90-second bipedal stance*

	ATS	df1	df2	p-value
Group	0.93	1	19.67	0.346
Vision	14.17	1		**<0.001**
Group:Vision	2.55	1		0.110

5.2.4 Centre of Pressure Median Power Frequency

The COP power spectral density for a representative participant is displayed in Figure 40, Appendix D.

There was no significant interaction of group and vision on COP MPF in the AP axis (Table 11). The main effect of vision was significant ($ATS(1)=14.97$, $p=<0.001$), while there was no significant main effect of group. Both groups displayed an increase in AP COP MPF when going from EO to EC, with a slightly larger increase for PNA than PWA (Figure 27).

Table 11. Two-way [2 group (PWA/PNA) x 2 vision (EO/EC)] non-parametric mixed ANOVA-type test of the median power frequency (Hz) of COP in the AP axis during 90-second bipedal stance

	ATS	*df1*	*df2*	*p*-value
Group	7.43e-4	1	20.68	0.978
Vision	14.97	1		**<0.001**
Group:Vision	0.10	1		0.755

No significant interaction or main effects were found for COP MPF in the ML axis (Table 12). Figure 27 shows minimal difference in ML COP MPF between the EO and EC condition for both groups.

Table 12. Two-way [2 group (PWA/PNA) x 2 vision (EO/EC)] non-parametric mixed ANOVA-type test of the median power frequency (Hz) of COP in the ML axis during 90-second bipedal stance

	ATS	*df1*	*df2*	*p*-value
Group	0.20	1	17.82	0.658
Vision	0.23	1		0.634
Group:Vision	4.34e-3	1		0.947
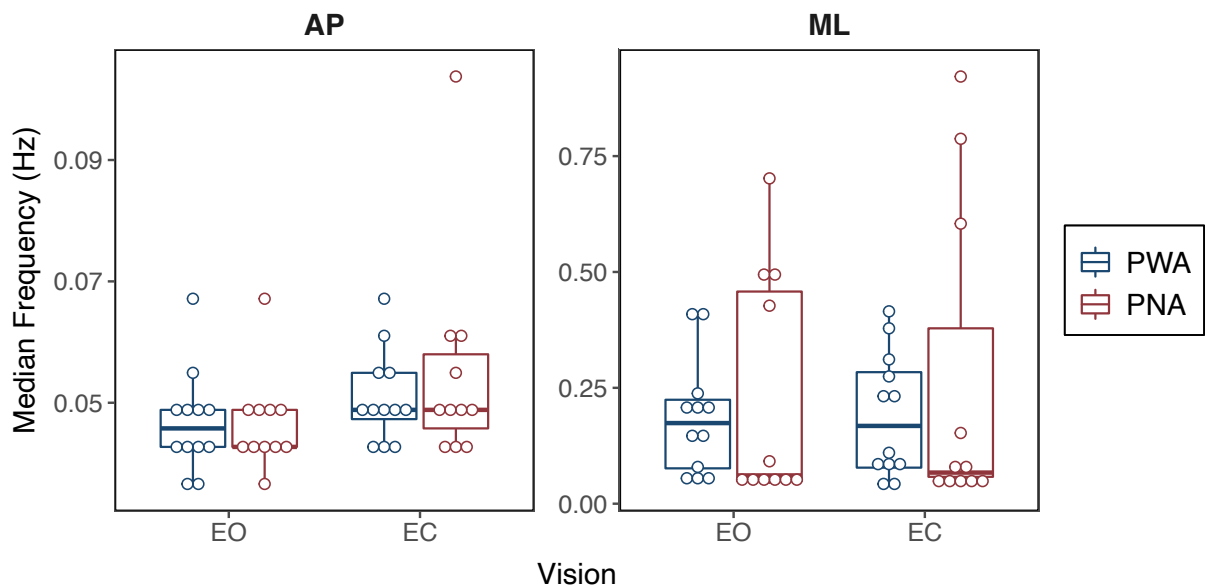
Figure 27. *COP median power frequency (Hz) in the anteroposterior (AP) and mediolateral (ML) axes during 90-second bipedal stance with eyes open (EO) and eyes closed (EC).*

5.2.5   Cross-correlation of Centre of Pressure and Centre of Mass

The COP and COM signals for three different participants are shown in Appendix F (Figure 42-44).

There was no significant interaction of group and vision on the cross-correlation between COP and COM in the AP axis (Table 13). There was a significant main effect of vision ($ATS(1)$=24.68, p=<0.001), while no significant main effect of group was found. The correlation between COP and COM decreased for both groups with EC compared to EO, with a greater decrease observed in PWA than PNA (Figure 28A).

There was no significant interaction effect or main effect of group and vision on the cross-correlation between COP and COM in the ML axis (Table 14). Figure 28A displays a slight decrease in the correlation between COP and COM for PWA with EC compared to

EO, while a slight increase in the correlation between COP and COM was observed for

PNA with EC compared to EO.

Table 13. *Two-way [2 group (PWA/PNA) x 2 vision (EO/EC)] non-parametric mixed ANOVA-type test of the cross-correlation coefficient between COP and COM in the AP axis during 90-second bipedal stance*

	ATS	*df1*	*df2*	*p*-value
Group	0.02	1	20.10	0.892
Vision	24.68	1		**<0.001**
Group:Vision	3.35	1		0.067

Table 14. *Two-way [2 group (PWA/PNA) x 2 vision (EO/EC)] non-parametric mixed ANOVA-type test of the cross-correlation coefficient between COP and COM in the ML axis during 90-second bipedal stance*

	ATS	*df1*	*df2*	*p*-value
Group	1.14	1	20.14	0.297
Vision	0.16	1		0.692
Group:Vision	0.28	1		0.596

No significant interaction effect or main effect of group and vision was found for

the time lag between COP and COM in the AP or ML axes (Table 15 and Table 16). Figure

28B reveals a negligible time lag between COP and COM for both groups in both visual

conditions in the AP axis. In the ML axis with EO, COP lags slightly behind COM for PNA

but not PWA, whereas with EC, both groups display negligible time lag between COP and

COM.

Table 15. *Two-way [2 group (PWA/PNA) x 2 vision (EO/EC)] non-parametric mixed ANOVA-type test of the time lag (ms) between COP and COM in the AP axis during 90-second bipedal stance*

	ATS	*df1*	*df2*	*p*-value
Group	0.08	1	19.53	0.774
Vision	0.13	1		0.721
Group:Vision	0.68	1		0.408

Table 16. *Two-way [2 group (PWA/PNA) x 2 vision (EO/EC)] non-parametric mixed ANOVA-type test of the time lag (ms) between COP and COM in the ML axis during 90-second bipedal stance*

|	ATS	*df1*	*df2*	*p*-value
Group	2.52	1	19.33	0.129
Vision	1.77	1		0.184
Group:Vision	1.64	1		0.200
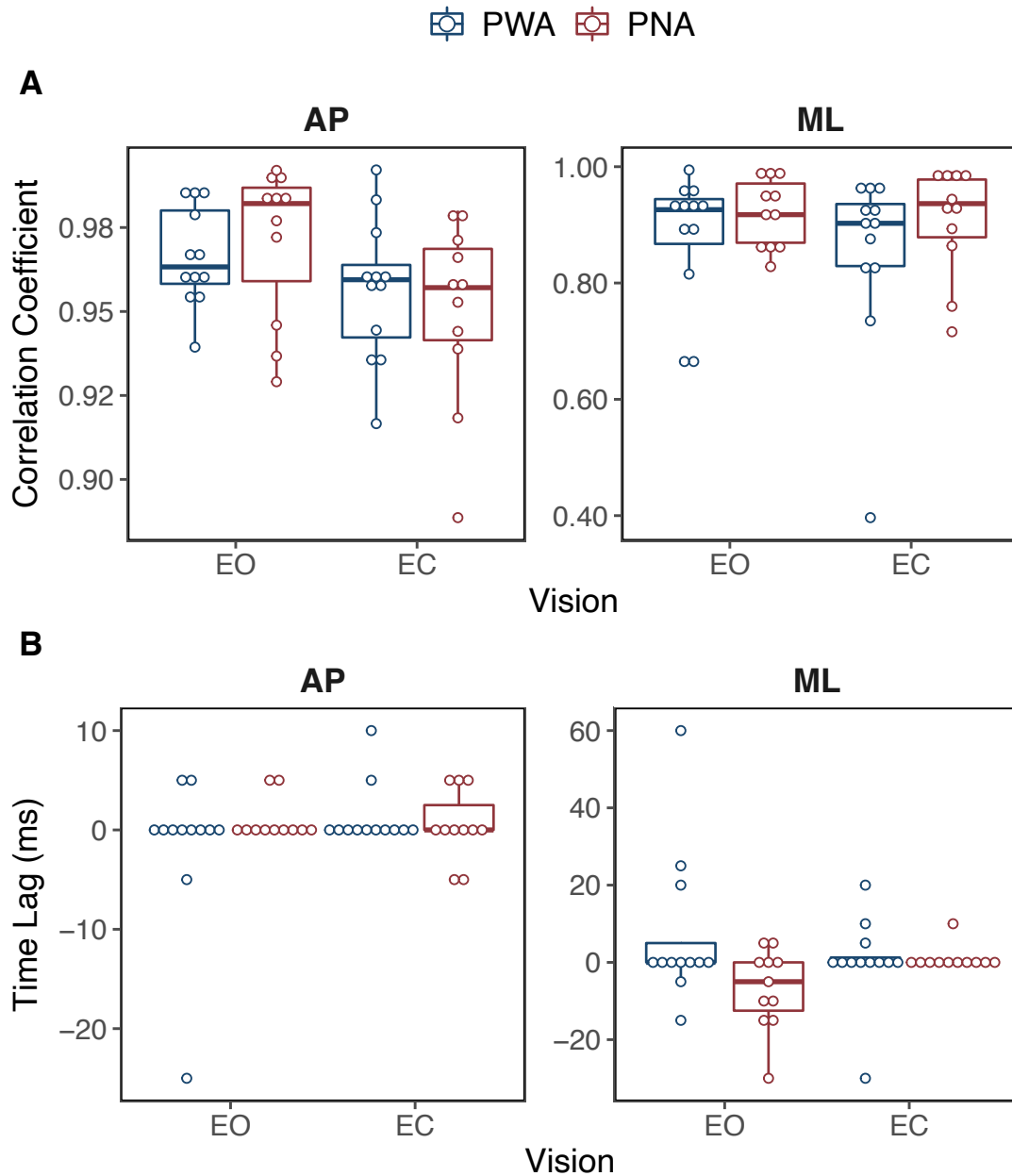
Figure 28. Cross-correlation (**A**) and time lag (ms; **B**) of COP and COM in the anteroposterior (AP) and mediolateral (ML) axes during 90-second bipedal stance with eyes open (EO) and eyes closed (EC)

5.2.6   Mean Absolute Deviation of Centre of Pressure and Centre of Mass

There was no significant interaction of group and vision or significant main effect of group or vision on COP-COM in the AP axis (Table 17). Figure 29 indicates that in the AP axis, there was negligible change in COP-COM between visual conditions for both groups. However, there was a trend towards a main effect of group, where median COP-COM was higher in PWA than PNA.

Table 17. Two-way [2 group (PWA/PNA) x 2 vision (EO/EC)] non-parametric mixed ANOVA-type test of COP-COM in the AP axis during 90-second bipedal stance

	ATS	df1	df2	p-value
Group	2.22	1	20.70	0.152
Vision	0.15	1		0.697
Group:Vision	0.01	1		0.903

There was no interaction of group and vision on COP-COM in the ML axis (Table 18). There was a main effect of group on COP-COM in the ML axis (ATS(1,20.63)=9.73, p=0.005), but no main effect of vision was found. The main effect of group for COP-COM in the ML axis can be observed in Figure 29, where COP-COM is larger in magnitude for PWA than PNA.

Table 18. Two-way [2 group (PWA/PNA) x 2 vision (EO/EC)] non-parametric mixed ANOVA-type test of COP-COM in the ML axis during 90-second bipedal stance

	ATS	df1	df2	p-value
Group	9.73	1	20.63	**0.005**
Vision	1.12e-4	1		0.992
Group:Vision	0.47	1		0.492

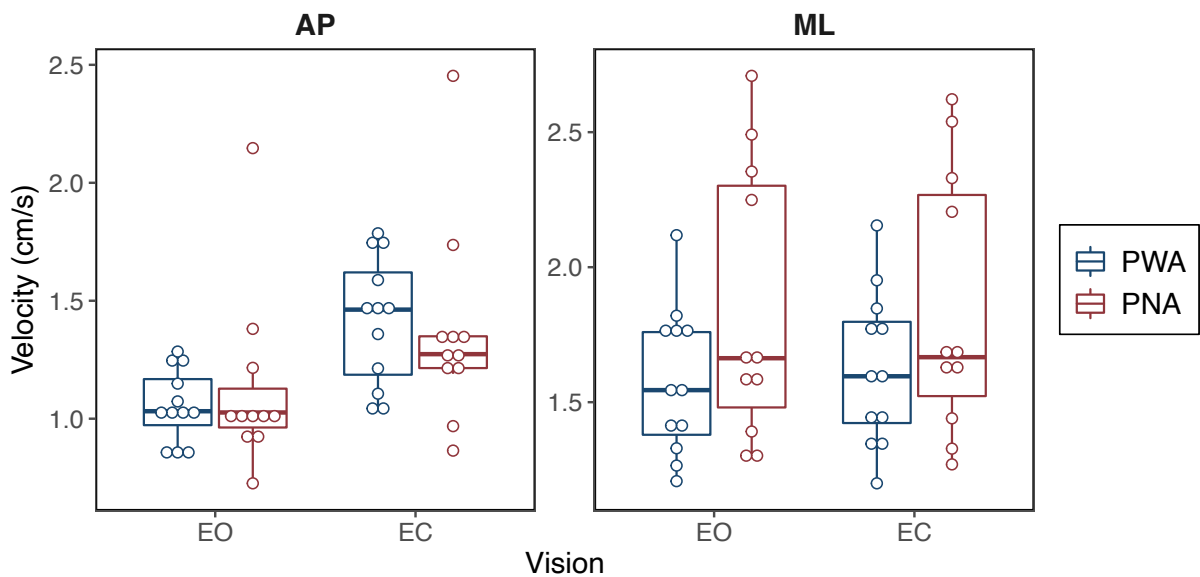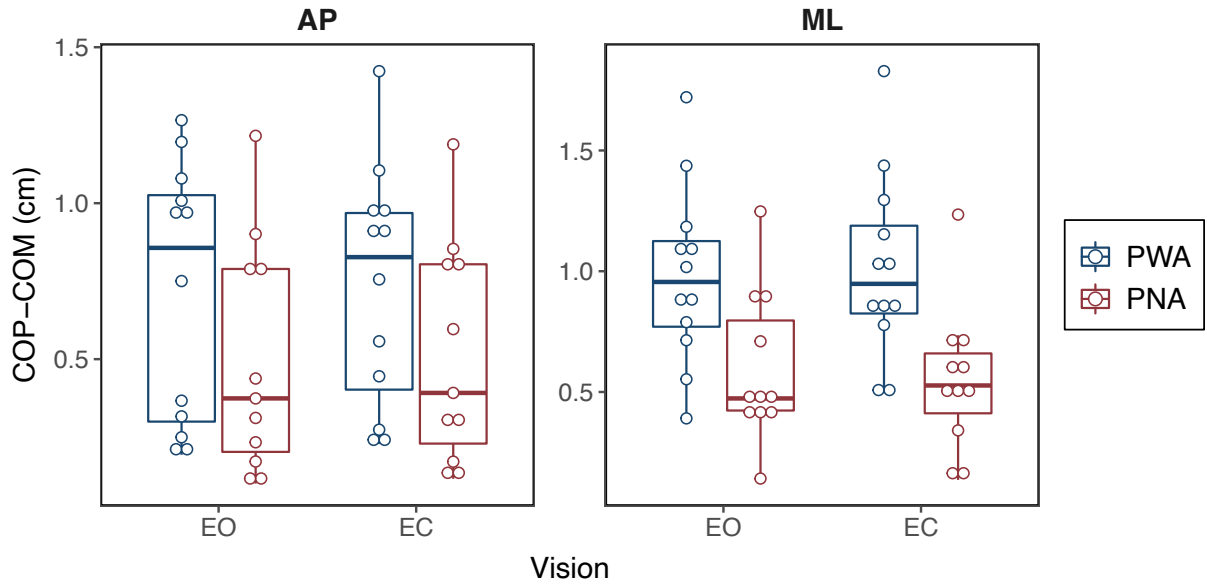*Figure 29.* *The mean absolute deviation between COP and COM (cm) in the anteroposterior (AP) and mediolateral (ML) axes during 90-second bipedal stance with eyes open (EO) and eyes closed (EC).*

Figure 30 exhibits the distance of COP and COM from the midpoint of the left and right ankle joint centres, showing the difference between the locations of COP and COM for each participant in PWA and PNA. In the AP axis (Figure 30A), the COM is anterior to the COP in approximately half of PWA in both visual conditions, while COM is anterior to the COP in the majority of PNA in both visual conditions. In the mediolateral axis (Figure 30B), all but one participant has a COM that is located to the right of the COP, and this trend appears to be independent of group and vision.
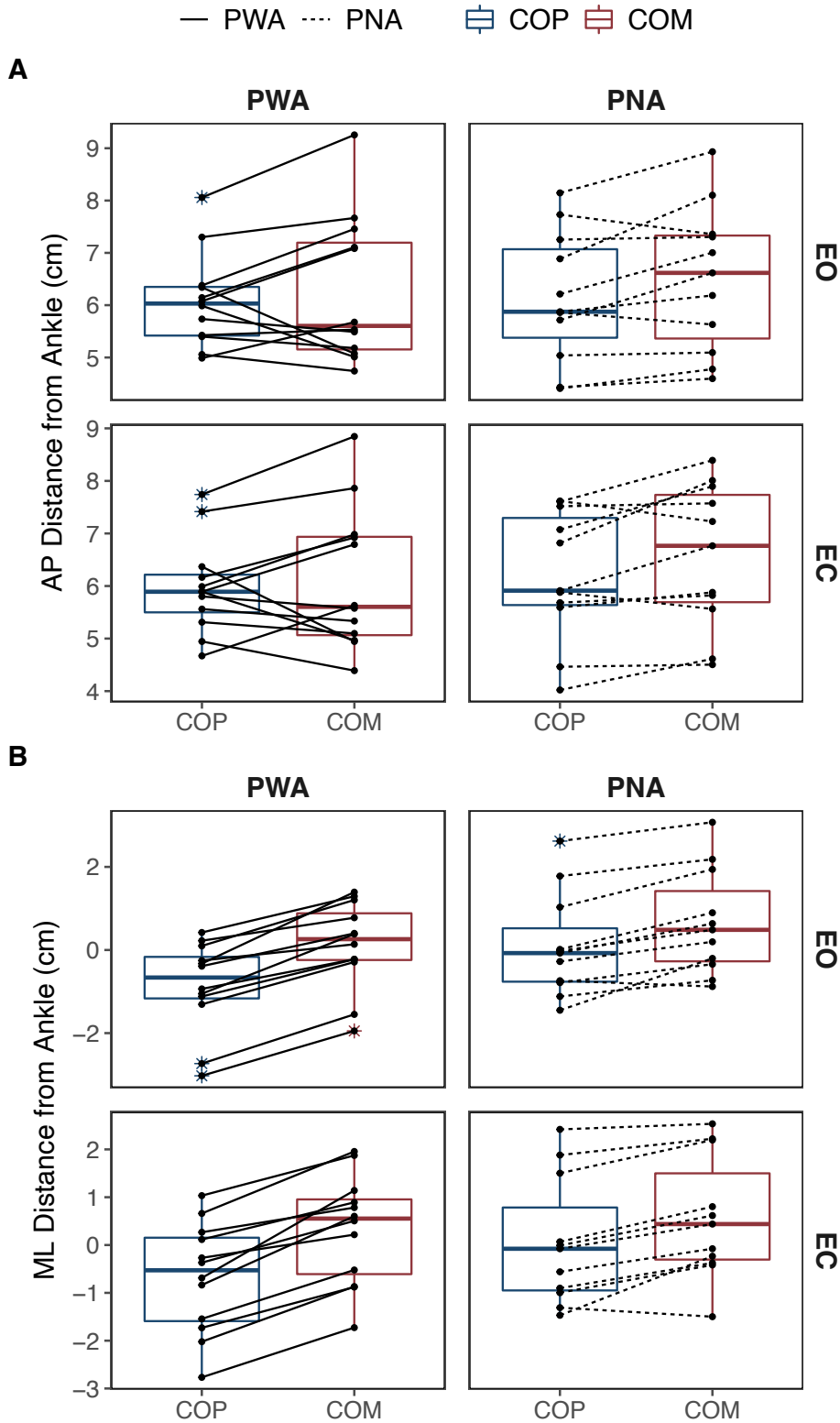
Figure 30. *The distance of COP (cm) and COM (cm) from the midpoint of the left and right ankle joint centres in the anteroposterior (AP; **A**) and mediolateral (ML; **B**) axes during 90-second bipedal stance with eyes open (EO) and eyes closed (EC).*

5.3 Unipedal Standing Balance

5.3.1 Unipedal Stance Time

No significant interaction between group and vision was found for unipedal stance time (Table 19). As observed in Figure 31, there was a significant decrease in unipedal stance time in both groups with EC compared to EO ($F(1,18)=47.61$, $p=<0.001$). No significant main effect of group was found. Figure 31 displays a trend towards a longer unipedal stance time for PWA than PNA in the EO condition, but the groups show similar unipedal stance times in the EC condition.
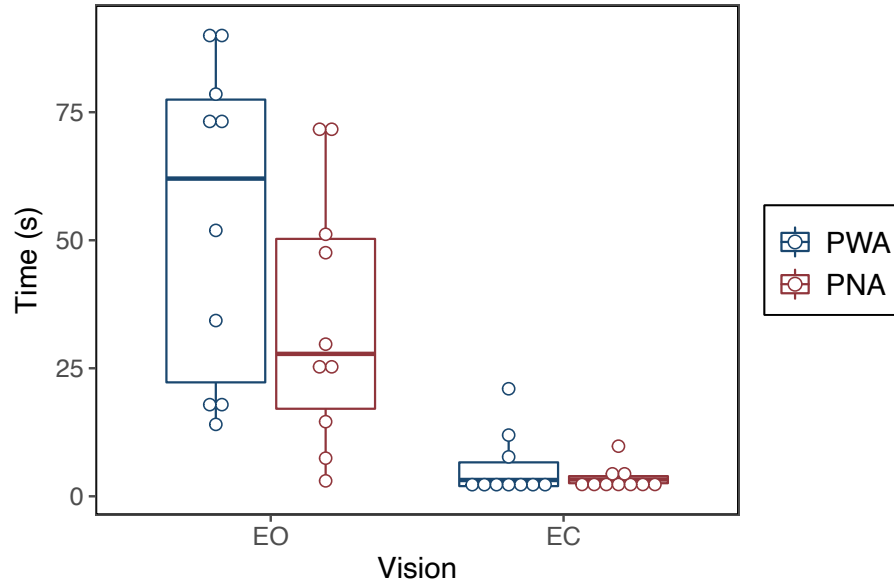
Figure 31. *Comparison of unipedal stance time (s) between groups and visual conditions*

Table 19. *Two-way [2 group (PWA/PNA) x 2 vision (EO/EC)] mixed ANOVA of unipedal stance time (s)*

Effect	df_n	df_d	F-stat	p-value	ω^2
(Intercept)	1	18	51.17	**<0.001**	
Group	1	18	2.45	0.135	0.07
Vision	1	18	47.61	**<0.001**	0.50
Group:Vision	1	18	2.23	0.152	0.03

5.3.2   Eyes Open

The results presented in the following subsections reflect the analyses performed on a subset of participants who maintained unipedal stance with EO for at least five seconds (PWA, n=10; PNA, n=9). Two PWA were unable to attempt the unipedal stance trials due to pain or fear of falling. One PNA completed the unipedal stance trials but was excluded as the force plate data was lost. The other PNA was excluded as they could not hold unipedal stance for at least five seconds.

5.3.2.1   Centre of Pressure 95% Prediction Ellipse Area

The COP 95% prediction ellipse for unipedal stance with EO for a representative participant can be found in Appendix E (Figure 41C and 41D).

There was no significant difference between PWA and PNA in the unipedal COP 95% PEA with EO (Table 20). The group medians for COP 95% PEA were similar, with greater variability observed in PWA than PNA (Figure 32).

Table 20. *Welch's t-test of COP 95% prediction ellipse area (cm^2) during unipedal stance with eyes open*

PWA (n)	PNA (n)	PWA (M)	PNA (M)	Mean Diff [95% CI]	t-stat	df	p-value	d
10	9	12.72	10.34	2.37 [-1.53, 6.27]	1.29	16.08	0.216	0.59
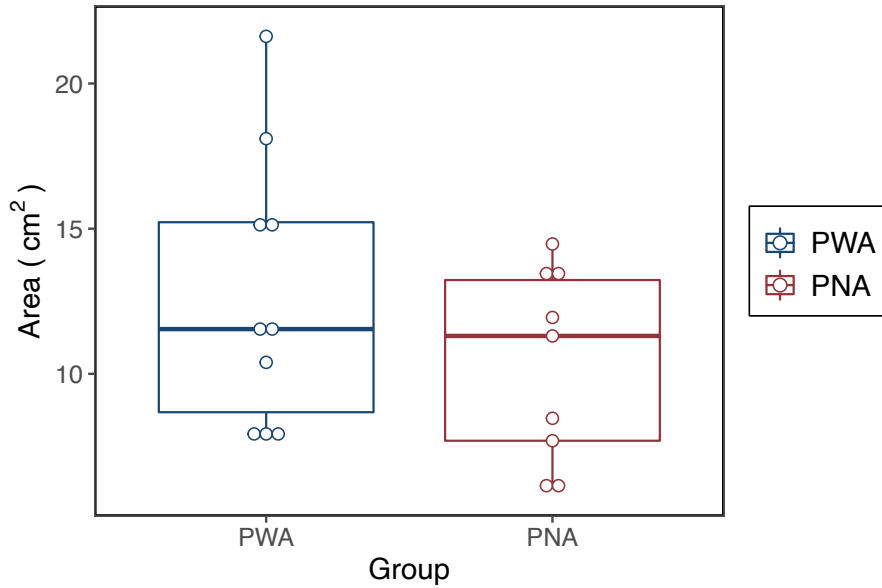
Figure 32. COP 95% prediction ellipse area (cm²) during unipedal stance with eyes open

5.3.2.2 Centre of Pressure Range

The unipedal COP range did not significantly different between groups for the EO condition in either the AP or ML axes (Table 21). Figure 33 displays that both groups had similar COP range in the AP axis, but a trend towards higher COP range values for PWA than PNA was observed in the ML axis.

Table 21. Welch's t-test of COP range (cm) in the anteroposterior (AP) and mediolateral (ML) axes during unipedal stance with eyes open

Axis	PWA (*n*)	PNA (*n*)	PWA (*M*)	PNA (*M*)	Mean Diff [95% CI]	*t*-stat	*df*	*p*-value	*d*
AP	10	9	5.32	4.99	0.33 [-1.35, 2.01]	0.41	16.65	0.686	0.19
ML	10	9	3.9	3.51	0.38 [-0.10, 0.86]	1.75	11.6	0.107	0.79
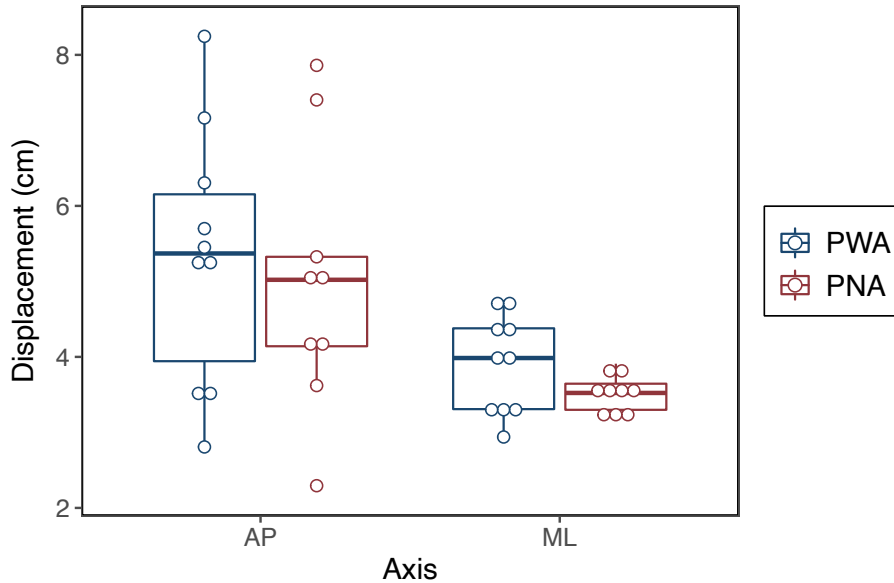
Figure 33. COP range (cm) in the anteroposterior (AP) and mediolateral (ML) axes during unipedal stance with eyes open

5.3.2.3 Centre of Pressure Mean Velocity

There was no significant difference in unipedal COP mean velocity between groups for the EO condition in either the AP or ML axes (Table 22). There was less variability of the COP mean velocity in the AP axis for PWA compared to PNA (Figure 34). In the ML axis, COP mean velocity trended lower for PWA than PNA.

Table 22. Welch's t-test of COP mean velocity (cm/s) in the anteroposterior (AP) and mediolateral (ML) axes during unipedal stance with eyes open

Axis	PWA (n)	PNA (n)	PWA (M)	PNA (M)	Mean Diff [95% CI]	t-stat	df	p-value	d
AP	10	9	3.35	3.60	-0.25 [-1.62, 1.11]	-0.40	12.65	0.694	-0.19
ML	10	9	3.53	4.08	-0.55 [-1.42, 0.32]	-1.33	15.64	0.201	-0.62
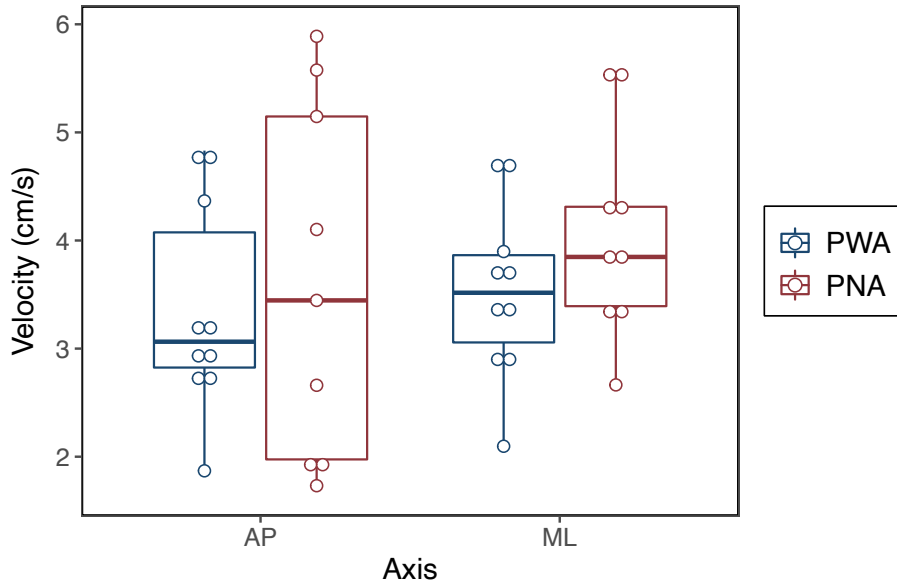
Figure 34. *COP mean velocity (cm/s) in the anteroposterior (AP) and mediolateral (ML) axes during unipedal stance with eyes open*

5.3.2.4   Centre of Pressure Median Power Frequency

The COP power spectral density for a representative participant is shown in Figure 40, Appendix D.

There was no significant difference between groups in the unipedal COP MPF for the EO condition in either the AP or ML axes (Table 23). Figure 35 shows a trend towards a lower COP MPF in the AP axis and higher COP MPF in the ML axis for PWA compared to PNA.

Table 23. *Welch's t-test of COP median power frequency (Hz) in the anteroposterior (AP) and mediolateral (ML) axes during unipedal stance with eyes open*

Axis	PWA (*n*)	PNA (*n*)	PWA (*M*)	PNA (*M*)	Mean Diff [95% CI]	*t*-stat	*df*	*p*-value	*d*
AP	10	9	0.11	0.14	-0.03 [-0.09, 0.03]	-1.17	12.07	0.265	-0.55
ML	10	9	0.44	0.41	0.03 [-0.08, 0.15]	0.59	15.97	0.561	0.27

113
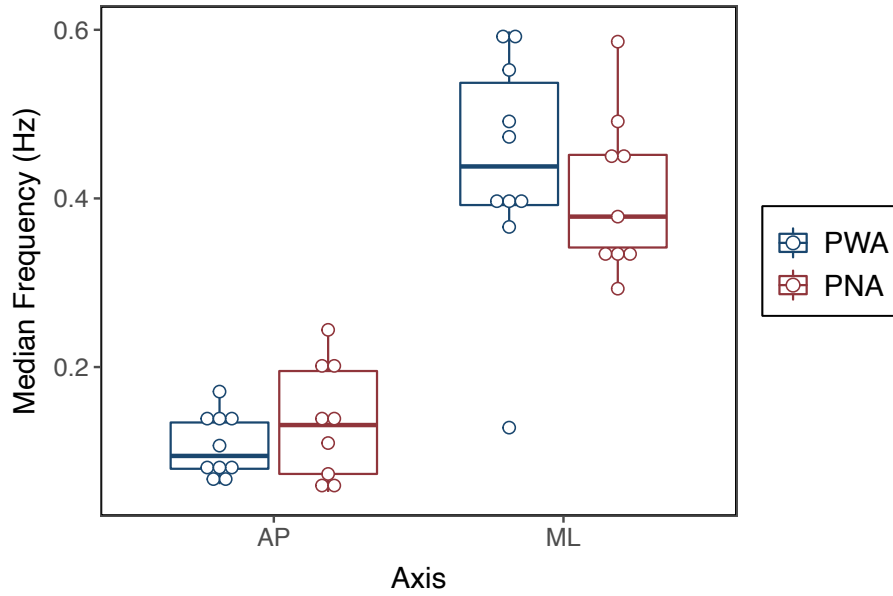
Figure 35. COP median power frequency (Hz) in the anteroposterior (AP) and mediolateral (ML) axes during unipedal stance with eyes open

5.3.3 Eyes Closed

The figures presented in the following subsections display trends in the outcome variables for a subset of participants who maintained unipedal stance with EC for at least five seconds (PWA, n=3; PNA, n=1). These participants were all males and tended to be of younger age and lower BMI compared to the group means. The PWA had no history of joint surgery, while the PNA underwent ankle tendon repair. PWA tended to have pain scores above the group median for the back, hip, and knee, while the PNA had higher back and ankle pain scores than the group median. The majority of these participants had higher balance confidence (ABC-6) than the group medians. One of three PWA experienced a fall over the past 12 months, while the PNA did not sustain a fall. All PWA had greater disability of the knee (KOOS, JR) than the group median, while two PWA had greater disability of the hip (HOOS, JR) and foot/ankle (Quick-FAAM) than the group median. The hip, knee, and foot/ankle disability scores for the PNA indicated optimal joint health.

5.3.3.1 Centre of Pressure 95% Prediction Ellipse Area

As shown in Figure 36, the COP 95% PEA during unipedal stance with EC trended higher for PWA than PNA.
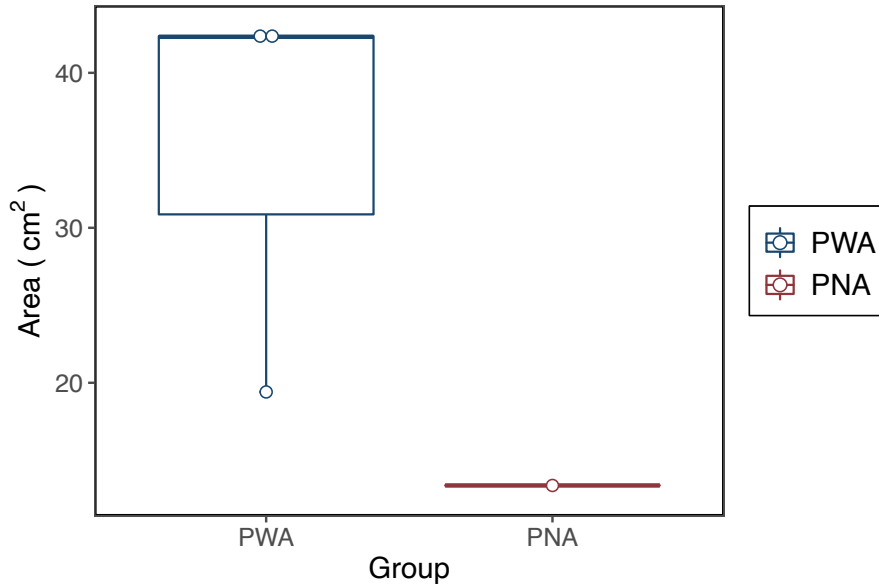
Figure 36. *COP 95% prediction ellipse area (cm²) during unipedal stance with eyes closed*

5.3.3.2 Centre of Pressure Range

Figure 37 indicated a greater COP range for PWA than PNA during unipedal stance with eyes closed in both the AP and ML axes.

115
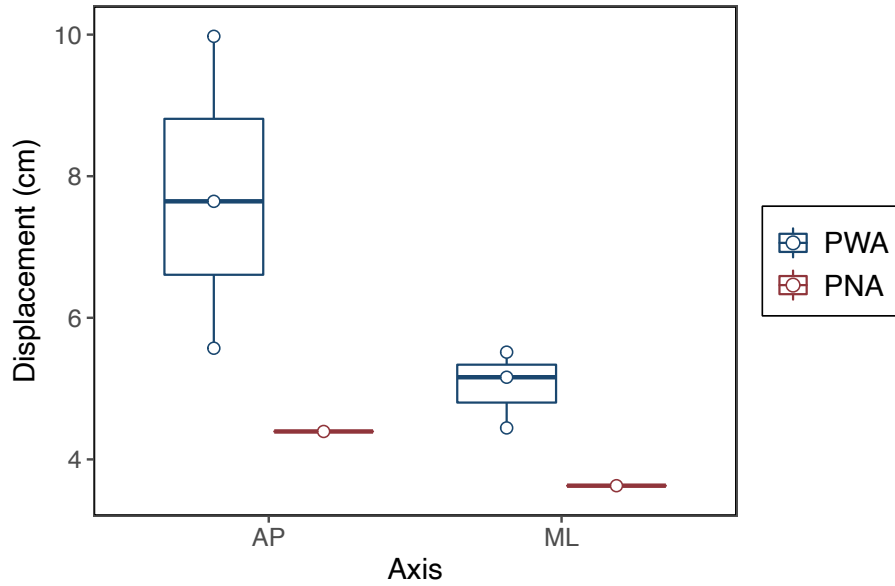
Figure 37. COP range (cm) in the anteroposterior (AP) and mediolateral (ML) axes during unipedal stance with eyes closed

5.3.3.3 Centre of Pressure Mean Velocity

COP mean velocity appeared similar between groups in both axes (Figure 38).
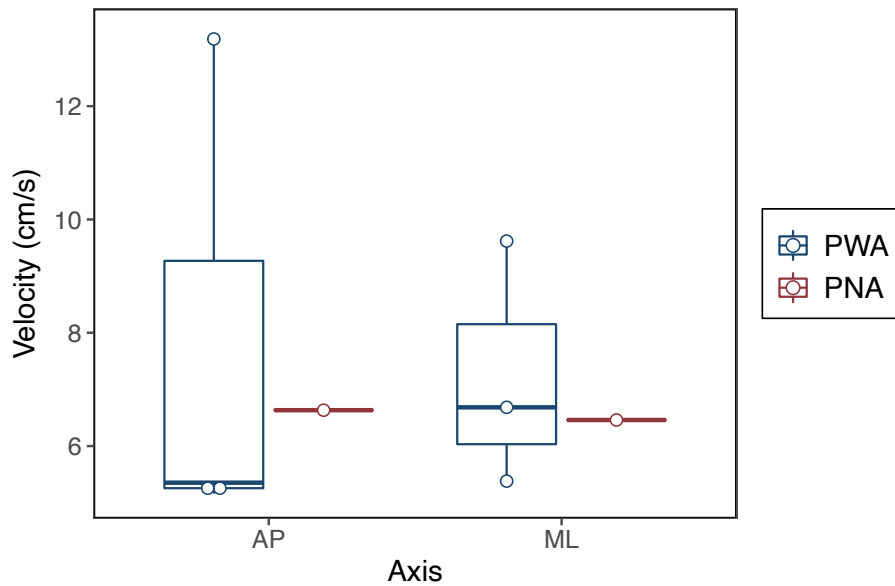
Figure 38. COP mean velocity (cm/s) in the anteroposterior (AP) and mediolateral (ML) axes during unipedal stance with eyes closed

5.3.3.4   Centre of Pressure Median Power Frequency

As seen in Figure 39, COP MPF was similar between groups in the AP and ML axes, with a higher MPF of COP in the ML axis than AP axis for both groups.
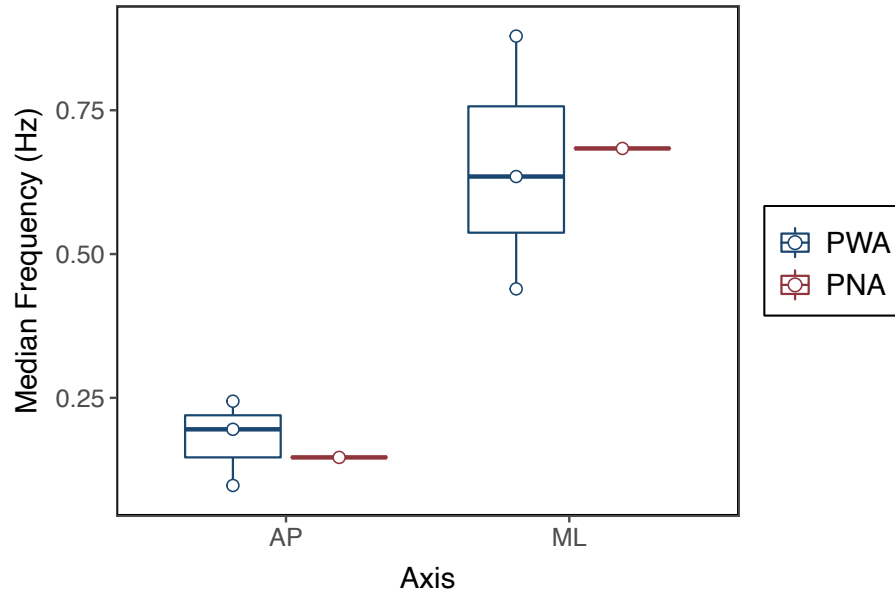
Figure 39. *COP median power frequency (Hz) in the anteroposterior (AP) and mediolateral (ML) axes during unipedal stance with eyes closed*

Chapter 6: Discussion

The aim of the present study was to determine if acromegaly had an effect on standing balance control. This aim was investigated using a study design that included a control group of PNA to control for the effects of the pituitary adenoma and included an EO and EC trial to control for the effect of vision while measuring COP and COM via synchronized force plate and motion capture analysis. The mechanisms of standing balance control were assessed not only through the manipulated variable of vision and the control group, but also by including outcome measures which are theorized to relate to different aspects of neuromuscular control of balance. While COP time domain parameters provide information regarding the extent or rate of body sway during standing balance, frequency domain parameters may help to elucidate the sensory mechanisms involved in balance control. Furthermore, assessment of the relationship between COP and COM can provide insight into the muscular control of the body's COM. Outcome measures were assessed for both bipedal and unipedal stance.

6.1   Bipedal Standing Balance

6.1.1   Centre of Pressure Time Domain Measures

Time domain parameters analyzed in the present study included COP 95% PEA, COP range, and COP mean velocity. COP 95% PEA was used to provide a measure of covariability of the AP and ML COP, while COP range was selected to indicate the variability of COP along the AP or ML axis. COP mean velocity was included to specify the rate of change in the COP position along the AP or ML axis.

In bipedal stance, a significant interaction between group and vision was found for AP COP mean velocity, where a greater increase in velocity with EC compared to EO was

observed for PWA than PNA, which was in support of the research hypothesis regarding the interaction of group and vision on standing balance control. Significant main effects of vision were found for ML COP range, AP COP mean velocity, and ML COP mean velocity, and independent of group, all three measures increased with EC compared to EO, which was in agreement with the research hypothesis regarding the main effect of vision. Additionally, there was a trend towards a main effect of vision for COP 95% PEA, with a larger sway area observed for EC compared to EO. In contrast to the research hypothesis, no significant main effect of group was found for any of the time domain COP parameters.

When comparing PWA to healthy controls, previous studies found significant differences in COP time domain measures between groups in EO with feet apart (Haliloglu et al., 2019; Homem et al., 2017; Lopes et al., 2014), EC with feet apart (Haliloglu et al., 2019), and EC with feet together (Homem et al., 2017; Lopes et al., 2014). In contrast, the present study found no group effects, with the exception of the interaction of group and vision for COP mean velocity in the AP axis. The predominant differences between the present study and previous studies is that the present study controlled for the effects of the pituitary adenoma by comparing PWA to a control group of PNA and the present study included only participants who underwent pituitary surgery and were in biochemical remission. The inclusion of PWA with active disease in prior studies may have revealed more severe balance impairments; however, depending on the cause of balance impairment, disease control could have little influence as some changes to musculoskeletal tissue in PWA have been shown to be irreversible (Biermasz et al., 2005; Claessen et al., 2012, 2015; Pelsma et al., 2021). Furthermore, the similarities between PWA and PNA in the present study may reveal that the balance impairments observed in previous studies of PWA could in part be related to lingering effects of the adenoma or adenoma removal surgery.

Previous studies of standing balance in PWA did not examine the interaction between acromegaly and vision; therefore, it is difficult to directly compare findings with the present study. When closing the eyes or when closing the eyes and concurrently narrowing the stance width, previous studies showed significant differences between PWA and healthy controls for measures of COP in the ML axis, but the measures of COP in the AP axis were not different between groups (Haliloglu et al., 2019; Homem et al., 2017; Lopes et al., 2014). In the present study, a significant interaction of effect group and vision was found in the AP axis, where AP COP mean velocity increased significantly more in PWA than PNA with EC compared to EO. This finding opposes all previous studies of balance in PWA and may indicate the need to control for effects of the pituitary adenoma to reveal additional mechanisms of balance impairment in PWA.

COP mean velocity has been shown to have greater reliability and greater ability to discern between different visual conditions than other COP parameters (Baig et al., 2012; Lafond et al., 2004). Additionally, this measure has been shown to discriminate between fallers and non-fallers (Pizzigalli et al., 2016; Quijoux et al., 2020). Therefore, based on the severe implications of falling, especially in clinical populations with increased levels of frailty, the significant interaction effect of group and vision on COP mean velocity should be considered clinically relevant.

Due to the main effect of vision on AP COP mean velocity, where velocity increased in EC compared to EO irrespective of group, visual impairment is unlikely as closing the eyes would theoretically decrease COP velocity for those with visual impairment. Furthermore, the larger increase in AP COP mean velocity with EC than EO in PWA compared to PNA may suggest that PWA have greater reliance on vision for the maintenance of quiet stance than PNA. Those with somatosensory or vestibular impairment

tend to reweight sensory information to prioritize the accurate sensory signals (Black et al., 1989). Somatosensory or vestibular impairment in PWA could potentially increase reliance on visual afferents and therefore increase COP velocity to a greater extent than PNA when visual feedback is absent.

Previous studies have suggested that increased sway in PWA may be related to impaired proprioception as a result of abnormal joint structure. However, joint receptors are only activated towards the end range of motion of a joint; therefore, they would not be involved in the control of quiet stance due to the small changes in joint position (Proske, 2023). If the argument was to be made that impaired somatosensory function influenced COP velocity in PWA, then it is more probable that it involves the muscle spindles, Golgi tendon organs, or plantar cutaneous receptors.

Hypertrophy and abnormal structure of muscles and tendons (Koçak, 2015; Mastaglia et al., 1970; Nagulesparen et al., 1976; Onal et al., 2016; Ozturk Gokce et al., 2020; Stern et al., 1974), and reduced muscular strength and endurance (Füchtbauer et al., 2017; Guedes da Silva et al., 2013; Homem et al., 2017; Walchan et al., 2016) have been reported in PWA. Although there is an absence of studies that examine muscle spindles and Golgi tendon organs in PWA, there is the potential that changes to muscle size and composition in PWA could alter the function of receptors located in the muscles and tendons of PWA. Several studies have found significantly thicker Achilles tendons in PWA compared to healthy controls (Colao et al., 1998; Koçak, 2015; Onal et al., 2016; Ozturk Gokce et al., 2020). Onal et al., (2016) found that Achilles tendons were significantly softer in PWA than healthy controls, which may suggest impaired passive and active stiffness of the plantar flexor muscles. Jamal (1987) noted that all PWA in their sample had absent ankle reflexes, which could suggest dysfunction of the Golgi tendon organs located in the tendons

that cross the ankle, perhaps related to the abnormal thickening or softening of the Achilles tendons in PWA. Furthermore, neuropathy of peripheral nerves may impair the transmission of sensory feedback from the cutaneous plantar receptors, muscle spindles, and Golgi tendon organs (Alibas et al., 2017; Ozata et al., 1997). Ozata et al. (1997) found greater latencies of the somatosensory evoked potentials in the tibial nerve in untreated PWA compared to controls, which is the nerve responsible for transmitting cutaneous information from the plantar surface of the foot. The link between AP COP velocity and plantar cutaneous sensation is supported by the findings of a study that examined the role of plantar cutaneous receptors in standing balance by using injections of local anaesthetic into the entire plantar surface of the foot (Meyer et al., 2004). The study revealed significant increases in AP COP velocity in EC but not EO conditions and no significant effect of impaired plantar cutaneous sensation on COP displacement, which are similar findings to the present study.

Vestibular function has not been addressed in the literature on acromegaly; however, there is a small body of literature that has performed audiological examinations of PWA. Although this research has not addressed vestibular function directly, some studies note hypertrophy of the temporal bone or otosclerosis, which could theoretically affect the function of middle or inner ear structures (Babic et al., 2006; Graham and Brackmann, 1978; Menzel, 1966; Richards, 1968). As overgrowth of facial bones is commonly reported in PWA (Abreu et al., 2016; Melmed, 2006; Reid et al., 2010), it may be worth investigating the vestibular function of PWA even if symptoms are not reported.

Lastly, PWA reported significantly higher pain scores for the back, hip, and knee than PNA. In a study of similar size to the present study, patients with low back pain exhibited a greater increase in AP COP mean velocity in more difficult stance conditions than healthy

participants, but no significant interaction of low back pain and task difficulty was found for ML COP mean velocity (Della Volpe et al., 2006). Although they found no significant differences between groups with EO or EC while standing on a stable surface, a trend could be observed where closing the eyes increased velocity for low back pain patients to a greater extent than healthy participants.

The absence of an interaction effect between group and vision or main effect of group on COP 95% PEA and AP and ML COP range suggests that there are similarities in balance control between PWA and PNA, which is in contrast to the research hypothesis. It should be noted that COP range has a high coefficient of variation (Doyle et al., 2005), likely due to the influence of noise on the magnitude of the COP range parameter. COP 95% PEA also has high degrees of error and may not be capable of detecting balance impairments specific to one axis of motion (Salavati et al., 2009). Although these findings may suggest similarities in balance performance between PWA and PNA, it is difficult to make any inferences regarding whether these balance parameters are within normal range without an additional control group of healthy participants. The high BMI in both groups would suggest greater instability compared to a normal BMI population (Hue et al., 2007; Neri et al., 2019; Teasdale et al., 2007); thus, comparison to a healthy population, who by definition typically have a normal BMI, would not allow for control of the effect of BMI on balance. Furthermore, it is difficult to find a set of normative values in the literature that come from a sample with similar BMI that are otherwise considered healthy.

It was hypothesized that there would be an effect of vision independent of group as many clinical populations are shown to have increased sway when closing the eyes (Caffaro et al., 2014; Da Silva et al., 2018; Masui et al., 2006). This hypothesis was supported by significant main effects of vision for AP and ML COP mean velocity and ML COP range.

These findings suggest that both groups of pituitary patients may not continue to experience significant visual impairment once the adenoma has been surgically removed. If visual impairment were present, increased sway with eyes open and decreased sway with eyes closed would likely be observed (Bednarczuk et al., 2021).

6.1.2   Centre of Pressure Median Power Frequency

Frequency analysis of the COP signal allows for discernment between different sensory mechanisms of balance control. For example, response to visual feedback has been proposed to primarily produce COP frequencies below 0.1 Hz (Dichgans and Brandt, 1978; Horak and Macpherson, 1996), while COP frequencies resulting from vestibular feedback are thought to occur below 0.5 Hz for the otolith organs (linear motion or head tilt) and in the range of 0.1-1 Hz for the semicircular canals (rotational motion) (Nashner, 1971; Nashner, 1972; Nashner et al., 1989). Somatosensory feedback is proposed to result in COP frequencies above 0.5 Hz, with frequencies above 1 Hz considered to be indicative of CNS dysfunction (Diener et al., 1984; Nashner et al., 1982; Oppenheim et al., 1999).

In the present study, no significant interactions of vision or group were found for COP MPF in either the AP or ML axis. There was a significant main effect of vision in the AP axis, in which AP COP MPF was significantly higher in EC than EO irrespective of group. No significant effect of group was found for either axis.

It was hypothesized that COP MPF would be significantly different between groups and the removal of visual feedback with EC would further differentiate groups. However, there were no interactions of group and vision or main effects of group for COP MPF in the AP or ML axis. This contradicts the finding of a significant interaction effect of vision and acromegaly on AP COP mean velocity, which suggested that there may be vestibular

or somatosensory impairment in PWA. Since mean velocity quantified the displacement per second of COP and MPF quantified the oscillations per second of COP, it is possible that PWA experienced the same number of oscillations per second as PNA but PWA had oscillations of higher amplitude than PNA, indicating a faster velocity of COP.

Closing the eyes has been shown to increase the MPF of the AP and ML COP power spectral densities in those with normal vision (Sozzi et al., 2021), which is in accordance with the theory that visual feedback produces lower frequencies of COP than feedback from other sensory systems. Increased MPF in EC compared to EO was observed in the AP axis but not the ML axis in the present study. Although the absence of difference between EO and EC COP MPF in the ML axis could indicate visual impairment, other findings of the present study are in disagreement. Future studies that compare the power across different frequency windows for various sensory conditions may be necessary to clarify the interpretation of this finding.

6.1.3   Comparison of Centre of Pressure and Centre of Mass

The relationship between the COP and COM can provide insight into the neuromuscular control of the body's COM. The present study performed a cross-correlation of COP and COM in the AP and ML axes to quantify the correlation and time lag between COP and COM. Additionally, the present study examined the difference between COP and COM in the AP and ML axes.

The correlation coefficient for the relationship between COP and COM in the AP axis was high (>0.9) in both groups with EO and EC. Despite the high correlation in both visual conditions, there was a significant main effect of vision, in which the correlation coefficient decreased with EC compared to EO independent of group. The median time lag

in both groups and visual conditions was zero, meaning that the COP and COM signals tended to be in phase with one another. No significant interaction of group and vision or main effect of group or vision was found for the time lag between COP and COM.

COP and COM signals have been shown to have a time lag of 4 ms in healthy participants (Winter et al., 1998). As the time resolution in the present study was 5 ms, the finding of no phase lag between COP and COM is in agreement with previous findings.

A previous study also explored the cross-correlation of COP and COM along the AP axis and the effect of vision on this correlation (Gatev et al., 1999). Similar to the present study, they found no time lag and a high positive correlation between COP and COM in the AP axis. However, they found no significant effect of vision on the correlation between COP and COM, which contradicts the findings of the present study. This further alludes to the previously proposed mechanism (see section 6.1.1) in which PWA and perhaps also PNA may experience dysfunction of the vestibular and/or somatosensory system. Vestibular or somatosensory dysfunction during quiet stance is thought to promote sensory re-weighting, in which greater dependency is placed on visual cues; therefore, the absence of visual feedback would influence balance control to a greater extent in individuals with vestibular or somatosensory dysfunction than individuals with normal sensory function (Black et al., 1988). However, without a healthy control group in the present study, it was difficult to determine if PWA and PNA show balance impairments that significantly differ from a healthy population.

In the AP axis, the present study found no interaction of group and vision on COP-COM. There was a trend towards a main effect of group, where PWA had a greater COP-COM than PNA, but there was no effect of vision. Although no interaction of group and vision or main effect of vision was found for ML COP-COM, a significant main effect of

126

group was revealed for COP-COM in the ML axis, which supports the research hypothesis regarding the main effect of group.

COP-COM has been referred to as the error in the balance control system and has been shown to be proportional to passive muscle stiffness and the horizontal acceleration of COM (Winter et al., 1998). Additionally, approximately half of the variance in COP-COM has been explained by somatosensory function in the AP axis and muscle strength in the ML axis (Corriveau et al., 2004). Furthermore, COP-COM has been shown to be discriminate between clinical populations and healthy controls, including diabetic neuropathy (Corriveau et al., 2000), visual impairment (Russo et al., 2017), and stroke (Corriveau et al., 2004).

PWA had significantly higher COP-COM in the ML axis and a trend towards higher COP-COM in the AP axis. Several variables could potentially explain this finding. Impaired plantar flexor muscle stiffness due to increased softness of Achilles tendons in PWA could increase the difference between COP and COM in the AP axis (Onal et al., 2016), while impaired somatosensory function due to peripheral neuropathy could explain increased COP-COM in both axes as observed in patients with diabetic neuropathy (Corriveau et al., 2000). The increase in COP-COM in the ML axis may be related to an impaired hip loading and unloading mechanism, possibly due to the significantly higher levels of low back and hip pain in PWA. The relationship between pain and an impaired frontal plane hip strategy while standing has been shown in patients with low back pain (Mok et al., 2004).

In the present study, both PWA and PNA had COP-COM values above those reported in healthy individuals. Hasan et al. (1996a) also calculated the mean absolute deviation of COP and COM and reported the mean values for six healthy, male, young

adults who each performed six 10-second trials of EO and EC bipedal stance. For EO, COP-COM was 0.48 mm in the ML axis and 0.82 mm in the AP axis, and for EC, COP-COM was 0.52 mm in the ML axis and 1.05 mm in the AP axis. In the present study, the mean values of COP-COM for each group were 5-20 times higher than the values reported by Hasan et al. (1996a). Furthermore, closing the eyes increased COP-COM to a greater extent in the ML axis than the AP axis in the present study, with almost no change between visual conditions in the AP axis, while Hasan et al. (1996a) found a greater increase in COP-COM with EC in the AP axis than ML axis.

In healthy participants, the COP will cross and overshoot the COM in each direction to control the COM position (see section 2.4.1). Therefore, the mean of the COP and COM trajectories are approximately equal despite the greater amplitude and frequency of COP. However, in the present study, many participants had COP and COM that never crossed in the AP axis. In approximately half of the participants, COP was always anterior to the COM, while in the other half, COP was always posterior to the COM. It was anticipated that participants with a larger BMI, who typically had more adiposity distributed on the anterior portion of the body around the abdomen, would have their COM anterior to their COP. However, although not significant, those with a larger BMI tended to have their COP anterior to their COM (Figure 45; Appendix G). This may reflect an error in the estimation of the COM as Hanavan's (1964) geometric model cannot account for additional mass distributed on the anterior portion of the trunk. This error would cause the COM estimate to be posterior to its true location and produce a greater difference between the COP and COM. For participants with COM anterior to COP, thoracic hyperkyphosis could be a possible explanation as it is highly prevalent in PWA (Cellini et al., 2021; de Azevedo Oliveira et al., 2019; Scarpa et al., 2004) and could shift the COM in the anterior direction.

128

6.2   *Unipedal Standing Balance*

6.2.1   Unipedal Stance Time

The present study did not find an interaction between group and vision or main effect of group on unipedal stance time; however, a significant main effect of vision indicated that independent of group, unipedal stance times were longer with EO than EC. A floor effect was observed for unipedal stance with eyes closed. All but four participants (PWA, n=3; PNA, n=1) were unable to hold unipedal stance for at least five seconds. Correlation analysis showed a significant relationship between unipedal stance time with age (see Figure 46, Appendix H), but not with BMI, height, weight, or sex of participants. This is in agreement with studies of healthy participants that show significantly shorter unipedal stance times in older adults compared to younger adults (da Silva et al., 2013).

Similar to the present study, Atmaca et al. (2013) found no significant difference in unipedal stance times between PWA and healthy controls. However, unipedal stance times were only recorded up to maximum of 30 seconds, which appeared to have created a ceiling effect in both groups.

Normative unipedal stance times for adults between the ages of 50-59 years, which is the age range represented by the mean age of participants in the present study, are 37 s for EO and 4.8 s with EC (Springer et al., 2007). With EO, PWA in the present study had above average unipedal stance times (*M*=54.1s; *SD*=30.8s), while PNA had similar stance times (*M*=34.7s; *SD*=24.8s) compared to normative values. In the EC condition, both groups had similar stance times to normative values (PWA, *M*=5.9s; *SD*=6.3s; PNA, *M*=3.7s; *SD*=2.4s). Therefore, it appears that PWA and PNA are similar to healthy

individuals in terms of their ability to maintain unipedal stance. However, unipedal stance times alone provide little information about unipedal balance control mechanisms.

6.2.2   Centre of Pressure Time and Frequency Domain Measures

COP range, mean velocity, and MPF in the AP and ML axes and COP 95% PEA were compared between PWA and PNA during EO unipedal stance. No significant effects of group were found for any COP measures during unipedal balance, which opposed the research hypothesis regarding a significant group effect.

The floor effect observed in both groups for unipedal stance with EC prevented analysis of the interaction of group and vision on COP measures of unipedal balance control. The absence of significant findings for unipedal stance could be due to the further reduction in sample size for unipedal balance trials; however, it is also possible that unipedal balance control is similar between PWA and PNA. Therefore, larger studies comparing unipedal stance in PWA and PNA are warranted.

Haliloglu et al. (2019) found significantly increased COP sway during unipedal stance in the AP and ML axes in PWA compared to healthy controls. However, PWA in the present study did not have significantly different COP range in the AP or ML axes compared to PNA. As the COP values were not reported in the previous study of PWA, comparison cannot be made with the COP range values obtained in the present study.

Compared to healthy younger adults and older adults (da Silva et al., 2013), PWA and PNA revealed COP 95% PEA values slightly closer to the values of healthy older adults than younger adults, which was expected as the majority of participants in the present study were middle age. Regarding COP mean velocity, the mean values for PWA and PNA in the AP and ML axes were lower than values for both healthy younger and older adults (da

Silva et al., 2013). Therefore, PWA and PNA appear to have a similar magnitude of sway to healthy populations, but the velocity of sway appears to be reduced in PWA and PNA.

6.3 *Balance Performance versus Balance Control*

In both bipedal and unipedal stance, PWA and PNA did not exhibit differences in measures of balance performance. This is in contrast to previous studies which have shown worse balance performance in PWA compared to healthy controls (Haliloglu et al., 2019; Homem et al., 2017; Lopes et al., 2014). Since the present study controlled for both the effects of the pituitary adenoma and active acromegaly, it is possible that the reduction in balance performance observed in previous studies was related to one or both of these effects.

In contrast to the findings for balance performance, PWA and PNA revealed differences in balance control for bipedal stance. This may suggest that in PWA, balance control is influenced by previous exposure to excess GH and IGF-1 since factors related to the pituitary adenoma and active disease were controlled in the present study. Contrary to bipedal stance, unipedal stance did not reveal any differences in balance control between groups. This could be related to the difference in muscular control strategies between bipedal and unipedal stance (García-Massó et al., 2016; Tropp and Odenrick, 1988). It should also be noted that the unipedal analysis had a smaller sample size, did not analyze the interaction of acromegaly and vision, and did not explore the relationship between COP and COM.

6.4   *Limitations*

The predominant limitation of the present study was the underpowered statistical analysis. A larger sample size may indicate significant effects that were missed or observed as trends in the present study.

The present study showed some similarities between PWA and PNA; however, without the addition of a healthy control group, it was difficult to discern whether patients with pituitary adenomas experience differences in balance control from a healthy population.

Although vision was manipulated in the present study, other sensory challenges were not included. Since somatosensory conditions, such as compliance of the support surface, were not manipulated in the present analysis, it was difficult to discern which sensory system was responsible for the increased AP COP velocity in PWA with EC.

This was the first study to perform a kinematic analysis of COM in PWA and PNA. Therefore, the validity of anthropometric models used to derive COM have not been evaluated in PWA or PNA. Dempster's regression equations (1955) are known to poorly estimate body segment parameters in young to middle-age adults, obese individuals, and females as the equations were derived using the anthropometric measurements of a sample of cadavers from Caucasian, male, older adults with low body mass (Durkin and Dowling, 2003). Furthermore, the segment inertial properties in Hanavan's geometric model (1964) are not representative of different body types as segment inertial properties vary by body composition and body mass distribution (Durkin and Dowling, 2003; Matrangola et al., 2008). As the present study contained both male and female participants with a high BMI, the validity of these models in the study population may be poor. Furthermore, due to hypertrophy and irregular composition of somatic tissues in PWA, there is the potential that

the inertial properties defined in these anthropometric models may not be generalizable to the acromegaly population.

The present study modelled the body as 14 rigid segments. The rigid segment assumption is fairly valid for a bony segment without moveable joints. However, in the present study, a few segments containing multiple joints were assumed to be rigid, including the joints of the head and cervical spine modelled as a single head segment and the joints of the thoracic and lumbar spine modelled as a single trunk segment. Therefore, the position of the COM may not accurately capture all changes in body position.

Soft-tissue artifact is a significant source of error in motion capture analysis and occurs due to movement of soft-tissues (e.g., skin, muscle, adipose tissue) that produces relative motion of the markers with respect to the underlying bone (Cappozzo et al., 1996). Soft-tissue artifact increases with an increase in BMI, especially for markers placed on the anterior superior iliac spines (Camomilla et al., 2017). Therefore, the COM estimates in the present study were likely limited by soft-tissue artifact.

6.5   *Future Directions*

Larger studies are necessary to further understand the relationship between acromegaly and standing balance control and the mechanisms involved. Biomechanical data collection and reduction are time demanding processes, thus sample sizes tend to be small. Furthermore, recruitment of PWA can be difficult due to the small population. To ease this difficulty, a multicentre study that recruits from several healthcare centres and performs data collection in several biomechanics laboratories would allow for a larger sample size and perhaps a more diverse sample of PWA.

In order to reveal neuromuscular mechanisms of balance control, future studies should manipulate variables related to different types of sensory feedback and consider including perturbations. Including the manipulation of both visual and somatosensory variables may help decipher whether PWA have sensory dysfunction and if so, which sensory systems are affected. The addition of anticipatory movements (e.g., voluntary movement of the arm) and external perturbations (e.g., unexpected push) that require feedforward and reactive balance control, respectively, may be necessary to observe deficits in neuromuscular control of standing balance in PWA (Horak and Macpherson, 1996). Finally, analyses that compare the total power in different frequency ranges of the COP power spectral density between various sensory conditions may provide further insight into mechanisms of standing balance control in PWA.

Chapter 7: Conclusion

The present study explored several novel aspects of standing balance control in PWA. This study was the first to perform a kinematic analysis of standing balance in PWA and thus, the first to examine the relationship between the trajectories of the COP and COM in PWA. Additionally, this was the first study to analyze the power spectrum of COP in PWA, which provided new insights into the sensory mechanisms of balance control in PWA. Finally, by using a control group of PNA, the present study was able to control for effects of the pituitary adenoma and its removal surgery on standing balance.

The findings of the present study suggest that PWA may experience impaired control of bipedal standing balance, particularly in the AP axis with EC and in the ML axis. Measures of bipedal and unipedal balance performance and unipedal balance control indicated similarities in standing balance between PWA and PNA. Larger studies that manipulate several sensory variables and that include an additional healthy control group are necessary to elucidate the neuromuscular mechanisms of standing balance control in PWA.

References

Aagaard, P., Andersen, J.L., Dyhre-Poulsen, P., Leffers, A., Wagner, A., Magnusson, S.P., Halkjær-Kristensen, J., Simonsen, E.B., 2001. A mechanism for increased contractile strength of human pennate muscle in response to strength training: changes in muscle architecture. The Journal of Physiology 534, 613–623. https://doi.org/10.1111/j.1469-7793.2001.t01-1-00613.x

Åberg, A.C., Thorstensson, A., Tarassova, O., Halvorsen, K., 2011. Calculations of mechanisms for balance control during narrow and single-leg standing in fit older adults: A reliability study. Gait & Posture 34, 352–357. https://doi.org/10.1016/j.gaitpost.2011.05.025

Abreu, A., Tovar, A., Castellanos, R., Valenzuela, A., Giraldo, C., Pinedo, A., Guerrero, D., Barrera, C., Franco, H., Ribeiro-Oliveira Jr., A., Vilar, L., Jallad, R., Duarte, F., Duarte, M., Boguszewski, C., Abucham, J., Naves, L., Musolino, N., de Faria, M., Rossato, C., Bronstein, M., 2016. Challenges in the diagnosis and management of acromegaly: a focus on comorbidities. Pituitary 19, 448–57. https://doi.org/10.1007/s11102-016-0725-2

Adbel-Aziz, Y., Karara, H., 1971. Direct Linear Transformation from Comparator Coordinates into Object Space in Close-Range Photogrammetry. Presented at the Proceedings of the Symposium on Close-Range Photogrammetry, Urbana, Illinois, pp. 1–18.

Akkaya, M., Pignataro, A., Sandiford, N., Gehrke, T., Citak, M., 2022. Clinical and functional outcome of total hip arthroplasty in patients with acromegaly: mean twelve year follow-up. International Orthopaedics (SICOT) 46, 1741–1747. https://doi.org/10.1007/s00264-022-05447-5

Alibas, H., Gogas Yavuz, D., Kahraman Koytak, P., Uygur, M., Tanridag, T., Uluc, K., 2017. Peripheral nervous system assessment in acromegaly patients under somatostatin analogue therapy. J Endocrinol Invest 40, 33–40. https://doi.org/10.1007/s40618-016-0522-9

Altman, R., Alarcon, G., Appelrouth, D., Bloch, D., Borenstein, D., Brandt, K., Brown, C., Cooke, T., Daniel, W., Gray, R., 1990. The American College of Rheumatology criteria for the classification and reporting of osteoarthritis of the hand. Arthritis & Rheumatism: Official Journal of the American College of Rheumatology 33, 1601–1610.

Altman, R., Alarcón, G., Appelrouth, D., Bloch, D., Borenstein, D., Brandt, K., Brown, C., Cooke, T.D., Daniel, W., Feldman, D., Greenwald, R., Hochberg, M., Howell, D., Ike, R., Kapila, P., Kaplan, D., Koopman, W., Marino, C., McDonald, E., McShane, D.J., Medsger, T., Michel, B., Murphy, W.A., Osial, T., Ramsey-Goldman, R., Rothschild, B., Wolfe, F., 1991. The American College of Rheumatology criteria for the classification and reporting of osteoarthritis of the hip. Arthritis & Rheumatism 34, 505–514. https://doi.org/10.1002/art.1780340502

Altman, R., Asch, E., Bloch, D., Bole, G., Borenstein, D., Brandt, K., Christy, W., Cooke, T.D., Greenwald, R., Hochberg, M., Howell, D., Kaplan, D., Koopman, W., Longley III, S., Mankin, H., McShane, D.J., Medsger Jr., T., Meenan, R., Mikkelsen, W., Moskowitz, R., Murphy, W., Rothschild, B., Segal, M., Sokoloff, L., Wolfe, F., 1986. Development of criteria for the classification and reporting of osteoarthritis: Classification of osteoarthritis of the knee. Arthritis & Rheumatism 29, 1039–1049. https://doi.org/10.1002/art.1780290816

Altman, R.D., Hochberg, M., Murphy, W.A.J., Wolfe, F., Lequesne, M., 1995. Atlas of individual radiographic features in osteoarthritis. Osteoarthritis Cartilage 3 Suppl A, 3–70.

Anderson, L.L., Jeftinija, S., Scanes, C.G., 2004. Growth Hormone Secretion: Molecular and Cellular Mechanisms and In Vivo Approaches. Exp Biol Med (Maywood) 229, 291–302. https://doi.org/10.1177/153537020422900403

Atmaca, A., Tander, B., Kan, E., Ulus, Y., Ecemis, G., Akyol, Y., Tomak, L., 2013. Assessment of balance performance and fear of falling in acromegalic patients: a comparative study. J Endocrinol Invest 36, 759–63. https://doi.org/10.3275/8944

Aydin, K., Ozturk, B., Turkyilmaz, M.D., Dagdelen, S., Ozgen, B., Unal, F., Erbas, T., 2012. Functional and structural evaluation of hearing in acromegaly. Clinical Endocrinology 76, 415–419. https://doi.org/10.1111/j.1365-2265.2011.04209.x

Babic, B.B., Petakov, M.S., Djukic, V.B., Ognjanovic, S.I., Arsovic, N.A., Isailovic, T.V., Milovanovic, J.D., Macut, D., Damjanovic, S.S., 2006. Conductive Hearing Loss in Patients with Active Acromegaly. Otology & Neurotology 27, 865–870. https://doi.org/10.1097/01.mao.0000201429.57746.1b

Baig, S., Dansereau, R.M., Chan, A.D.C., Remaud, A., Bilodeau, M., 2012. Cluster Analysis of Center-of-Pressure Measures. IJECS. https://doi.org/10.11159/ijecs.2012.002

Baylan, M.Y., Gokalp, D., Celik, Y., Tuzcu, A., Meric, F., Topcu, I., 2011. Audiological Findings in Acromegaly Patients. Int. Adv. Otol. 7, 87–90.

Bednarczuk, G., Wiszomirska, I., Rutkowska, I., Skowroński, W., 2021. Role of vision in static balance in persons with and without visual impairments. Eur J Phys Rehabil Med 57. https://doi.org/10.23736/S1973-9087.21.06425-X

Bell, A.L., Brand, R.A., Pedersen, D.R., 1989. Prediction of hip joint centre location from external landmarks. Human Movement Science 8, 3–16. https://doi.org/10.1016/0167-9457(89)90020-1

Bellamy, N., Buchanan, W.W., Goldsmith, C.H., Campbell, J., Stitt, L.W., 1988. Validation study of WOMAC: a health status instrument for measuring clinically important patient relevant outcomes to antirheumatic drug therapy in patients with osteoarthritis of the hip or knee. Journal of rheumatology.

Bellamy, N., Campbell, J., Haraoui, B., Gerecz-Simon, E., Buchbinder, R., Hobby, K., MacDermid, J.C., 2002. Clinimetric properties of the AUSCAN Osteoarthritis Hand Index: an evaluation of reliability, validity and responsiveness. Osteoarthritis and Cartilage 10, 863–869. https://doi.org/10.1053/joca.2002.0838

Berelowitz, M., Szabo, M., Frohman, L.A., Firestone, S., Chu, L., Hintz, R.L., 1981. Somatomedin-C Mediates Growth Hormone Negative Feedback by Effects on Both the Hypothalamus and the Pituitary. Science 212, 1279–1281. https://doi.org/10.1126/science.6262917

Biermasz, N., Pereira, A., Smit, J., Romijn, J., Roelfsema, F., 2005. Morbidity after long-term remission for acromegaly: persisting joint-related complaints cause reduced quality of life. J Clin Endocrinol Metab 90, 2731–9. https://doi.org/10.1210/jc.2004-2297

Biermasz, N., van 't Klooster, R., Wassenaar, M., Malm, S., Claessen, K., Nelissen, R., Roelfsema, F., Pereira, A., Kroon, H., Stoel, B., Romijn, J., Kloppenburg, M., 2012. Automated image analysis of hand radiographs reveals widened joint spaces in patients with long-term control of acromegaly: relation to disease activity and symptoms. Eur J Endocrinol 166, 407–13. https://doi.org/10.1530/EJE-11-0795

Biermasz, N., Wassenaar, M., van der Klaauw, A., Pereira, A., Smit, J., Roelfsema, F., Wolterbeek, R., Kroon, H., Kloppenburg, M., Romijn, J., 2009. Pretreatment insulin-like growth factor-I concentrations predict radiographic osteoarthritis in acromegalic patients with long-term cured disease. J Clin Endocrinol Metab 94, 2374–9. https://doi.org/10.1210/jc.2008-2393

Bigland, B., Jehring, B., 1952. Muscle performance in rats, normal and treated with growth hormone. The Journal of Physiology 116, 129–136. https://doi.org/10.1113/jphysiol.1952.sp004694

Bingham, J.T., Choi, J.T., Ting, L.H., 2011. Stability in a frontal plane model of balance requires coupled changes to postural configuration and neural feedback control. Journal of Neurophysiology 106, 437–448. https://doi.org/10.1152/jn.00010.2011

Black, F.O., Peterka, R.J., Shupert, C.L., Nashner, L.M., 1989. Effects of Unilateral Loss of Vestibular Function on the Vestibulo-Ocular Reflex and Postural Control. Ann Otol Rhinol Laryngol 98, 884–889. https://doi.org/10.1177/000348948909801109

Black, F.O., Shupert, C.L., Horak, F.B., Nashner, L.M., 1988. Abnormal postural control associated with peripheral vestibular disorders, in: Pompeiano, O., Allum, J.H.J. (Eds.), Progress in Brain Research. Elsevier, pp. 263–275. https://doi.org/10.1016/S0079-6123(08)64513-6

Bluestone, R., Bywaters, E.G., Hartog, M., Holt, P.J., Hyde, S., 1971. Acromegalic arthropathy. Ann Rheum Dis 30, 243–258. https://doi.org/10.1136/ard.30.3.243

Bohl, A.A., Fishman, P.A., Ciol, M.A., Williams, B., LoGerfo, J., Phelan, E.A., 2010. A Longitudinal Analysis of Total 3-Year Healthcare Costs for Older Adults Who Experience a Fall Requiring Medical Care. Journal of the American Geriatrics Society 58, 853–860. https://doi.org/10.1111/j.1532-5415.2010.02816.x

Bolfi, F., Neves, A.F., Boguszewski, C.L., Nunes-Nogueira, V.S., 2018. Mortality in acromegaly decreased in the last decade: a systematic review and meta-analysis. European Journal of Endocrinology 179, 59–71. https://doi.org/10.1530/EJE-18-0255

Buczek, F.L., Rainbow, M.J., Cooney, K.M., Walker, M.R., Sanders, J.O., 2010. Implications of using hierarchical and six degree-of-freedom models for normal gait analyses. Gait & Posture 31, 57–63. https://doi.org/10.1016/j.gaitpost.2009.08.245

Burns, E.R., Stevens, J.A., Lee, R., 2016. The direct costs of fatal and non-fatal falls among older adults — United States. Journal of Safety Research 58, 99–103. https://doi.org/10.1016/j.jsr.2016.05.001

Butenschoen, V.M., Schwendinger, N., Von Werder, A., Bette, S., Wienke, M., Meyer, B., Gempt, J., 2021. Visual acuity and its postoperative outcome after transsphenoidal adenoma resection. Neurosurg Rev 44, 2245–2251. https://doi.org/10.1007/s10143-020-01408-x

Caffaro, R.R., França, F.J.R., Burke, T.N., Magalhães, M.O., Ramos, L.A.V., Marques, A.P., 2014. Postural control in individuals with and without non-specific chronic low back pain: a preliminary case–control study. Eur Spine J 23, 807–813. https://doi.org/10.1007/s00586-014-3243-9

Camomilla, V., Bonci, T., Cappozzo, A., 2017. Soft tissue displacement over pelvic anatomical landmarks during 3-D hip movements. Journal of Biomechanics 62, 14–20. https://doi.org/10.1016/j.jbiomech.2017.01.013

Cappozzo, A., Cappello, A., Croce, U.D., Pensalfini, F., 1997. Surface-marker cluster design criteria for 3-D bone movement reconstruction. IEEE Trans. Biomed. Eng. 44, 1165–1174. https://doi.org/10.1109/10.649988

Cappozzo, A., Catani, F., Leardini, A., Benedetti, M., Della Croce, U., 1996. Position and orientation in space of bones during movement: experimental artefacts. Clinical Biomechanics 11, 90–100. https://doi.org/10.1016/0268-0033(95)00046-1

Carpenter, M.G., Frank, J.S., Winter, D.A., Peysar, G.W., 2001. Sampling duration effects on centre of pressure summary measures. Gait & Posture 13, 35–40. https://doi.org/10.1016/S0966-6362(00)00093-X

Casadio, M., Morasso, P.G., Sanguineti, V., 2005. Direct measurement of ankle stiffness during quiet standing: implications for control modelling and clinical application. Gait & Posture 21, 410–424. https://doi.org/10.1016/j.gaitpost.2004.05.005

Castle-Kirszbaum, M., Wang, Y.Y., King, J., Goldschlager, T., 2022. Predictors of visual and endocrine outcomes after endoscopic transsphenoidal surgery for pituitary adenomas. Neurosurg Rev 45, 843–853. https://doi.org/10.1007/s10143-021-01617-y

Cellini, M., Biamonte, E., Mazza, M., Trenti, N., Ragucci, P., Milani, D., Ferrante, E., Rossini, Z., Lavezzi, E., Sala, E., Mantovani, G., Arosio, M., Fornari, M., Balzarini, L., Lania, A.G., Mazziotti, G., 2021. Vertebral Fractures Associated with Spinal Sagittal Imbalance and Quality of Life in Acromegaly: A Radiographic Study with EOS 2D/3D Technology. Neuroendocrinology 111, 775–785. https://doi.org/10.1159/000511811

Chesnin, K.J., Selby-Silverstein, L., Besser, M.P., 2000. Comparison of an in-shoe pressure measurement device to a force plate: concurrent validity of center of pressure measurements. Gait and Posture.

Chevalier, T.L., Hodgins, H., Chockalingam, N., 2010. Plantar pressure measurements using an in-shoe system and a pressure platform: A comparison. Gait & Posture 31, 397–399. https://doi.org/10.1016/j.gaitpost.2009.11.016

Claessen, K., Canete, A., de Bruin, P., Pereira, A., Kloppenburg, M., Kroon, H., Biermasz, N., 2017. Acromegalic arthropathy in various stages of the disease: an MRI study. Eur J Endocrinol 176, 779–790. https://doi.org/10.1530/EJE-16-1073

Claessen, K., Kloppenburg, M., Kroon, H., Romijn, J., Pereira, A., Biermasz, N., 2013. Two phenotypes of arthropathy in long-term controlled acromegaly? A comparison between patients with and without joint space narrowing (JSN). Growth Horm IGF Res 23, 159–64. https://doi.org/10.1016/j.ghir.2013.05.003

Claessen, K., Mazziotti, G., Biermasz, N., Giustina, A., 2016. Bone and Joint Disorders in Acromegaly. Neuroendocrinology 103, 86–95. https://doi.org/10.1159/000375450

Claessen, K., Ramautar, S., Pereira, A., Romijn, J., Kroon, H., Kloppenburg, M., Biermasz, N., 2014. Increased clinical symptoms of acromegalic arthropathy in patients with long-term disease control: a prospective follow-up study. Pituitary 17, 44–52. https://doi.org/10.1007/s11102-013-0464-6

Claessen, K., Ramautar, S., Pereira, A., Smit, J., Barbe, F., Romijn, J., Kroon, H., Kloppenburg, M., Biermasz, N., 2012. Progression of acromegalic arthropathy despite long-term biochemical control: a prospective, radiological study. Eur J Endocrinol 167, 235–44. https://doi.org/10.1530/EJE-12-0147

Claessen, K.M., Pereira, A.M., Biermasz, N.R., 2015. Outcome of complications in acromegaly patients after long-term disease remission. Expert Review of Endocrinology & Metabolism 10, 499–510. https://doi.org/10.1586/17446651.2015.1068116

Cohen, A.R., Cooper, P.R., Kupersmith, M.J., Flamm, E.S., Ransohoff, J., 1985. Visual recovery after transsphenoidal removal of pituitary adenomas. Neurosurgery 17, 446–452.

Colao, A., Cannavo, S., Marzullo, P., Pivonello, R., Squadrito, S., Vallone, G., Almoto, B., Bichisao, E., Trimarchi, F., Lombardi, G., 2003. Twelve months of treatment with octreotide-LAR reduces joint thickness in acromegaly. Eur J Endocrinol 148, 31–8. https://doi.org/10.1530/eje.0.1480031

Colao, A., Ferone, D., Marzullo, P., Lombardi, G., 2004. Systemic complications of acromegaly: epidemiology, pathogenesis, and management. Endocr Rev 25, 102–52. https://doi.org/10.1210/er.2002-0022

Colao, A., Marzullo, P., Vallone, G., Giaccio, A., Ferone, D., Rossi, E., Scarpa, R., Smaltino, F., Lombardi, G., 1999. Ultrasonographic evidence of joint thickening reversibility in acromegalic patients treated with lanreotide for 12 months: Reversibility of acromegalic arthropathy. Clinical Endocrinology 51, 611–618. https://doi.org/10.1046/j.1365-2265.1999.00851.x

Colao, A., Marzullo, P., Vallone, G., Marino, V., Annecchino, M., Ferone, D., Lombardi, G., 1998. Reversibility of Joint Thickening in Acromegalic Patients: An Ultrasonography Study. Journal of Clinical Endocrinology and Metabolism 83, 2121–2125.

Collins, T.D., Ghoussayni, S.N., Ewins, D.J., Kent, J.A., 2009. A six degrees-of-freedom marker set for gait analysis: repeatability and comparison with a modified Helen Hayes set. Gait & posture 30, 173–180.

Constantin, T., Tangpricha, V., Shah, R., Oyesiku, N.M., Ioachimescu, O.C., Ritchie, J., Ioachimescu, A.G., 2017. Calcium and Bone Turnover Markers in Acromegaly: A Prospective, Controlled Study. The Journal of Clinical Endocrinology & Metabolism 102, 2416–2424. https://doi.org/10.1210/jc.2016-3693

Corriveau, H., Hébert, R., Prince, F., Raîche, M., 2000. Intrasession reliability of the "center of pressure minus center of mass" variable of postural control in the healthy elderly. Archives of Physical Medicine and Rehabilitation 81, 45–48. https://doi.org/10.1016/S0003-9993(00)90220-X

Corriveau, H., Hébert, R., Raîche, M., Dubois, M.-F., Prince, F., 2004a. Postural stability in the elderly: empirical confirmation of a theoretical model. Archives of Gerontology and Geriatrics 39, 163–177. https://doi.org/10.1016/j.archger.2004.03.001

Corriveau, H., Hébert, R., Raîche, M., Prince, F., 2004b. Evaluation of postural stability in the elderly with stroke. Archives of Physical Medicine and Rehabilitation 85, 1095–1101. https://doi.org/10.1016/j.apmr.2003.09.023

Corriveau, H., Prince, F., Hébert, R., Raîche, M., Tessier, D., Maheux, P., Ardilouze, J.L., 2000. Evaluation of postural stability in elderly with diabetic neuropathy. Diabetes Care 23, 1187–1191. https://doi.org/10.2337/diacare.23.8.1187

da Silva, R.A., Bilodeau, M., Parreira, R.B., Teixeira, D.C., Amorim, C.F., 2013. Age-related differences in time-limit performance and force platform-based balance measures during one-leg stance. Journal of Electromyography and Kinesiology 23, 634–639. https://doi.org/10.1016/j.jelekin.2013.01.008

Da Silva, R.A., Vieira, E.R., Carvalho, C.E., Oliveira, M.R., Amorim, C.F., Neto, E.N., 2016. Age-related differences on low back pain and postural control during one-leg stance: a case–control study. Eur Spine J 25, 1251–1257. https://doi.org/10.1007/s00586-015-4255-9

Da Silva, R.A., Vieira, E.R., Fernandes, K.B.P., Andraus, R.A., Oliveira, M.R., Sturion, L.A., Calderon, M.G., 2018. People with chronic low back pain have poorer balance than controls in challenging tasks. Disability and Rehabilitation 40, 1294–1300. https://doi.org/10.1080/09638288.2017.1294627

Davis, J.R., Campbell, A.D., Adkin, A.L., Carpenter, M.G., 2009. The relationship between fear of falling and human postural control. Gait & Posture 29, 275–279. https://doi.org/10.1016/j.gaitpost.2008.09.006

Day, B.L., Steiger, M.J., Thompson, P.D., Marsden, C.D., 1993. Effect of vision and stance width on human body motion when standing: implications for afferent control of lateral sway. The Journal of Physiology 469, 479–499. https://doi.org/10.1113/jphysiol.1993.sp019824

de Azevedo Oliveira, B., Araujo, B., dos Santos, T.M., Ongaratti, B.R., Rech, C.G.S.L., Ferreira, N.P., Pereira-Lima, J.F.S., da Costa Oliveira, M., 2019. The acromegalic spine: fractures, deformities and spinopelvic balance. Pituitary 22, 601–606. https://doi.org/10.1007/s11102-019-00991-7

DeBerardinis, J., Neilsen, C., Lidstone, D.E., Dufek, J.S., Trabia, M.B., 2020. A comparison of two techniques for center of pressure measurements. Journal of Rehabilitation and Assistive Technologies Engineering 7, 205566832092106. https://doi.org/10.1177/2055668320921063

Degache, F., Goy, Y., Vat, S., Haba Rubio, J., Contal, O., Heinzer, R., 2016. Sleep-disordered breathing and daytime postural stability. Thorax 71, 543–548. https://doi.org/10.1136/thoraxjnl-2015-207490

Dekkers, O.M., Biermasz, N.R., Pereira, A.M., Romijn, J.A., Vandenbroucke, J.P., 2008. Mortality in Acromegaly: A Metaanalysis. The Journal of Clinical Endocrinology & Metabolism 93, 61–67. https://doi.org/10.1210/jc.2007-1191

Della Volpe, R., Popa, T., Ginanneschi, F., Spidalieri, R., Mazzocchio, R., Rossi, A., 2006. Changes in coordination of postural control during dynamic stance in chronic low back pain patients. Gait & Posture 24, 349–355. https://doi.org/10.1016/j.gaitpost.2005.10.009

Dempster, W.T. (Wilfrid T., 1955. Space requirements of the seated operator : geometrical, kinematic, and mechanical aspects of the body, with special reference to the limbs.

Denko, C., Boja, B., Moskowitz, R., 1990. Growth promoting peptides in osteoarthritis: insulin, insulin-like growth factor-1, growth hormone. The Journal of Rheumatology 17, 1217–1221.

Denko, C.W., Boja, B., Moskowitz, R.W., 1996. Growth factors, insulin-like growth factor-1 and growth hormone, in synovial fluid and serum of patients with rheumatic disorders. Osteoarthritis and Cartilage 4, 245–249. https://doi.org/10.1016/S1063-4584(05)80102-5

Derrick, T.R., Thomas, J.M., 2004. Time-Series Analysis: The cross-correlation function, in: Stergiou, N. (Ed.), Innovative Analyses of Human Movement. Human Kinetics Publishers, Champaign, Illinois, pp. 189–205.

Detenbeck, L.C., Tressler, H.A., O'Duffy, J.D., Randall, R.V., 1973. Peripheral joint manifestations of acromegaly. Clin Orthop Relat Res 119–127. https://doi.org/10.1097/00003086-197303000-00017

Dichgans, J., Brandt, T., 1978. Visual-Vestibular Interaction: Effects on Self-Motion Perception and Postural Control, in: Anstis, S.M., Atkinson, J., Blakemore, C., Braddick, O., Brandt, T., Campbell, F.W., Coren, S., Dichgans, J., Dodwell, P.C., Eimas, P.D., Foley, J.M., Fox, R., Ganz, L., Garrett, M., Gibson, E.J., Girgus, J.S., Haith, M.M., Hatwell, Y., Hilgard, E.R., Ingle, D., Johansson, G., Julesz, B., Konishi, M., Lackner, J.R., Levinson, E., Liberman, A.M., Maffei, L., Oyama, T., Pantle, A., Pöppel, E., Sekuler, R., Stromeyer, C.F., Studdert-Kennedy, M., Teuber, H.-L., Yin, R.K., Held, R., Leibowitz, H.W., Teuber, Hans-Lukas (Eds.), Perception. Springer Berlin Heidelberg, Berlin, Heidelberg, pp. 755–804. https://doi.org/10.1007/978-3-642-46354-9_25

Diener, H.C., Dichgans, J., Guschlbauer, B., Mau, H., 1984. The significance of proprioception on postural stabilization as assessed by ischemia. Brain Research 296, 103–109. https://doi.org/10.1016/0006-8993(84)90515-8

Dinn, J.J., Dinn, E.I., 1985. Natural History of Acromegalic Peripheral Neuropathy. Quarterly Journal of Medicine 57, 833–842.

Dixit, M., Poudel, S.B., Yakar, S., 2021. Effects of GH/IGF axis on bone and cartilage. Molecular and Cellular Endocrinology 519, 111052. https://doi.org/10.1016/j.mce.2020.111052

Do, M.T., Chang, V.C., Kuran, N., Thompson, W., 2015. Fall-related injuries among Canadian seniors, 2005–2013: an analysis of the Canadian Community Health Survey. Health Promot Chronic Dis Prev Can 35, 99–108.

Doessing, S., Holm, L., Heinemeier, K.M., Feldt-Rasmussen, U., Schjerling, P., Qvortrup, K., Larsen, J.O., Nielsen, R.H., Flyvbjerg, A., Kjaer, M., 2010. GH and IGF1 levels are positively associated with musculotendinous collagen expression: experiments in acromegalic and GH deficiency patients. European Journal of Endocrinology 163, 853–862. https://doi.org/10.1530/EJE-10-0818

Dos Santos, C., Essioux, L., Teinturier, C., Tauber, M., Goffin, V., Bougnères, P., 2004. A common polymorphism of the growth hormone receptor is associated with increased responsiveness to growth hormone. Nat Genet 36, 720–724. https://doi.org/10.1038/ng1379

Doyle, T.L., Newton, R.U., Burnett, A.F., 2005. Reliability of Traditional and Fractal Dimension Measures of Quiet Stance Center of Pressure in Young, Healthy People. Archives of Physical Medicine and Rehabilitation 86, 2034–2040. https://doi.org/10.1016/j.apmr.2005.05.014

Durkin, J.L., Dowling, J.J., 2003. Analysis of Body Segment Parameter Differences Between Four Human Populations and the Estimation Errors of Four Popular Mathematical Models. Journal of Biomechanical Engineering 125, 515–522. https://doi.org/10.1115/1.1590359

Ekenstedt, K.J., Sonntag, W.E., Loeser, R.F., Lindgren, B.R., Carlson, C.S., 2006. Effects of chronic growth hormone and insulin-like growth factor 1 deficiency on osteoarthritis severity in rat knee joints. Arthritis Rheum 54, 3850–3858. https://doi.org/10.1002/art.22254

Fatti, L., Cangiano, B., Vitale, G., Persani, L., Mantovani, G., Sala, E., Arosio, M., Maffei, P., Dassie, F., Mormando, M., Giampietro, A., Tanda, L., Masiello, E., Nazzari, E., Ferone, D., Corbetta, S., Passeri, E., Guaraldi, F., Grottoli, S., Cannavò, S., Torre, M., Soranna, D., Zambon, A., Cavagnini, F., Scacchi, M., 2019. Arthropathy in acromegaly: a questionnaire-based estimation of motor disability and its relation with quality of life and work productivity. Pituitary 22, 552–560. https://doi.org/10.1007/s11102-019-00966-8

Felson, D.T., Anderson, J.J., Hannan, M.T., Milton, R.C., Wilson, P.W., Kiel, D.P., 1989. Impaired vision and hip fracture: The Framingham Study. Journal of the American Geriatrics Society 37, 495–500.

Ferrante, E., Ferraroni, M., Castrignanò, T., Menicatti, L., Anagni, M., Reimondo, G., Del Monte, P., Bernasconi, D., Loli, P., Faustini-Fustini, M., Borretta, G., Terzolo, M., Losa, M., Morabito, A., Spada, A., Beck-Peccoz, P., Lania, A.G., 2006. Non-functioning pituitary adenoma database: a useful resource to improve the clinical management of pituitary tumors. eur j endocrinol 155, 823–829. https://doi.org/10.1530/eje.1.02298

Fleseriu, M., Biller, B.M.K., Freda, P.U., Gadelha, M.R., Giustina, A., Katznelson, L., Molitch, M.E., Samson, S.L., Strasburger, C.J., van der Lely, A.J., Melmed, S., 2021. A Pituitary Society update to acromegaly management guidelines. Pituitary 24, 1–13. https://doi.org/10.1007/s11102-020-01091-7

Forbes, P.A., Chen, A., Blouin, J.-S., 2018. Sensorimotor control of standing balance, in: Handbook of Clinical Neurology. Elsevier, pp. 61–83. https://doi.org/10.1016/B978-0-444-63916-5.00004-5

Freeman, E.E., Mun~oz, B., Rubin, G., West, S.K., 2007. Visual Field Loss Increases the Risk of Falls in Older Adults: The Salisbury Eye Evaluation. Invest. Ophthalmol. Vis. Sci. 48, 4445. https://doi.org/10.1167/iovs.07-0326

Friedrich, M., Grein, H.-J., Wicher, C., Schuetze, J., Mueller, A., Lauenroth, A., Hottenrott, K., Schwesig, R., 2008. Influence of pathologic and simulated visual dysfunctions on the postural system. Exp Brain Res 186, 305–314. https://doi.org/10.1007/s00221-007-1233-4

Frohman, L.A., Jansson, J.-O., 1986. Growth Hormone-Releasing Hormone. Endocrine Reviews 7, 223–253.

Füchtbauer, L., Olsson, D.S., Bengtsson, B.-Å., Norrman, L.-L., Sunnerhagen, K.S., Johannsson, G., 2017. Muscle strength in patients with acromegaly at diagnosis and during long-term follow-up. European Journal of Endocrinology 177, 217–226. https://doi.org/10.1530/EJE-17-0120

Gage, W.H., Winter, D.A., Frank, J.S., Adkin, A.L., 2004. Kinematic and kinetic validity of the inverted pendulum model in quiet standing. Gait & posture 19, 124–132.

García-Massó, X., Pellicer-Chenoll, M., Gonzalez, L.M., Toca-Herrera, J.L., 2016. The difficulty of the postural control task affects multi-muscle control during quiet standing. Exp Brain Res 234, 1977–1986. https://doi.org/10.1007/s00221-016-4602-z

Gatev, P., Thomas, S., Kepple, T., Hallett, M., 1999. Feedforward ankle strategy of balance during quiet stance in adults. The Journal of physiology 514, 915–928.

Gonticas, S.K., Ikkos, D.G., Stergiou, L.H., 1969. Evaluation of the Diagnostic Value of Heel-Pad Thickness in Acromegaly. Radiology 92, 304–307. https://doi.org/10.1148/92.2.304

Goodworth, A.D., Peterka, R.J., 2010. Influence of Stance Width on Frontal Plane Postural Dynamics and Coordination in Human Balance Control. Journal of Neurophysiology 104, 1103–1118. https://doi.org/10.1152/jn.00916.2009

Gordon, M., Zajac, F., Hoy, M., 1986. Postural synergies dictated by segmental accelerations from muscles and physical constraints. Presented at the Society of Neuroscience Abstracts, p. 1425.

Graham, M.D., Brackmann, D.E., 1978. Acromegaly and the temporal bone. J. Laryngol. Otol. 92, 275–279. https://doi.org/10.1017/S0022215100085352

Guedes da Silva, D.P., Guimarães, F.S., Dias, C.M., Guimarães, S. de A., Kasuki, L., Gadelha, M.R., Camilo, G.B., Lopes, A.J., 2013. On the Functional Capacity and Quality of Life of Patients with Acromegaly: Are They Candidates for Rehabilitation Programs? J Phys Ther Sci 25, 1497–1501. https://doi.org/10.1589/jpts.25.1497

Haliloglu, O., Topsakal, N., Camliguney, F., Polat Korkmaz, O., Sahin, S., Cotuk, B., Kadioglu, P., Erkut, O., 2019. Static and dynamic balances of patients with acromegaly and impact of exercise on balance. Pituitary 22, 497–506. https://doi.org/10.1007/s11102-019-00979-3

Hanavan, E.P., 1964. A mathematical model of the human body. AMRL TR 1–149.

Hasan, S.S., Lichtenstein, M.J., Shiavi, R.G., 1990. Effect of loss of balance on biomechanics platform measures of sway: Influence of stance and a method for adjustment. Journal of Biomechanics 23, 783–789. https://doi.org/10.1016/0021-9290(90)90025-X

Hasan, S.S., Robin, D.W., Szurkus, D.C., Ashmead, D.H., Peterson, S.W., Shiavi, R.G., 1996a. Simultaneous measurement of body center of pressure and center of gravity during upright stance. Part II: Amplitude and frequency data. Gait & Posture 4, 11–20. https://doi.org/10.1016/0966-6362(95)01031-9

Hasan, S.S., Robin, D.W., Szurkus, D.C., Ashmead, D.H., Peterson, S.W., Shiavi, R.G., 1996b. Simultaneous measurement of body center of pressure and center of gravity during upright stance. Part I: Methods. Gait & Posture 4, 1–10. https://doi.org/10.1016/0966-6362(95)01030-0

Hassan, B.S., 2001. Static postural sway, proprioception, and maximal voluntary quadriceps contraction in patients with knee osteoarthritis and normal control subjects. Annals of the Rheumatic Diseases 60, 612–618. https://doi.org/10.1136/ard.60.6.612

Hatipoglu, E., Topsakal, N., Atilgan, O.E., Alcalar, N., Camliguney, A.F., Niyazoglu, M., Cotuk, H.B., Kadioglu, P., 2014. Impact of exercise on quality of life and body-self perception of patients with acromegaly. Pituitary 17, 38–43. https://doi.org/10.1007/s11102-013-0463-7

Hatipoglu, E., Topsakal, N., Erkut Atilgan, O., Camliguney, A.F., Ikitimur, B., Ugurlu, S., Niyazoglu, M., Cotuk, H.B., Kadioglu, P., 2015. Physical and cardiovascular performance in cases with acromegaly after regular short-term exercise. Clin Endocrinol 83, 91–97. https://doi.org/10.1111/cen.12708

Hirata, R.P., Skou, S.T., Simonsen, O., Rasmussen, S., Laursen, M., Graven-Nielsen, T., 2019. Increased postural stiffness during challenging postural tasks in patients with knee osteoarthritis with high pain sensitization. Clinical Biomechanics 61, 129–135. https://doi.org/10.1016/j.clinbiomech.2018.12.004

Hochberg, M.C., Lethbridge-Cejku, M., Scott Jr, W.W., Reichle, R., Plato, C.C., Tobin, J.D., 1994. Serum levels of insulin-like growth factor 1 in subjects with osteoarthritis of the knee. Data from the baltimore longitudinal study of aging. Arthritis & Rheumatism: Official Journal of the American College of Rheumatology 37, 1177–1180.

Hoffman, G.J., Hays, R.D., Shapiro, M.F., Wallace, S.P., Ettner, S.L., 2017. The Costs of Fall-Related Injuries among Older Adults: Annual Per-Faller, Service Component, and Patient Out-of-Pocket Costs. Health Serv Res 52, 1794–1816. https://doi.org/10.1111/1475-6773.12554

Holdaway, I.M., Bolland, M.J., Gamble, G.D., 2008. A meta-analysis of the effect of lowering serum levels of GH and IGF-I on mortality in acromegaly. European Journal of Endocrinology 159, 89–95. https://doi.org/10.1530/EJE-08-0267

Holdaway, I.M., Rajasoorya, C., 1999. Epidemiology of Acromegaly. Pituitary 2, 29–41. https://doi.org/10.1023/A:1009965803750

Homem, T.S., Guimarães, F.S., Soares, M.S., Kasuki, L., Gadelha, M.R., Lopes, A.J., 2017. Balance Control and Peripheral Muscle Function in Aging: A Comparison Between Individuals with Acromegaly and Healthy Subjects. Journal of Aging and Physical Activity 25, 218–227. https://doi.org/10.1123/japa.2016-0100

Hong, T., Mitchell, P., Burlutsky, G., Samarawickrama, C., Wang, J.J., 2014. Visual Impairment and the Incidence of Falls and Fractures Among Older People: Longitudinal Findings From the Blue Mountains Eye Study. Invest. Ophthalmol. Vis. Sci. 55, 7589. https://doi.org/10.1167/iovs.14-14262

Horak, F., Moore, S., 1993. The effect of prior leaning on human postural responses. Gait & Posture 1, 203–210. https://doi.org/10.1016/0966-6362(93)90047-5

Horak, F.B., Macpherson, J.M., 1996. Postural orientation and equilibrium., in: Handbook of Physiology. Exercise: Regulation and Integration of Multiple Systems. Oxford University Press, New York, pp. 255–292.

Horak, F.B., Nashner, L.M., 1986. Central programming of postural movements: adaptation to altered support-surface configurations. Journal of Neurophysiology 55, 1369–1381. https://doi.org/10.1152/jn.1986.55.6.1369

Horak, F.B., Shupert, C.L., Mirka, A., 1989. Components of postural dyscontrol in the elderly: a review. Neurobiol Aging 10, 727–738.

Hoshino, Y., Hidaka, N., Kato, H., Koga, M., Taniguchi, Y., Kobayashi, H., Nangaku, M., Makita, N., Ito, N., 2022. Incidence of ossification of the spinal ligaments in acromegaly patients. Bone Reports 17, 101628. https://doi.org/10.1016/j.bonr.2022.101628

Hue, O., Simoneau, M., Marcotte, J., Berrigan, F., Doré, J., Marceau, P., Marceau, S., Tremblay, A., Teasdale, N., 2007. Body weight is a strong predictor of postural stability. Gait & Posture 26, 32–38. https://doi.org/10.1016/j.gaitpost.2006.07.005

Imran, S.A., Tiemensma, J., Kaiser, S.M., Vallis, M., Doucette, S., Abidi, E., Yip, C.-E., De Tugwell, B., Siddiqi, F., Clarke, D.B., 2016. Morphometric changes correlate with poor psychological outcomes in patients with acromegaly. European Journal of Endocrinology 174, 41–50. https://doi.org/10.1530/EJE-15-0888

Ivers, R.Q., Cumming, R.G., Mitchell, P., Attebo, K., 1998. Visual Impairment and Falls in Older Adults: The Blue Mountains Eye Study. Journal of the American Geriatrics Society 46, 58–64. https://doi.org/10.1111/j.1532-5415.1998.tb01014.x

Jamal, G.A., Kerr, D.J., McLellan, A.R., Weir, A.I., Davies, D.L., 1987. Generalised peripheral nerve dysfunction in acromegaly: a study by conventional and novel neurophysiological techniques. Journal of Neurology, Neurosurgery & Psychiatry 50, 886–894. https://doi.org/10.1136/jnnp.50.7.886

James, S.L., Castle, C.D., Dingels, Z.V., Fox, J.T., Hamilton, E.B., Liu, Z., S Roberts, N.L., Sylte, D.O., Henry, N.J., LeGrand, K.E., Abdelalim, A., Abdoli, A., Abdollahpour, I., Abdulkader, R.S., Abedi, A., Abosetugn, A.E., Abushouk, A.I., Adebayo, O.M., Agudelo-Botero, M., …, Vos, T., 2020. Global injury morbidity and mortality from 1990 to 2017: results from the Global Burden of Disease Study 2017. Inj Prev 26, i96–i114. https://doi.org/10.1136/injuryprev-2019-043494

Jeka, J., Kiemel, T., Creath, R., Horak, F., Peterka, R., 2004. Controlling Human Upright Posture: Velocity Information Is More Accurate Than Position or Acceleration. Journal of Neurophysiology 92, 2368–2379. https://doi.org/10.1152/jn.00983.2003

Johanson, N.A., Vigorita, V.J., Goldman, A.B., Salvati, E.A., 1983. Acromegalic Arthropathy of the Hip. Clin Orthop Relat Res 173, 130–139. https://doi.org/10.1097/00003086-198303000-00017

Jørgensen, A.E.M., Schjerling, P., DellaValle, B., Rungby, J., Kjær, M., 2023. Acute loading has minor influence on human articular cartilage gene expression and glycosaminoglycan composition in late-stage knee osteoarthritis: a randomised controlled trial. Osteoarthritis and Cartilage S1063458423003357. https://doi.org/10.1016/j.joca.2023.01.317

Juraschek, S.P., Simpson, L.M., Davis, B.R., Beach, J.L., Ishak, A., Mukamal, K.J., 2019. Effects of Antihypertensive Class on Falls, Syncope, and Orthostatic Hypotension in Older Adults: The ALLHAT Trial. Hypertension 74, 1033–1040. https://doi.org/10.1161/HYPERTENSIONAHA.119.13445

Kan, E., Kan, E.K., Atmaca, A., Atmaca, H., Colak, R., 2013. Visual field defects in 23 acromegalic patients. Int Ophthalmol 33, 521–525. https://doi.org/10.1007/s10792-013-9733-7

Katznelson, L., Laws, E.R., Melmed, S., Molitch, M.E., Murad, M.H., Utz, A., Wass, J.A.H., 2014. Acromegaly: An Endocrine Society Clinical Practice Guideline. The Journal of Clinical Endocrinology & Metabolism 99, 3933–3951. https://doi.org/10.1210/jc.2014-2700

Kellgren, J.H., Lawrence, J.S., 1957. Radiological assessment of osteo-arthritis. Annals of the Rheumatic Diseases 16, 494–502.

Kepple, T.M., Sommer III, H.J., Siegel, K.L., Stanhope, S.J., 1997. A three-dimensional musculoskeletal database for the lower extremities. Journal of Biomechanics 31, 77–80. https://doi.org/10.1016/S0021-9290(97)00107-3

Khaleeli, A.A., Levy, R.D., Edwards, R.H., McPhail, G., Mills, K.R., Round, J.M., Betteridge, D.J., 1984. The neuromuscular features of acromegaly: a clinical and pathological study. Journal of Neurology, Neurosurgery & Psychiatry 47, 1009–1015. https://doi.org/10.1136/jnnp.47.9.1009

Kho, K.M., Wright, A.D., Doyle, F.H., 1970. Heel pad thickness in acromegaly. BJR 43, 119–125. https://doi.org/10.1259/0007-1285-43-506-119

Killinger, Z., Payer, J., Lazúrová, I., Imrich, R., Homérová, Z., Kužma, M., Rovenský, J., 2010. Arthropathy in acromegaly. Rheum Dis Clin North Am 36, 713–20. https://doi.org/10.1016/j.rdc.2010.09.004

Koçak, M., 2015. Ultrasonographic Assessment of Soft Tissues in Patients With Acromegaly. Arch Rheumatol 30, 138–143. https://doi.org/10.5606/ArchRheumatol.2015.5158

Kojima, M., Hosoda, H., Date, Y., Nakazato, M., Matsuo, H., Kangawa, K., 1999. Ghrelin is a growth-hormone-releasing acylated peptide from stomach. Nature 402, 656–660. https://doi.org/10.1038/45230

Kosk, K., Luukinen, H., Laippala, P., Kivelä, S.-L., 1996. Physiological Factors and Medications as Predictors of Injurious Falls by Elderly People: A Prospective Population-based Study. Age Ageing 25, 29–38. https://doi.org/10.1093/ageing/25.1.29

Kropf, L.L., Madeira, M., Neto, L.V., Roberto Gadelha, M., de Farias, M.L.F., 2013. Functional evaluation of the joints in acromegalic patients and associated factors. Clin Rheumatol 32, 991–998. https://doi.org/10.1007/s10067-013-2219-1

Lafond, D., Champagne, A., Descarreaux, M., Dubois, J.-D., Prado, J.M., Duarte, M., 2009. Postural control during prolonged standing in persons with chronic low back pain. Gait & Posture 29, 421–427. https://doi.org/10.1016/j.gaitpost.2008.10.064

Lafond, D., Corriveau, H., Hébert, R., Prince, F., 2004. Intrasession reliability of center of pressure measures of postural steadiness in healthy elderly people. Archives of Physical Medicine and Rehabilitation 85, 896–901. https://doi.org/10.1016/j.apmr.2003.08.089

Lafond, D., Duarte, M., Prince, F., 2004. Comparison of three methods to estimate the center of mass during balance assessment. Journal of Biomechanics 37, 1421–1426. https://doi.org/10.1016/S0021-9290(03)00251-3

Lakie, M., Caplan, N., Loram, I.D., 2003. Human balancing of an inverted pendulum with a compliant linkage: neural control by anticipatory intermittent bias. The Journal of Physiology 551, 357–370. https://doi.org/10.1113/jphysiol.2002.036939

Lestienne, F., Soechting, J., Berthoz, A., 1977. Postural readjustments induced by linear motion of visual scenes. Exp Brain Res 28–28. https://doi.org/10.1007/BF00235717

Lestienne, F.G., Gurfinkel, V.S., 1988. Postural control in weightlessness: a dual process underlying adaptation to an unusual environment. Trends in Neurosciences 11, 359–363.

Lima, T.R.L., Kasuki, L., Gadelha, M., Lopes, A.J., 2019. Physical exercise improves functional capacity and quality of life in patients with acromegaly: a 12-week follow-up study. Endocrine 66, 301–309. https://doi.org/10.1007/s12020-019-02011-x

Lloyd, M.E., Hart, D.J., Nandra, D., McAlindon, T.E., Wheeler, M., Doyle, D.V., Spector, T.D., 1996. Relation between insulin-like growth factor-I concentrations, osteoarthritis, bone density, and fractures in the general population: the Chingford study. Annals of the Rheumatic Diseases 55, 870–874. https://doi.org/10.1136/ard.55.12.870

Lopes, A.J., da Silva, D.P.G., Kasuki, L., Gadelha, M.R., Camilo, G.B., Guimarães, F.S., 2014. Posture and balance control in patients with acromegaly: Results of a cross-sectional study. Gait & Posture 40, 154–159. https://doi.org/10.1016/j.gaitpost.2014.03.014

Lopes, A.J., Ferreira, A.S., Walchan, E.M., Soares, M.S., Bunn, P.S., Guimarães, F.S., 2016. Explanatory models of muscle performance in acromegaly patients evaluated by knee isokinetic dynamometry: Implications for rehabilitation. Human Movement Science 49, 160–169. https://doi.org/10.1016/j.humov.2016.07.005

Lopes, A.J., Guedes da Silva, D.P., Ferreira, A. de S., Kasuki, L., Gadelha, M.R., Guimarães, F.S., 2015. What is the effect of peripheral muscle fatigue, pulmonary function, and body composition on functional exercise capacity in acromegalic patients? J Phys Ther Sci 27, 719–724. https://doi.org/10.1589/jpts.27.719

Loram, I.D., Lakie, M., 2002a. Direct measurement of human ankle stiffness during quiet standing: the intrinsic mechanical stiffness is insufficient for stability. The Journal of Physiology 545, 1041–1053. https://doi.org/10.1113/jphysiol.2002.025049

Loram, I.D., Lakie, M., 2002b. Human balancing of an inverted pendulum: position control by small, ballistic-like, throw and catch movements. The Journal of Physiology 540, 1111–1124. https://doi.org/10.1113/jphysiol.2001.013077

Loram, I.D., Maganaris, C.N., Lakie, M., 2005. Active, non-spring-like muscle movements in human postural sway: how might paradoxical changes in muscle length be produced?: Muscle movements in human standing. The Journal of Physiology 564, 281–293. https://doi.org/10.1113/jphysiol.2004.073437

Low, P.A., Mcleod, J.G., Turtle, J.R., Donnelly, P., Wright, R.G., 1974. Peripheral neuropathy in acromegaly. Brain 97, 139–152. https://doi.org/10.1093/brain/97.1.139

Lu, M., Flanagan, J.U., Langley, R.J., Hay, M.P., Perry, J.K., 2019. Targeting growth hormone function: strategies and therapeutic applications. Signal Transduction and Targeted Therapy 4, 3. https://doi.org/10.1038/s41392-019-0036-y

Lu, T., O'Connor, J.J., 1999. Bone position estimation from skin marker co-ordinates using global optimisation with joint constraints. Journal of Biomechanics 32, 129–134. https://doi.org/10.1016/S0021-9290(98)00158-4

Lyman, S., Lee, Y., Franklin, P.D., Li, W., Cross, M.B., Padgett, D.E., 2016a. Validation of the KOOS, JR: A Short-form Knee Arthroplasty Outcomes Survey. Clinical Orthopaedics and Related Research® 474, 1461–1471. https://doi.org/10.1007/s11999-016-4719-1

Lyman, S., Lee, Y., Franklin, P.D., Li, W., Mayman, D.J., Padgett, D.E., 2016b. Validation of the HOOS, JR: A Short-form Hip Replacement Survey. Clinical Orthopaedics and Related Research® 474, 1472–1482. https://doi.org/10.1007/s11999-016-4718-2

Macpherson, J., Horak, F., Dunbar, D., Dow, R., 1989. Stance dependence of automatic postural adjustments in humans. Exp Brain Res 78, 557–566.

Manal, K., McClay, I., Stanhope, S., Richards, J., Galinat, B., 2000. Comparison of surface mounted markers and attachment methods in estimating tibial rotations during walking: an in vivo study. Gait & Posture 11, 38–45. https://doi.org/10.1016/S0966-6362(99)00042-9

Mastaglia, F., Barwick, D., Hall, R., 1970. Myopathy in acromegaly. The Lancet 296, 907–909.

Masui, T., Hasegawa, Y., Yamaguchi, J., Kanoh, T., Ishiguro, N., Suzuki, S., 2006. Increasing postural sway in rural-community-dwelling elderly persons with knee osteoarthritis. Journal of Orthopaedic Science 11, 353–358. https://doi.org/10.1007/s00776-006-1034-9

Matrangola, S.L., Madigan, M.L., Nussbaum, M.A., Ross, R., Davy, K.P., 2008. Changes in body segment inertial parameters of obese individuals with weight loss. Journal of Biomechanics 41, 3278–3281. https://doi.org/10.1016/j.jbiomech.2008.08.026

McAlindon, T.E., Teale, J.D., Dieppe, P.A., 1993. Levels of insulin related growth factor 1 in osteoarthritis of the knee. Annals of the Rheumatic Diseases 52, 229–231. https://doi.org/10.1136/ard.52.3.229

Melmed, S., 2006. Acromegaly. N Engl J Med 355, 2558–2573. https://doi.org/10.1056/NEJMra062453

Melmed, S., Bronstein, M.D., Chanson, P., Klibanski, A., Casanueva, F.F., Wass, J.A.H., Strasburger, C.J., Luger, A., Clemmons, D.R., Giustina, A., 2018. A Consensus Statement on acromegaly therapeutic outcomes. Nature Reviews Endocrinology 14, 552–561. https://doi.org/10.1038/s41574-018-0058-5

Menezes, M., De Mello Meziat-Filho, N.A., Araújo, C.S., Lemos, T., Ferreira, A.S., 2020. Agreement and predictive power of six fall risk assessment methods in community-dwelling older adults. Archives of Gerontology and Geriatrics 87, 103975. https://doi.org/10.1016/j.archger.2019.103975

Menzel, O., 1966. Hearing loss secondary to acromegaly: case report. Eye, Ear, Nose and Throat Monthly 45, 84–85.

Mercado, M., González, B., Sandoval, C., Esquenazi, Y., Mier, F., Vargas, G., de los Monteros, A.L.E., Sosa, E., 2008. Clinical and Biochemical Impact of the d3 Growth Hormone Receptor Genotype in Acromegaly. The Journal of Clinical Endocrinology & Metabolism 93, 3411–3415. https://doi.org/10.1210/jc.2008-0391

Meyer, P.F., Oddsson, L.I.E., De Luca, D.L., 2004. The role of plantar cutaneous sensation in unperturbed stance. Experimental Brain Research 156, 505–512. https://doi.org/10.1007/s00221-003-1804-y

Micarelli, A., Liguori, C., Viziano, A., Izzi, F., Placidi, F., Alessandrini, M., 2017. Integrating postural and vestibular dimensions to depict impairment in moderate-to-severe obstructive sleep apnea syndrome patients. J Sleep Res 26, 487–494. https://doi.org/10.1111/jsr.12516

Middleton, J., Arnott, N., Walsh, S., Beresford, J., 1995. Osteoblasts and osteoclasts in adult human osteophyte tissue express the mRNAs for insulin-like growth factors I and II and the type 1 IGF receptor. Bone 16, 287–293. https://doi.org/10.1016/8756-3282(94)00040-9

Miller, A., Doll, H., David, J., Wass, J., 2008. Impact of musculoskeletal disease on quality of life in long-standing acromegaly. Eur J Endocrinol 158, 587–593. https://doi.org/10.1530/EJE-07-0838

Mok, N.W., Brauer, S.G., Hodges, P.W., 2004. Hip Strategy for Balance Control in Quiet Standing Is Reduced in People With Low Back Pain: Spine 29, E107–E112. https://doi.org/10.1097/01.BRS.0000115134.97854.C9

Molitch, M.E., 1992. Clinical Manifestations of Acromegaly. Endocrinology and Metabolism Clinics of North America 21, 597–614. https://doi.org/10.1016/S0889-8529(18)30204-4

Moore, S., Horak, F., Nashner, L., 1986. Influence of stimulus anticipation on human postural responses. North Am Soc Psychol Sport Phys Activity, Scottsdale, Arizona.

Morasso, P.G., Sanguineti, V., 2002. Ankle Muscle Stiffness Alone Cannot Stabilize Balance During Quiet Standing. Journal of Neurophysiology 88, 2157–2162. https://doi.org/10.1152/jn.2002.88.4.2157

Morasso, P.G., Schieppati, M., 1999. Can Muscle Stiffness Alone Stabilize Upright Standing? Journal of Neurophysiology 82, 1622–1626. https://doi.org/10.1152/jn.1999.82.3.1622

Mori, S., 1973. Discharge patterns of soleus motor units with associated changes in force exerted by foot during quiet stance in man. Journal of neurophysiology 36, 458–471.

Mosca, S., Paolillo, S., Colao, A., Bossone, E., Cittadini, A., Iudice, F.L., Parente, A., Conte, S., Rengo, G., Leosco, D., Trimarco, B., Filardi, P.P., 2013. Cardiovascular involvement in patients affected by acromegaly: An appraisal. International Journal of Cardiology 167, 1712–1718. https://doi.org/10.1016/j.ijcard.2012.11.109

Müslüman, A.M., Cansever, T., Yılmaz, A., Kanat, A., Oba, E., Çavuşoğlu, H., Şirinoğlu, D., Aydın, Y., 2011. Surgical Results of Large and Giant Pituitary Adenomas with Special Consideration of Ophthalmologic Outcomes. World Neurosurgery 76, 141–148. https://doi.org/10.1016/j.wneu.2011.02.009

Nagulesparen, M., Trickey, R., Davies, M.J., Jenkins, J.S., 1976. Muscle changes in acromegaly. BMJ 2, 914–915. https://doi.org/10.1136/bmj.2.6041.914

Nashner, L., 1971. A model describing vestibular detection of body sway motion. Acta Oto-Laryngologica 72, 429–436.

Nashner, L., Berthoz, A., 1978. Visual contribution to rapid motor responses during postural control. Brain Research 150, 403–407. https://doi.org/10.1016/0006-8993(78)90291-3

Nashner, L.M., 1976. Adapting reflexes controlling the human posture. Exp Brain Res 26. https://doi.org/10.1007/BF00235249

Nashner, L.M., 1972. Vestibular postural control model. Kybernetik 10, 106–110. https://doi.org/10.1007/BF00292236

Nashner, L.M., 1970. Sensory feedback in human posture control.

Nashner, L.M., Black, F.O., Wall, C., 1982. Adaptation to altered support and visual conditions during stance: patients with vestibular deficits. Journal of Neuroscience 2, 536–544.

Nashner, L.M., McCollum, G., 1985. The organization of human postural movements: A formal basis and experimental synthesis. Behavioral and Brain Sciences 8, 135–150. https://doi.org/10.1017/S0140525X00020008

Nashner, L.M., Shupert, C.L., Horak, F.B., Black, F.O., 1989. Organization of posture controls: an analysis of sensory and mechanical constraints, in: Allum, J.H.J., Hulliger, M. (Eds.), Progress in Brain Research. Elsevier, pp. 411–418. https://doi.org/10.1016/S0079-6123(08)62237-2

Neri, S.G.R., Gadelha, A.B., De David, A.C., Ferreira, A.P., Safons, M.P., Tiedemann, A., Lima, R.M., 2019. The Association Between Body Adiposity Measures, Postural Balance, Fear of Falling, and Fall Risk in Older Community-Dwelling Women. Journal of Geriatric Physical Therapy 42, E94–E100. https://doi.org/10.1519/JPT.0000000000000165

Nevitt, M.C., 1989. Risk Factors for Recurrent Nonsyncopal Falls: A Prospective Study. JAMA 261, 2663. https://doi.org/10.1001/jama.1989.03420180087036

Nevitt, M.C., Cummings, S.R., Hudes, E.S., 1991. Risk Factors for Injurious Falls: a Prospective Study. Journal of Gerontology 46, M164–M170. https://doi.org/10.1093/geronj/46.5.M164

Niiori-Onishi, A., Iwasaki, Y., Mutsuga, N., Oiso, Y., Inoue, K., Saito, H., 1999. Molecular Mechanisms of the Negative Effect of Insulin- Like Growth Factor-I on Growth Hormone Gene Expression in MtT/S Somatotroph Cells. Endocrinology 140, 344–349.

Noguchi, K., Gel, Y.R., Brunner, E., Konietschke, F., 2012. nparLD: An R Software Package for the Nonparametric Analysis of Longitudinal Data in Factorial Experiments. J. Stat. Soft. 50, 1–23. https://doi.org/10.18637/jss.v050.i12

Oerbekke, M.S., Stukstette, M.J., Schütte, K., De Bie, R.A., Pisters, M.F., Vanwanseele, B., 2017. Concurrent validity and reliability of wireless instrumented insoles measuring postural balance and temporal gait parameters. Gait & Posture 51, 116–124. https://doi.org/10.1016/j.gaitpost.2016.10.005

Ogra, S., Nichols, A.D., Stylli, S., Kaye, A.H., Savino, P.J., Danesh-Meyer, H.V., 2014. Visual acuity and pattern of visual field loss at presentation in pituitary adenoma. Journal of Clinical Neuroscience 21, 735–740. https://doi.org/10.1016/j.jocn.2014.01.005

Okazaki, K., Jingushi, S., Ikenoue, T., Urabe, K., Sakai, H., Ohtsuru, A., Akino, K., Yamashita, S., Nomura, S., Iwamoto, Y., 1999. Expression of Insulin-Like Growth Factor I Messenger Ribonucleic Acid in Developing Osteophytes in Murine Experimental Osteoarthritis and in Rats Inoculated with Growth Hormone-Secreting Tumor. Endocrinology 140, 4821–4830.

Omma, T., Tunc, A.R., Fırat, S.N., Taskaldıran, I., Culha, C., Ersoz Gulcelik, N., 2022. Pedabarography May Play a Role in Foot Plantar Scanning in Acromegaly. International Journal of Clinical Practice 2022, 1–7. https://doi.org/10.1155/2022/9882896

Onal, E.D., Ipek, A., Evranos, B., Idilman, I.S., Cakir, B., Ersoy, R., 2016. Structural tendon changes in patients with acromegaly: assessment of Achilles tendon with sonoelastography. Med Ultrason 18, 30. https://doi.org/10.11152/mu.2013.2066.181.edo

Oppenheim, U., Kohen-Raz, R., Alex, D., Kohen-Raz, A., Azarya, M., 1999. Postural characteristics of diabetic neuropathy. Diabetes Care 22, 328–332. https://doi.org/10.2337/diacare.22.2.328

Ozata, M., Ozkardes, A., Beyhan, Z., Corakci, A., Gundogan, M.A., 1997. Central and Peripheral Neural Responses in Acromegaly. Endocrine Practice 3, 118–122. https://doi.org/10.4158/EP.3.3.118

Ozturk Gokce, B., Gogus, F., Bolayir, B., Tecer, D., Gokce, O., Eroglu Altinova, A., Balos Toruner, F., Akturk, M., 2020. The evaluation of the tendon and muscle changes of lower extremity in patients with acromegaly. Pituitary 23, 338–346. https://doi.org/10.1007/s11102-020-01037-z

Pantel, J., Machinis, K., Sobrier, M.-L., Duquesnoy, P., Goossens, M., Amselem, S., 2000. Species-specific Alternative Splice Mimicry at the Growth Hormone Receptor Locus Revealed by the Lineage of Retroelements during Primate Evolution. Journal of Biological Chemistry 275, 18664–18669. https://doi.org/10.1074/jbc.M001615200

Parolin, M., Dassie, F., Alessio, L., Wennberg, A., Rossato, M., Vettor, R., Maffei, P., Pagano, C., 2020. Obstructive Sleep Apnea in Acromegaly and the Effect of Treatment: A Systematic Review and Meta-Analysis. The Journal of Clinical Endocrinology & Metabolism 105, e23–e31. https://doi.org/10.1210/clinem/dgz116

Pasma, J.H., Engelhart, D., Maier, A.B., Schouten, A.C., van der Kooij, H., Meskers, C.G.M., 2015. Changes in sensory reweighting of proprioceptive information during standing balance with age and disease. Journal of Neurophysiology 114, 3220–3233. https://doi.org/10.1152/jn.00414.2015

Peel, N.M., 2011. Epidemiology of Falls in Older Age. Can. J. Aging 30, 7–19. https://doi.org/10.1017/S071498081000070X

Pelsma, I., Biermasz, N., van Furth, W., Pereira, A., Kroon, H., Kloppenburg, M., Claessen, K., 2021. Progression of acromegalic arthropathy in long-term controlled acromegaly patients: 9 years of longitudinal follow-up. J Clin Endocrinol Metab 106, 188–200. https://doi.org/10.1210/clinem/dgaa747

Pelsma, I., Kroon, H., van Trigt, V., Pereira, A., Kloppenburg, M., Biermasz, N., Claessen, K., 2022. Clinical and radiographic assessment of peripheral joints in controlled acromegaly. Pituitary 25, 622–635. https://doi.org/10.1007/s11102-022-01233-z

Peretz, C., Herman, T., Hausdorff, J.M., Giladi, N., 2006. Assessing fear of falling: Can a short version of the Activities-specific Balance Confidence scale be useful? Movement Disorders 21, 2101–2105. https://doi.org/10.1002/mds.21113

Peterka, R.J., 2000. Postural control model interpretation of stabilogram diffusion analysis. Biol. Cybern. 82, 335–343.

Pickett, J.B.E., Layzer, R.B., Levin, S.R., Schneider, V., Campbell, M.J., Sumner, A.J., 1975. Neuromuscular complications of acromegaly. Neurology 25, 638–638. https://doi.org/10.1212/WNL.25.7.638

Pizzigalli, L., Micheletti Cremasco, M., Mulasso, A., Rainoldi, A., 2016. The contribution of postural balance analysis in older adult fallers: A narrative review. Journal of Bodywork and Movement Therapies 20, 409–417. https://doi.org/10.1016/j.jbmt.2015.12.008

Plard, C., Hochman, C., Hadjadj, S., Le Goff, B., Maugars, Y., Cariou, B., Drui, D., Guillot, P., 2020. Acromegaly is associated with vertebral deformations but not vertebral fractures: Results of a cross-sectional monocentric study. Joint Bone Spine 87, 618–624. https://doi.org/10.1016/j.jbspin.2020.04.020

Podgorski, M., Robinson, B., Weissberger, A., Stiel, J., Wang, S., Brooks, P.M., 1988. Articular manifestations of acromegaly. Australian and New Zealand Journal of Medicine 18, 28–35. https://doi.org/10.1111/j.1445-5994.1988.tb02236.x

Powell, M., 1995. Recovery of vision following transsphenoidal surgery for pituitary adenomas. British Journal of Neurosurgery 9, 367–374. https://doi.org/10.1080/02688699550041377

Prencipe, N., Scarati, M., Manetta, T., Berton, A., Parisi, S., Bona, C., Parasiliti-Caprino, M., Ditto, M., Gasso, V., Fusaro, E., Grottoli, S., 2020. Acromegaly and joint pain: is there something more? A cross-sectional study to evaluate rheumatic disorders in growth hormone secreting tumor patients. J Endocrinol Invest 43, 1661–1667. https://doi.org/10.1007/s40618-020-01268-8

Proske, U., 2023. A reassessment of the role of joint receptors in human position sense. Exp Brain Res 241, 943–949. https://doi.org/10.1007/s00221-023-06582-0

Qiu, F., Cole, M.H., Davids, K.W., Hennig, E.M., Silburn, P.A., Netscher, H., Kerr, G.K., 2012. Enhanced somatosensory information decreases postural sway in older people. Gait & Posture 35, 630–635. https://doi.org/10.1016/j.gaitpost.2011.12.013

Quijoux, F., Vienne-Jumeau, A., Bertin-Hugault, F., Zawieja, P., Lefèvre, M., Vidal, P.-P., Ricard, D., 2020. Center of pressure displacement characteristics differentiate fall risk in older people: A systematic review with meta-analysis. Ageing Research Reviews 62, 101117. https://doi.org/10.1016/j.arr.2020.101117

Rab, G., Petuskey, K., Bagley, A., 2002. A method for determination of upper extremity kinematics. Gait & Posture 15, 113–119. https://doi.org/10.1016/S0966-6362(01)00155-2

Reid, T.J., Kalmon D Post, Bruce, J.N., Nabi Kanibir, M., Reyes-Vidal, C.M., Freda, P.U., 2010. Features at diagnosis of 324 patients with acromegaly did not change from 1981 to 2006: acromegaly remains under-recognized and under-diagnosed. Clin Endocrinol (Oxf) 72, 203–208. https://doi.org/10.1111/j.1365-2265.2009.03626.x

Resmini, E., Tagliafico, A., Nizzo, R., Bianchi, F., Minuto, F., Derchi, L., Martinoli, C., Ferone, D., 2009. Ultrasound of peripheral nerves in acromegaly: changes at 1-year follow-up. Clinical Endocrinology 71, 220–225. https://doi.org/10.1111/j.1365-2265.2008.03468.x

Richards, S., 1968. Deafness in Acromegaly. J. Laryngol. Otol. 82, 1053–1065. https://doi.org/10.1017/S0022215100069887

Rietdyk, S., Patla, A.E., Winter, D.A., Ishac, M.G., Little, C.E., 1999. Balance recovery from medio-lateral perturbations of the upper body during standing. Journal of Biomechanics 32, 1149–1158. https://doi.org/10.1016/S0021-9290(99)00116-5

Rivoal, O., Brézin, A.P., Feldman-Billard, S., Luton, J.-P., 2000. Goldmann perimetry in acromegaly. Ophthalmology 107, 991–997. https://doi.org/10.1016/S0161-6420(00)00060-9

Rizzo, J.A., Friedkin, R., Williams, C.S., Nabors, J., Acampora, D., Tinetti, M.E., 1998. Health care utilization and costs in a Medicare population by fall status. Medical care 1174–1188.

Robertson, D., Caldwell, G., Hamill, J., Kamen, G., Whittlesey, S., 2013. Research Methods in Biomechanics: Second edition (eBook).

Roerink, S.H.P.P., Wagenmakers, M.A.E.M., Wessels, J.F., Sterenborg, R.B.T.M., Smit, J.W., Hermus, A.R.M.M., Netea-Maier, R.T., 2015. Persistent self-consciousness about facial appearance, measured with the Derriford appearance scale 59, in patients after long-term biochemical remission of acromegaly. Pituitary 18, 366–375. https://doi.org/10.1007/s11102-014-0583-8

Rosselet, P., Pastakia, B., Doppman, J., Gorden, P., 1988. Arthropathy in acromegaly patients before and after treatment: a long-term follow-up study. Clin Endocrinol 28, 515–524. https://doi.org/10.1111/j.1365-2265.1988.tb03686.x

Rougier, P., Belaid, D., Cantalloube, S., Lamotte, D., Deschamps, J., 2008. Quiet Postural Control of Patients with Total Hip Arthroplasty Following Joint Arthritis. Motor Control 12, 136–150. https://doi.org/10.1123/mcj.12.2.136

Rowles, S.V., Prieto, L., Badia, X., Shalet, S.M., Webb, S.M., Trainer, P.J., 2005. Quality of Life (QOL) in Patients with Acromegaly Is Severely Impaired: Use of a Novel Measure of QOL: Acromegaly Quality of Life Questionnaire. The Journal of Clinical Endocrinology & Metabolism 90, 3337–3341. https://doi.org/10.1210/jc.2004-1565

Ruhe, A., Fejer, R., Walker, B., 2010. The test–retest reliability of centre of pressure measures in bipedal static task conditions – A systematic review of the literature. Gait & Posture 32, 436–445. https://doi.org/10.1016/j.gaitpost.2010.09.012

Russo, M.M., Lemos, T., Imbiriba, L.A., Ribeiro, N.L., Vargas, C.D., 2017. Beyond deficit or compensation: new insights on postural control after long-term total visual loss. Exp Brain Res 235, 437–446. https://doi.org/10.1007/s00221-016-4799-x

Salavati, M., Hadian, M.R., Mazaheri, M., Negahban, H., Ebrahimi, I., Talebian, S., Jafari, A.H., Sanjari, M.A., Sohani, S.M., Parnianpour, M., 2009. Test–retest reliabty of center of pressure measures of postural stability during quiet standing in a group with musculoskeletal disorders consisting of low back pain, anterior cruciate ligament injury and functional ankle instability. Gait & Posture 29, 460–464. https://doi.org/10.1016/j.gaitpost.2008.11.016

Santos, B.R., Delisle, A., Larivière, C., Plamondon, A., Imbeau, D., 2008. Reliability of centre of pressure summary measures of postural steadiness in healthy young adults. Gait & Posture 27, 408–415. https://doi.org/10.1016/j.gaitpost.2007.05.008

Sasagawa, Y., Tachibana, O., Doai, M., Tonami, H., Iizuka, H., 2015. Median nerve conduction studies and wrist magnetic resonance imaging in acromegalic patients with carpal tunnel syndrome. Pituitary 18, 695–700. https://doi.org/10.1007/s11102-015-0642-9

Scarpa, R., De Brasi, D., Pivonello, R., Marzullo, P., Manguso, F., Sodano, A., Oriente, P., Lombardi, G., Colao, A., 2004. Acromegalic axial arthropathy: a clinical case-control study. J Clin Endocrinol Metab 89, 598–603. https://doi.org/10.1210/jc.2003-031283

Schepens, S., Goldberg, A., Wallace, M., 2010. The short version of the Activities-specific Balance Confidence (ABC) scale: its validity, reliability, and relationship to balance impairment and falls in older adults. Archives of gerontology and geriatrics 51. https://doi.org/10.1016/j.archger.2009.06.003

Schmitz, A., Buczek, F.L., Bruening, D., Rainbow, M.J., Cooney, K., Thelen, D., 2016. Comparison of hierarchical and six degrees-of-freedom marker sets in analyzing gait kinematics. Computer Methods in Biomechanics and Biomedical Engineering 19, 199–207. https://doi.org/10.1080/10255842.2015.1006208

Schouten, J.S.A.G., Van Den Ouweland, F.A., Valkenburg, H.A., Lamberts, S.W.J., 1993. Insulin-like growth factor-1: A prognostic factor of knee osteoarthritis. Rheumatology 32, 274–280. https://doi.org/10.1093/rheumatology/32.4.274

Schubert, P., Kirchner, M., 2014. Ellipse area calculations and their applicability in posturography. Gait & Posture 39, 518–522. https://doi.org/10.1016/j.gaitpost.2013.09.001

Sendur, S.N., Oguz, S., Dagdelen, S., Erbas, T., 2019. Assessment of static and dynamic plantar data of patients with acromegaly. Pituitary 22, 373–380. https://doi.org/10.1007/s11102-019-00964-w

Shumway-Cook, A., Ciol, M.A., Hoffman, J., Dudgeon, B.J., Yorkston, K., Chan, L., 2009. Falls in the Medicare Population: Incidence, Associated Factors, and Impact on Health Care. Physical Therapy 89, 324–332. https://doi.org/10.2522/ptj.20070107

Sobrier, M.-L., Duquesnoy, P., Duriez, B., Amselem, S., Goossens, M., 1993. Expression and binding properties of two isoforms of the human growth hormone receptor. FEBS Letters 319, 16–20. https://doi.org/10.1016/0014-5793(93)80028-S

Sozzi, S., Nardone, A., Schieppati, M., 2021. Specific Posture-Stabilising Effects of Vision and Touch Are Revealed by Distinct Changes of Body Oscillation Frequencies. Front. Neurol. 12, 756984. https://doi.org/10.3389/fneur.2021.756984

Spoor, C.W., Veldpaus, F.E., 1980. Rigid body motion calculated from spatial co-ordinates of markers. Journal of Biomechanics 13, 391–393. https://doi.org/10.1016/0021-9290(80)90020-2

Springer, B.A., Marin, R., Cyhan, T., Roberts, H., Gill, N.W., 2007. Normative Values for the Unipedal Stance Test with Eyes Open and Closed: Journal of Geriatric Physical Therapy 30, 8–15. https://doi.org/10.1519/00139143-200704000-00003

Stagni, R., Leardini, A., Cappozzo, A., Benedetti, M.G., Cappello, A., 2000. Effects of hip joint centre mislocation on gait analysis results. Journal of Biomechanics 33, 1479–87. https://doi.org/10.1016/s0021-9290(00)00093-2

Steinbach, H.L., Russell, W., 1964. Measurement of the Heel-Pad as an Aid to Diagnosis of Acromegaly. Radiology 82, 418–423. https://doi.org/10.1148/82.3.418

Stern, L.Z., Payne, C.M., Hannapel, L.K., 1974. Acromegaly: Histochemical and electron microscopic changes in deltoid and intercostal muscle. Neurology 24, 589–589. https://doi.org/10.1212/WNL.24.6.589

Stevens, D., Jackson, B., Carberry, J., McLoughlin, J., Barr, C., Mukherjee, S., Oh, A., McEvoy, R.D., Crotty, M., Vakulin, A., 2020. The Impact of Obstructive Sleep Apnea on Balance, Gait, and Falls Risk: A Narrative Review of the Literature. The Journals of Gerontology: Series A 75, 2450–2460. https://doi.org/10.1093/gerona/glaa014

Stewart, B.M., 1966. The Hypertrophic Neuropathy of Acromegaly: A Rare Neuropathy Associated With Acromegaly. Arch Neurol 14, 107. https://doi.org/10.1001/archneur.1966.00470070111014

Sugihara, H., Emoto, N., Tamura, H., Kamegai, J., Shibasaki, T., Minami, S., Wakabayashi, I., 1999. Effect of insulin-like growth factor-I on growth hormone-releasing factor receptor expression in primary rat anterior pituitary cell culture. Neuroscience Letters 276, 87–90. https://doi.org/10.1016/S0304-3940(99)00801-0

Tabur, S., Korkmaz, H., Baysal, E., Hatipoglu, E., Aytac, I., Akarsu, E., 2017. Auditory changes in acromegaly. J Endocrinol Invest 40, 621–626. https://doi.org/10.1007/s40618-016-0602-x

Tagliafico, A., Resmini, E., Ferone, D., Martinoli, C., 2011. Musculoskeletal complications of acromegaly: what radiologists should know about early manifestations. Radiol Med 116, 781–92. https://doi.org/10.1007/s11547-011-0671-z

Tannenbaum, G.S., 1980. Evidence for autoregulation of growth hormone secretion via the central nervous system. Endocrinology 107, 2117–2120. https://doi.org/10.1210/endo-107-6-2117

Teasdale, N., Hue, O., Marcotte, J., Berrigan, F., Simoneau, M., Doré, J., Marceau, P., Marceau, S., Tremblay, A., 2007. Reducing weight increases postural stability in obese and morbid obese men. Int J Obes 31, 153–160. https://doi.org/10.1038/sj.ijo.0803360

Thorner, M., Vance, M.L., Hartman, M., Holl, R., Evans, W., Veldhuis, J., Van Cauter, E., Copinschi, G., Bowers, C., 1990. Physiological role of somatostatin on growth hormone regulation in humans. Metabolism 39, 40–42.

Tinetti, M.E., Kumar, C., 2010. The Patient Who Falls: "It's Always a Trade-off." JAMA 303, 258. https://doi.org/10.1001/jama.2009.2024

Title, M., Wang, Y., Steeves, K., Chen, K., Ahmad, S., Tramble, L., Yusuf Ibrahim, A., Van Uum, S., Chik, C.L., Clarke, D.B., Ladouceur, M., Imran, S.A., 2023. Joint pain, physical function, and balance self-confidence in acromegaly versus nonfunctioning pituitary adenoma patients. European Journal of Endocrinology 189, 156–163. https://doi.org/10.1093/ejendo/lvad090

Tornero, J., Castaneda, S., Vidal, J., Herrero-Beaumont, G., 1990. Differences between radiographic abnormalities of acromegalic arthropathy and those of osteoarthritis. Arthritis & Rheumatism 33, 455–456. https://doi.org/10.1002/art.1780330332

Tropp, H., Odenrick, P., 1988. Postural control in single-limb stance. Journal of Orthopaedic Research 6, 833–839. https://doi.org/10.1002/jor.1100060607

Tsang, C., Leung, J., Kwok, T., 2022. Self-perceived balance confidence is independently associated with any subsequent falls and injurious falls among community-dwelling older fallers: A prospective cohort study. Arch Gerontol Geriatr 103, 104776. https://doi.org/10.1016/j.archger.2022.104776

van der Klaauw, A.A., Kars, M., Biermasz, N.R., Roelfsema, F., Dekkers, O.M., Corssmit, E.P., van Aken, M.O., Havekes, B., Pereira, A.M., Pijl, H., Smit, J.W., Romijn, J.A., 2008. Disease-specific impairments in quality of life during long-term follow-up of patients with different pituitary adenomas. Clinical Endocrinology 69, 775–784. https://doi.org/10.1111/j.1365-2265.2008.03288.x

van der Meulen, M., Zamanipoor Najafabadi, A.H., Broersen, L.H.A., Schoones, J.W., Pereira, A.M., van Furth, W.R., Claessen, K.M.J.A., Biermasz, N.R., 2022. State of the Art of Patient-reported Outcomes in Acromegaly or GH Deficiency: A Systematic Review and Meta-analysis. The Journal of Clinical Endocrinology & Metabolism 107, 1225–1238. https://doi.org/10.1210/clinem/dgab874

Vilar, L., Vilar, C.F., Lyra, Ruy, Lyra, Raissa, Naves, L.A., 2017. Acromegaly: clinical features at diagnosis. Pituitary 20, 22–32. https://doi.org/10.1007/s11102-016-0772-8

Virnes, R.-E., Tiihonen, M., Karttunen, N., Van Poelgeest, E.P., Van Der Velde, N., Hartikainen, S., 2022. Opioids and Falls Risk in Older Adults: A Narrative Review. Drugs Aging 39, 199–207. https://doi.org/10.1007/s40266-022-00929-y

Walchan, E.M., Guimarães, F.S., Soares, M.S., Kasuki, L., Gadelha, M.R., Lopes, A.J., 2016. Parameters of knee isokinetic dynamometry in individuals with acromegaly: Association with growth hormone levels and general fatigue. IES 24, 331–340. https://doi.org/10.3233/IES-160635

Wassenaar, M., Biermasz, N., Bijsterbosch, J., Pereira, A., Meulenbelt, I., Smit, J., Roelfsema, F., Kroon, H., Romijn, J., Kloppenburg, M., 2011. Arthropathy in long-term cured acromegaly is characterised by osteophytes without joint space narrowing: a comparison with generalised osteoarthritis. Ann Rheum Dis 70, 320–5. https://doi.org/10.1136/ard.2010.131698

Wassenaar, M., Biermasz, N., Kloppenburg, M., van der Klaauw, A., Tiemensma, J., Smit, J., Pereira, A., Roelfsema, F., Kroon, H., Romijn, J., 2010. Clinical osteoarthritis predicts physical and psychological QoL in acromegaly patients. Growth Horm IGF Res 20, 226–33. https://doi.org/10.1016/j.ghir.2010.02.003

Wassenaar, M., Biermasz, N., Pereira, A., van der Klaauw, A., Roelfsema, F., van der Straaten, T., Cazemier, M., Hommes, D., Kroon, H., Kloppenburg, M., Guchelaar, H., Romijn, J., 2009a. The Exon-3 Deleted Growth Hormone Receptor Polymorphism Predisposes to Long-Term Complications of Acromegaly. The Journal of Clinical Endocrinology & Metabolism 94, 4671–4678. https://doi.org/10.1210/jc.2009-1172

Wassenaar, M., Biermasz, N., van Duinen, N., van der Klaauw, A., Pereira, A., Roelfsema, F., Smit, J., Kroon, H., Kloppenburg, M., Romijn, J., 2009b. High prevalence of arthropathy, according to the definitions of radiological and clinical osteoarthritis, in patients with long-term cure of acromegaly: a case-control study. Eur J Endocrinol 160, 357–65. https://doi.org/10.1530/EJE-08-0845

Webster, J.G. (Ed.), 2009. Medical instrumentation: application and design, 4th Edition. ed. John Wiley & Sons.

Wennberg, A., Lorusso, R., Dassie, F., Benavides-Varela, S., Parolin, M., De Carlo, E., Fallo, F., Mioni, R., Vettor, R., Semenza, C., Maffei, P., 2019. Sleep disorders and cognitive dysfunction in acromegaly. Endocrine 66. https://doi.org/10.1007/s12020-019-02061-1

Whitehouse, S.L., Crawford, R., Learmonth, I., 2008. Validation for the reduced Western Ontario and McMaster Universities Osteoarthritis Index function scale. Journal of Orthopaedic Surgery 16, 50–53.

Winter, D., 1995. Human balance and posture control during standing and walking. Gait & Posture 3, 193–214. https://doi.org/10.1016/0966-6362(96)82849-9

Winter, D.A., 2009. Biomechanics and motor control of human movement, 4th ed. ed. Wiley, Hoboken, N.J.

Winter, D.A., Patla, A.E., Frank, J.S., 1990. Assessment of balance control in humans. Med Prog Technol 16, 31–51.

Winter, D.A., Patla, A.E., Prince, F., Ishac, M., Gielo-Perczak, K., 1998. Stiffness Control of Balance in Quiet Standing. Journal of Neurophysiology 80, 1211–1221. https://doi.org/10.1152/jn.1998.80.3.1211

Winter, D.A., Patla, A.E., Rietdyk, S., Ishac, M.G., 2001. Ankle muscle stiffness in the control of balance during quiet standing. Journal of neurophysiology 85, 2630–2633.

Winter, D.A., Prince, F., Frank, J.S., Powell, C., Zabjek, K.F., 1996. Unified theory regarding A/P and M/L balance in quiet stance. Journal of Neurophysiology 75, 2334–2343. https://doi.org/10.1152/jn.1996.75.6.2334

Winter, D.A., Prince, F., Stergiou, P., Powell, C., 1993. Medial-lateral and anterior-posterior motor responses associated with centre of pressure changes in quiet standing. Neuroscience Research Communications 12, 141–148.

Woolcott, J.C., 2009. Meta-analysis of the Impact of 9 Medication Classes on Falls in Elderly Persons. Arch Intern Med 169, 1952. https://doi.org/10.1001/archinternmed.2009.357

Woollacott, M.H., Shumway-Cook, A., Nashner, L.M., 1986. Aging and posture control: changes in sensory organization and muscular coordination. The International Journal of Aging and Human Development 23, 97–114.

Yamasaki, H., Prager, D., Gebremedhin, S., Moise, L., Melmed, S., 1991. Binding and Action of Insulin-Like Growth Factor I in Pituitary Tumor Cells. Endocrinology 128, 857–862. https://doi.org/10.1210/endo-128-2-857

Yamashita, S., Melmed, S., 1987. Insulinlike growth factor I regulation of growth hormone gene transcription in primary rat pituitary cells. J. Clin. Invest. 79, 449–452. https://doi.org/10.1172/JCI112832

Yamashita, S., Melmed, S., 1986. Insulin-Like Growth Factor I Action on Rat Anterior Pituitary Cells: Suppression of Growth Hormone Secretion and Messenger Ribonucleic Acid Levels. Endocrinology 118, 176–182. https://doi.org/10.1210/endo-118-1-176

Yang, J.F., Winter, D.A., Wells, R.P., 1990. Postural dynamics in the standing human. Biological Cybernetics 62, 309–320. https://doi.org/10.1007/BF00201445

Yilmaz Gokmen, G., Gurses, H.N., Zeren, M., Ozyilmaz, S., Kansu, A., Akkoyunlu, M.E., 2021. Postural stability and fall risk in patients with obstructive sleep apnea: a cross-sectional study. Sleep Breath 25, 1961–1967. https://doi.org/10.1007/s11325-021-02322-2

Żuk, M., Pezowicz, C., 2015. Kinematic Analysis of a Six-Degrees-of-Freedom Model Based on ISB Recommendation: A Repeatability Analysis and Comparison with Conventional Gait Model. Applied Bionics and Biomechanics 2015, 1–9. https://doi.org/10.1155/2015/503713

Informed Consent Form Non-Interventional Study

STUDY TITLE:	The comparison of standing posture and walking patterns between acromegaly patients and able-bodied individuals.
PRINCIPAL INVESTIGATOR:	Dr. Michel Ladouceur School of Health and Human Performance Dalhousie University Phone: (902) 494-2754 Yuqi Wang, Michaela Title Graduate Student Department of Health and Human Performance, Dalhousie University Phone: (902) 401-6753, (902) 293-0616

1. Introduction

You have been invited to take part in a research study. A research study is a way of gathering information on a treatment, procedure or medical device or to answer a question about something that is not well understood. Taking part in this study is voluntary. It is up to you to decide whether to be in the study or not. Before you decide, you need to understand what the study is for, what risks you might take and what benefits you might receive. This consent form explains the study. The research team will tell you if there are any study timelines for making your decision.

Please ask the research team to clarify anything you do not understand or would like to know more about. Make sure all your questions are answered to your satisfaction before deciding whether to participate in this research study.

The researchers will:
- Discuss the study with you
- Answer your questions
- Be available during the study to deal with problems and answer questions

You are being asked to consider participating in this study because you are between the ages of 18-65 and were diagnosed with acromegaly, also, you do not have any physical disability not related to acromegaly, neurological or vestibular disorders, inflammatory arthritis, amputation or drug or alcohol abuse.

If you decide not to take part or if you leave the study early, your usual health care will not be affected.

2. Why is there a need for this study?

The purpose of the study is to observe the differences of standing posture and walking patterns between acromegaly patients and able-bodied individuals and find out possible mechanical changes leading to the differences. Posture and balance are necessary to human's ability to perform normal gait and activities of daily living and play an important role in prevent falls and injuries. It is important to explore whether the standing posture and walking patterns reveal significant differences between acromegaly patients and able-bodied individuals and what possible factors leading to the differences so that find out more applicable physiotherapy interventions to help the patients rehabilitate.

There has been limited research investigating the static posture, static balance and dynamic balance of acromegaly patients. Several previous studies have found possible mechanical factors leading to imbalance of acromegaly patients for static balance, such as different joint alignment and weaker muscle function. However, for dynamic balance, most of the studies used subjective methods to assess the participants' dynamic balance. The majority of the methods used in previous studies to assess dynamic balance were based on tester's subjective interpretation, the results are obtained by observing the movements of the subjects and then giving them a score, which lacks theoretical stringency, compared with some tests that provide objective data. Thus, in our experiment, we will use a force plate system and motion capture system to obtain objective data and do a full kinematic and kinetic gait analysis to evaluate individuals' dynamic balance during walking and obstructed walking. Additionally, none of the studies has considered the impact of joint laxity on acromegalic patients' posture and gait. Therefore, we will use well-established clinical tests to manually evaluate joint laxity.

3. How Long Will I Be In The Study?

All of the tests will be completed in only one session. The total duration from the time of entry into the Lab to the end of the experiment will be no longer than 150 minutes. The results should be known in 1 year.

4. How Many People Will Take Part In This Study?

It is anticipated that about 5 people will participate in this study at BEN lab of the department of Kinesiology of Dalhousie University.

5. How Is The Study Being Done?

The study will involve one session in which you will be asked to complete timed up and go test, dynamic gait index test, posturography, Romberg test, and do the 10-meter walking and obstructed walking. We will be using Motion capture system (14-camera system which only captures the movement of markers) and force plate system (a rectangular plate embedded in the floor) to assess your standing posture and walking patterns. The total duration from the time you enter the Lab to the end of the experiment will be no longer than 150 minutes.

nova scotia health authority

6. What Will Happen If I Take Part In This Study?

If you agree to take part in this study, you will be asked to do the following tests.

Timed up and go test: stand up from chair, walk straight for 3 meters, turn around, walk back and sit down

Dynamic gait index test: modify gait based on 8 different instructions, such as change in gait speed, gait with horizontal head turn, step over obstacle

Posturography: patient standing in anatomical position for 3 seconds

Dual leg stance & Single leg stance: stand still to maintain balance in both eyes open condition and eyes close condition

10-meter walking and obstructed walking: the participants are expected to walk a 10-meter walkway with and without obstacles for 10 times each. The participants will do several practice trials (not recorded) before the formal trial to familiarize them with the setting.

You may choose not to continue participating in the study at any time. If you decide not to take part in the study or if you leave the session early, your data will automatically be withdrawn from the study. Additionally, you may choose to withdraw after participating in the study, but this will not be possible after the data has been analyzed. We will hold off analyzing data for 1 week following collection from the final participant to allow you to withdraw after you have participated.

7. Are There Risks To The Study?

The foreseeable risk in this experiment include muscle fatigue. If this happens, you are encouraged to keep stretching and moving the muscle and apply mild heat. There is minimal chance of muscle injury. Some people may experience personal discomfort in the form of irritated or itchy skin due to marker placement. If this happens, apply a topical moisturizer and cold compresses. To diminish personal discomfort due to the site of marker placement, a research assistant whose gender matches yours will be on hand to apply these markers.

8. Are There Benefits Of Participating In This Study?

We cannot guarantee or promise that you will receive any benefits from this research. Participating in the study might not benefit you directly, but we might learn things that will help you rehabilitate in the future, in terms of the appropriate intervention to use for relieving joint symptoms.

9. What Happens at the End of the Study?

We will provide a short description of group results when the study is finished. There will be no access to individual results. You can obtain these results by including your email at the end of the signature/ consent page.

10. What Are My Responsibilities?

As a study participant you will be expected to:
- Follow the directions of the research team;

Romeo File No. xxxxxx   2020/01/26

- Report all medications being taken or that you plan on taking;
- Report any changes in your health to the research team;
- Report any problems that you experience that you think might be related to participating in the study;

11. Can My Participation in this Study End Early?

Yes. If you chose to participate and later change your mind, you can say no and stop the research at any time. If you wish to withdraw your consent, please inform the research team. If you choose to withdraw from this study, your decision will have no effect on your current or future medical treatment and healthcare.

Also, the Nova Scotia Health Authority Research Ethics Board and the principal investigator have the right to stop patient recruitment or cancel the study at any time.

Lastly, the principal investigator may decide to remove you from this study without your consent for any of the following reasons:

➢ You do not follow the directions of the research team;
➢ There is new information that shows that being in this study is not in your best interests;

13. What About New Information?

You will be told about any other new information that might affect your health, welfare, or willingness to stay in the study and will be asked whether you wish to continue taking part in the study or not.

14. Will It Cost Me Anything?

Compensation
You may be reimbursed for some study related expenses such as parking. Please bring your receipts with you.

Research Related Injury

If you become ill or injured as a direct result of participating in this study, necessary medical treatment will be available at no additional cost to you. Your signature on this form only indicates that you have understood to your satisfaction the information regarding your participation in the study and agree to participate as a subject. In no way does this waive your legal rights nor release the principal investigator, the research staff, the study sponsor or involved institutions from their legal and professional responsibilities.

15. What About My Privacy and Confidentiality?

Protecting your privacy is an important part of this study. Every effort to protect your privacy will be made. If the results of this study are presented to the public, nobody will be able to tell that you were in the study.

However, complete privacy cannot be guaranteed. For example, the principal investigator may be required by law to allow access to research records.

If you decide to participate in this study, the research team will look at your personal health information and collect only the information they need for this study. << "Personal health information" is health information about you that could identify you because it includes information such as your;
- Name,
- Address,
- Telephone number,
- Age or month/year of birth (MM/YY),
- Information from the study interviews and questionnaires;
- New and existing medical records, or
- The types, dates and results of various tests and procedures. >>

Access to Records
Other people may need to look at your personal health information to check that the information collected for the study is correct and to make sure the study followed the required laws and guidelines. These people might include:

o The Nova Scotia Health Authority Research Ethics Board (NSHA REB) and people working for or with the NSHA REB because they oversee the ethical conduct of research studies within the Nova Scotia Health Authority;

Use of Your Study Information
Any study data about you that is sent outside of the Nova Scotia Health Authority will have a code and will not contain your name or address, or any information that directly identifies you.

De-identified study data may be transferred to:
- <<The sponsor and companies working for and with the sponsor>>; and
- <<Regulatory authorities within and outside Canada>>.

Study data that is sent outside of the Nova Scotia Health Authority will be used for the research purposes explained in this consent form.

The research team and the other people listed above will keep the information they see or receive about you confidential, to the extent permitted by applicable laws. Even though the risk of identifying you from the study data is very small, it can never be completely eliminated.

The research team will keep any personal health information about you in a secure and confidential location for 1 year and then destroy it according to NSHA policy. Your personal health information will not be shared with others without your permission.

Romeo File No. xxxxxx   2020/01/26

170

After your part in the study ends, we may continue to review your health records for safety and data accuracy until the study is finished or you withdraw your consent.

You have the right to be informed of the results of this study once the entire study is complete.

The REB and people working for or with the REB may also contact you personally for quality assurance purposes.

Please be aware that once your *de-identified* data is sent outside of Canada it may be accessed by regulatory authorities in other countries who may not have the same privacy laws as we do.

Your access to records
You have the right to access, review, and request changes to your study data.

16. Declaration of Financial Interest
This study is unfunded. The PI has no vested financial interest in conducting this study.

17. What About Questions or Problems?
For further information about the study you may call the principal investigator, who is the person in charge of this study.
The principal investigator is Yuqi Wang
Telephone: 902-401-6753

18. What Are My Rights?
You have the right to all information that could help you make a decision about participating in this study. You also have the right to ask questions about this study and your rights as a research participant, and to have them answered to your satisfaction before you make any decision. You also have the right to ask questions and to receive answers throughout this study. You have the right to withdraw your consent at any time.

If you have questions about your rights as a research participant, and/or concerns or complaints about this research study, you can contact the Nova Scotia Health Authority Research Ethics Board manager at 902-473-8426 or Patient Relations at (902) 473-2133 or 1-855-799-0990 or healthcareexperience@nshealth.ca.

In the next part you will be asked if you agree (consent) to join this study. If the answer is "yes", please sign the form.

19. Consent Form Signature Page
I have reviewed all of the information in this consent form related to the study called:

nova scotia
health authority

The comparison of standing posture and walking patterns between acromegaly patients and able-bodied individuals.

I have been given the opportunity to discuss this study. All of my questions have been answered to my satisfaction.

I authorize access to my personal health information, and research study data as explained in this form.

This signature on this consent form means that I agree to take part in this study. I understand that I am free to withdraw at any time without affecting my future care.

E-messaging (email and texting) can be used by a member or members of the research team to communicate with you while you are in this study. All communication done with you will be done only through a NSHA Webmail account, or text by a phone issued to a research member through NSHA. All efforts are made to keep information sent or received private, but it is possible other people may be able to see, read, and change messages sent to or from NSHA.

☐ I give my permission to be contacted by a member or members of the research team from an NSHA Webmail account or an NSHA cell phone by research staff to communicate during this study. _____ (initials and date).

      Email   yes ☐   no ☐
      Text message   yes ☐   no ☐

☐ I do not wish to be contacted by email or text message, unless I otherwise give permission at another time during this study _____ (initial and date).

☐ Not applicable.

_____   _____   ____ / _____ / ___
Signature of Participant   Name (Printed)   Year Month Day*

_____   _____   ____ / _____ / ___
Signature of Person Conducting   Name (Printed)   Year Month Day*
Consent Discussion

_____   _____   ____ / _____ / ___
Signature of Principal Investigator Name (Printed)   Year Month Day*

I will be given a signed copy of this consent form.

Romeo File No. xxxxxx   2020/01/26

Appendix B: Data Collection Sheet

Acromegaly Study Data Collection Sheet

Patient ID		Date of assessment (YYYY/MM/DD)	
Date of birth (YYYY/MM/DD)		Sex	

LOPES Asset

Posturography: <mark>(Anatomical 3s)</mark>

Trial	Start Time (hh:mm)	File Name
1		
Notes:		

6DoF upper +lower Asset + rigid bodies Asset

Anthropometry:

Weight (kg)	
Height (m)	
RASIS → LASIS (m)	
Circumference of distal end of Thigh (m) LFME → LFLE RFME → RFLE	L: R:
Length of Shank (m) LFLE → LFAL RFLE → RFAL	L: R:
Circumference of distal end of Shank (m) LFAL → LTAM RFAL → RTAM	L: R:
Length of Foot (m) LTAM → LTOE RTAM → RTOE	L: R:
Circumference of distal end of Foot (m) L5MH → L1MH R5MH → R1MH	L: R:

1

Static!

	Trial	Start Time	File Name
Static (T-pose 10s)	1		

Stabilometry (Romberg Test): (natural 90s)

	Trial	Start Time (hh:mm)	File Name
Dual Eyes Open	1		
Dual Eyes Closed	1		
Left Single EO	1		
Right Single EO	1		
Left Single EC	1		
Right Single EC	1		
Notes:			

Remove 6DoF upper Asset & upper rigid bodies Asset

Gait Analysis: (15s)

	First foot strike	Trial		Start Time (hh:mm)	File Name
Level Surface	Right	1			
		2			
		3			
		4			
		5			
		6			
		7			
		8			
		9			
		10			
		11			
		12			
		13			
		14			
		15			

2

Obstacle	First foot strike	Trial		Start Time (hh:mm)	File Name
		1			
		2			
		3			
		4			
		5			
		6			
		7			
	Right	8			
		9			
		10			
		11			
		12			
		13			
		14			
		15			

Timed Up and Go Test:

Trial	Time to Complete (s)	Start Time (hh:mm)	File Name
1			
2			
Notes:			

Dynamic Gait Index:

	Item	Score (0-3)	Start Time (hh:mm)
1	Gait on level surface		
2	Change in gait speed		
3	Gait with horizontal head turn		
4	Gait with vertical head turn		
5	Gait and pivot turn		
6	Stepping over an obstacle		
7	Stepping around an obstacle		
8	Steps		
Total			

3

Appendix C: Sample Calculations for Defining Segment Coordinate Systems

The following equations are sample calculations of the pelvis and right thigh SCS. The origin of the pelvis will be calculated by finding the midpoint (mean) of the right and left ASIS:

$$\vec{O}_{Pelvis} = 0.5 * \left(\vec{P}_{RIAS} + \vec{P}_{LIAS} \right) \qquad (21)$$

The ML component of the pelvis SCS will be defined by the unit vector $\hat{\imath}$ in the direction of the pelvis origin to the right ASIS. The unit vector will be obtained by dividing the directional vector by its norm:

$$\hat{\imath} = \frac{\vec{P}_{RIAS} - \vec{O}_{Pelvis}}{\left| \vec{P}_{RIAS} - \vec{O}_{Pelvis} \right|} \qquad (22)$$

A unit vector, $\hat{v}$, will be calculated from the midpoint (mean) of the right and left PSIS to the origin of the pelvis:

$$\hat{v} = \frac{\vec{O}_{Pelvis} - 0.5 * \left(\vec{P}_{RIPS} + \vec{P}_{LIPS} \right)}{\left| \vec{O}_{Pelvis} - 0.5 * \left(\vec{P}_{RIPS} + \vec{P}_{LIPS} \right) \right|} \qquad (23)$$

The vertical component of the pelvis SCS will be defined by the unit vector $\hat{k}$, which is directed superiorly and orthogonal to the plane containing unit vectors $\hat{\imath}$ and $\hat{v}$. Unit vector $\hat{k}$ will be calculated by taking the cross product of $\hat{\imath}$ and $\hat{v}$. The right-hand rule will be used to determine the order in which to cross $\hat{\imath}$ and $\hat{v}$ so that a superiorly directed vector will be produced:

$$\hat{k} = \hat{\imath} \times \hat{v} \qquad (24)$$

The anterior component of the pelvis SCS will be determined by calculating unit vector $\hat{j}$, which is orthogonal to the plane containing unit vectors $\hat{k}$ and $\hat{i}$. Unit vector $\hat{j}$ will be computed by taking the cross product of unit vectors $\hat{k}$ and $\hat{i}$:

$$\hat{j} = \hat{k} \times \hat{i} \tag{25}$$

Unit vectors $\hat{i}$, $\hat{j}$, and $\hat{k}$ will be vertically concatenated to form the rotation matrix defining the orientation of the pelvis:

$$R_{Pelvis} = \begin{bmatrix} \hat{i}_x & \hat{i}_y & \hat{i}_z \\ \hat{j}_x & \hat{j}_y & \hat{j}_z \\ \hat{k}_x & \hat{k}_y & \hat{k}_z \end{bmatrix} \tag{26}$$

Next, the thigh SCS will be defined. The origin of the thigh will be determined by the hip joint centre in the GCS. However, the hip joint centre will first be calculated relative to the pelvis SCS using the regression equations derived by Bell et al. (1989). The regression coefficients will be multiplied by the distance between the right and left ASIS, which will be calculated by finding the norm of the vector from the left to the right ASIS:

$$\vec{P}_{RHip} = \begin{bmatrix} 0.36 * \left| \vec{P}_{RIAS} - \vec{P}_{LIAS} \right| \\ -0.19 * \left| \vec{P}_{RIAS} - \vec{P}_{LIAS} \right| \\ -0.30 * \left| \vec{P}_{RIAS} - \vec{P}_{LIAS} \right| \end{bmatrix} \tag{27}$$

Note that for calculation of the left hip joint centre, the coefficient for the x component will be -0.36. The hip joint centre will then be transformed from the pelvis SCS to the GCS:

$$\vec{O}_{RThigh} = R'_{Pelvis} * \vec{P}_{RHip} + \vec{O}_{Pelvis} \tag{28}$$

The superiorly directed component of the right thigh SCS, unit vector $\hat{k}$, will be determined by the vector from the midpoint of the right MFE and right LFE to the origin of the right thigh divided by its norm:

$$\hat{k} = \frac{\vec{O}_{RThigh} - 0.5 * (\vec{P}_{RFLE} + \vec{P}_{RFME})}{\left|\vec{O}_{RThigh} - 0.5 * (\vec{P}_{RFLE} + \vec{P}_{RFME})\right|} \tag{29}$$

A unit vector, $\hat{v}$, in the direction of the right MFE to the right LFE will be calculated by subtracting the two points to define the directional vector and dividing the vector by its norm:

$$\hat{v} = \frac{(\vec{P}_{RFLE} - \vec{P}_{RFME})}{\left|\vec{P}_{RFLE} - \vec{P}_{RFME}\right|} \tag{30}$$

The anterior unit vector, $\hat{j}$, will be calculated by taking the cross product of unit vectors $\hat{k}$ and $\hat{v}$:

$$\hat{j} = \hat{k} \times \hat{v} \tag{31}$$

Similarly, the lateral unit vector, $\hat{i}$, will be determined by crossing unit vectors $\hat{j}$ and $\hat{k}$:

$$\hat{i} = \hat{j} \times \hat{k} \tag{32}$$

The rotation matrix of the right thigh will be constructed from the unit vectors $\hat{i}, \hat{j},$ and $\hat{k}$:

$$R_{RThigh} = \begin{bmatrix} \hat{i}_x & \hat{i}_y & \hat{i}_z \\ \hat{j}_x & \hat{j}_y & \hat{j}_z \\ \hat{k}_x & \hat{k}_y & \hat{k}_z \end{bmatrix} \tag{33}$$
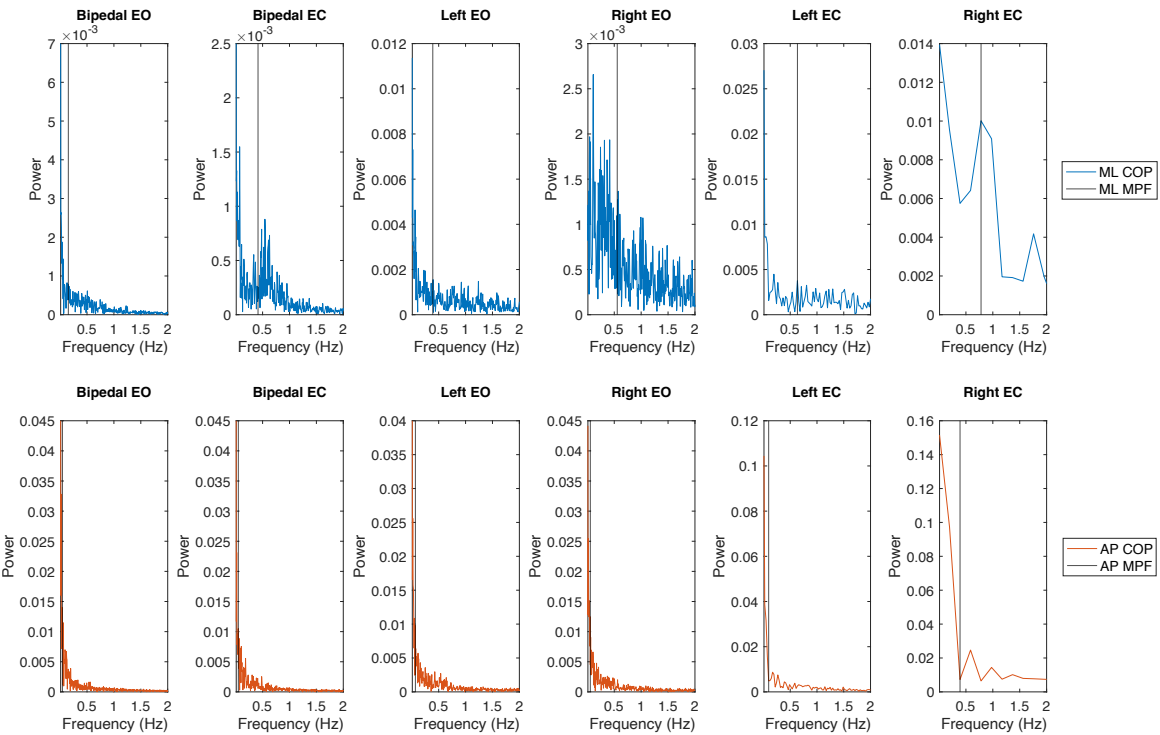
Figure 40. Power spectral density of centre of pressure up to 2 Hz for a representative participant in the mediolateral (ML; top row) and anteroposterior (AP; bottom row) axes during bipedal and unipedal stance with eyes open (EO) and eyes closed (EC)

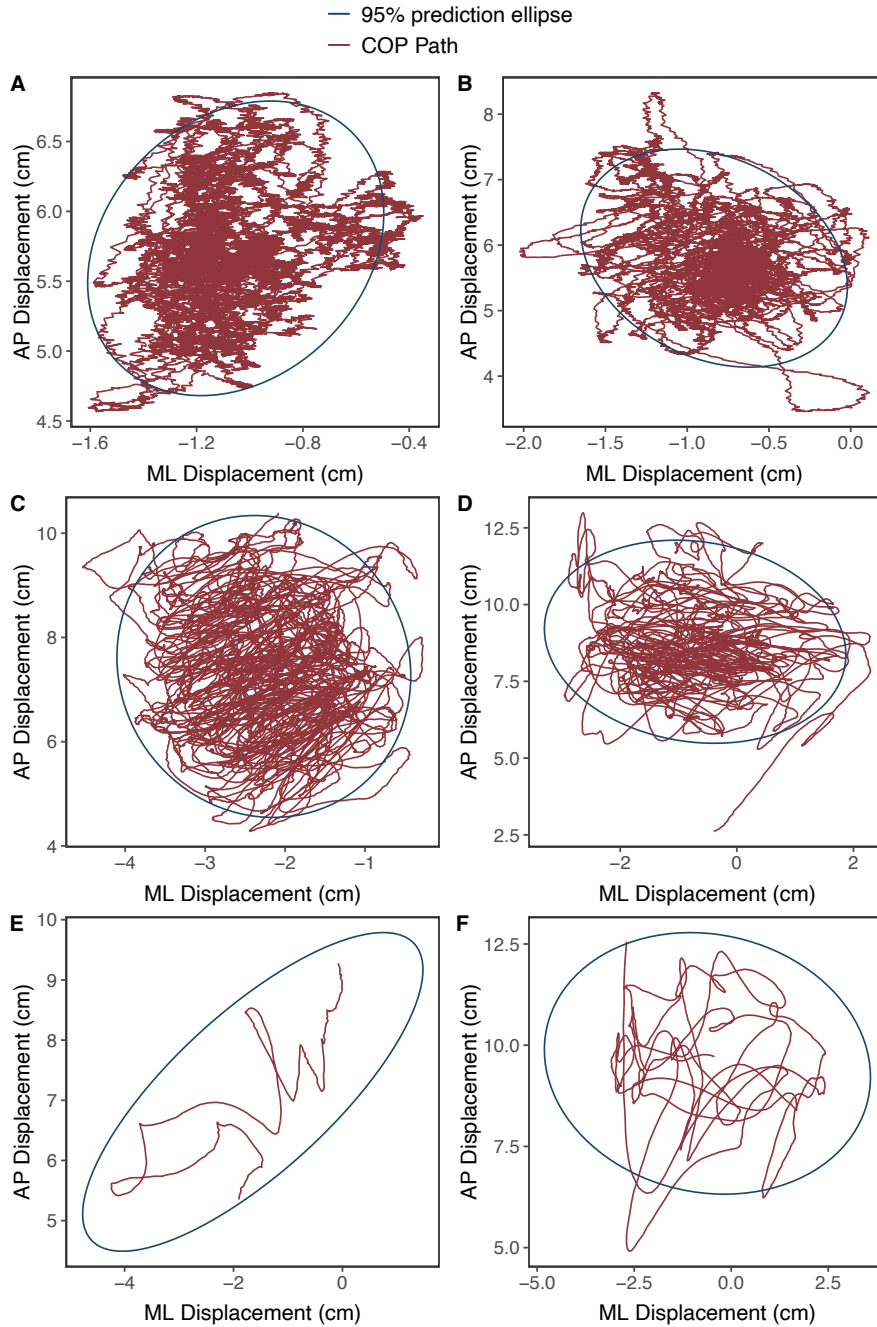# Appendix E: Centre of Pressure 95% Prediction Ellipse

Figure 41. Centre of pressure (COP) 95% prediction ellipse and centre of pressure path expressed relative to the mediolateral (ML) and anteroposterior (AP) axes during (A) bipedal eyes open, (B) bipedal eyes closed, (C) left foot eyes open, (D) right foot eyes open, (E) left foot eyes closed, and (F) right foot eyes closed for a representative participant
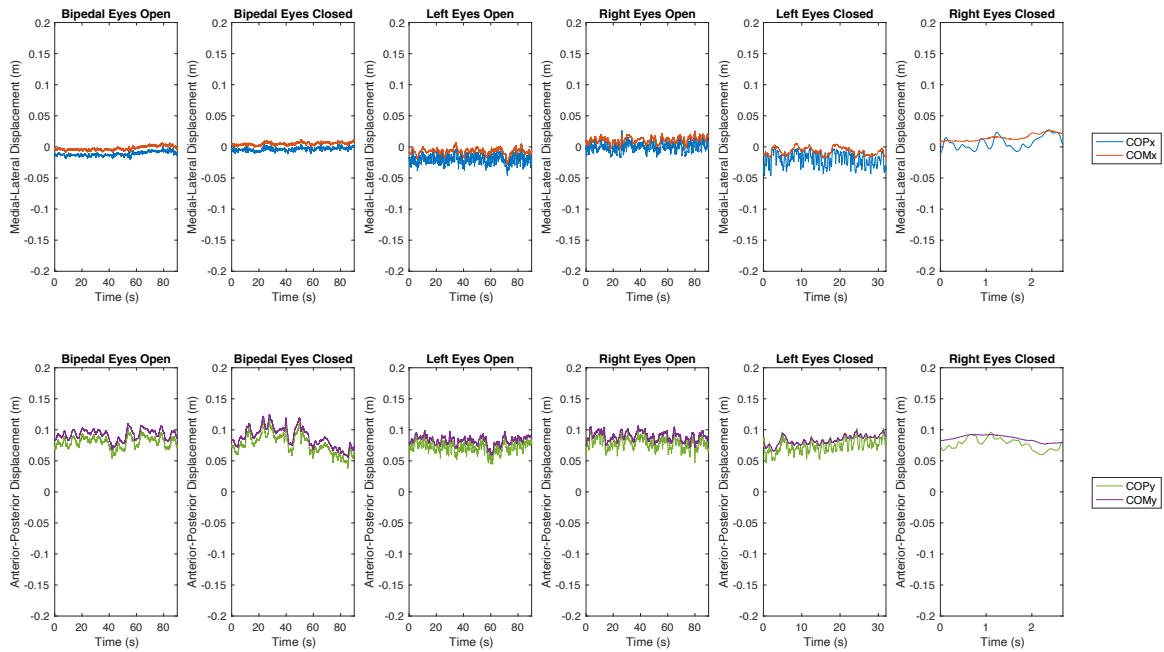
Figure 42. *Trajectories of centre of pressure (COP; m) and centre of mass (COM; m) along the mediolateral (top row) and anteroposterior (bottom row) axes for a representative participant with COM anterior to COP in bipedal trials.*
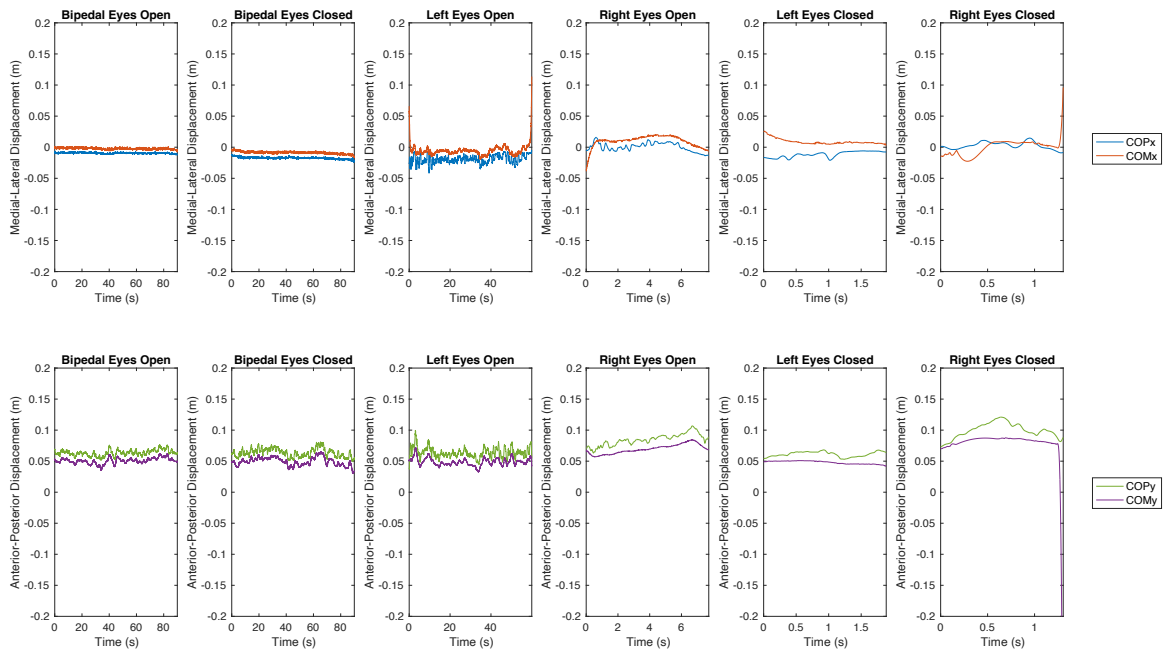

Figure 43. *Trajectories of centre of pressure (COP; m) and centre of mass (COM; m) along the mediolateral (top row) and anteroposterior (bottom row) axes for a representative participant with COP anterior to COM in bipedal trials.*
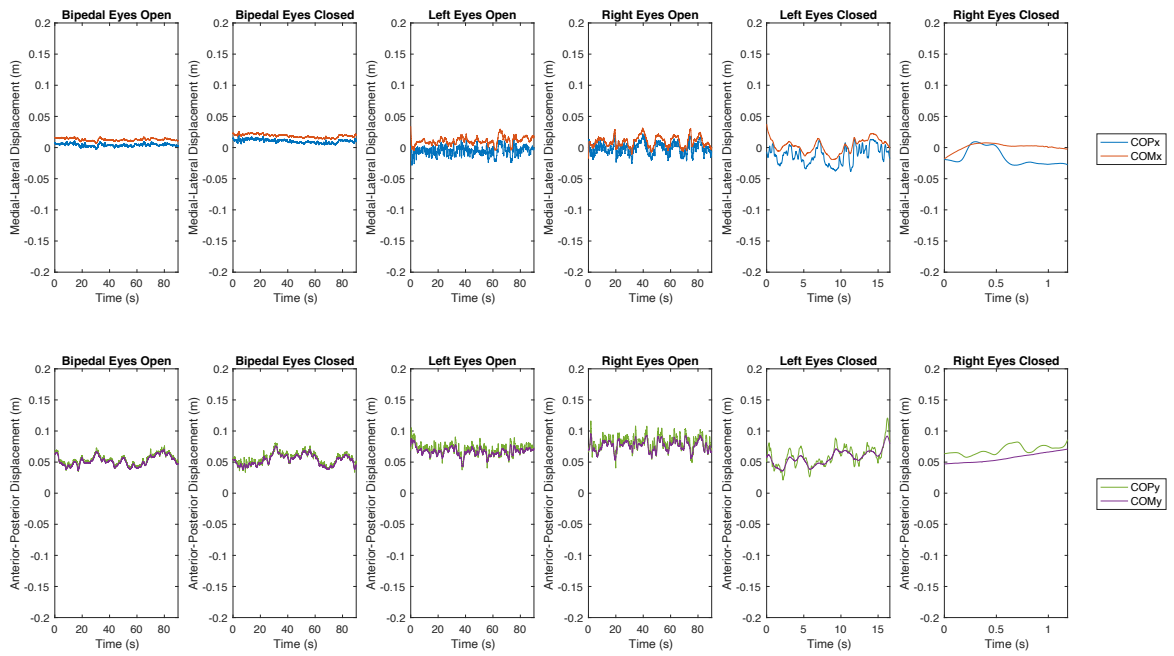
Figure 44. *Trajectories of centre of pressure (COP; m) and centre of mass (COM; m) along the mediolateral (top row) and anteroposterior (bottom row) axes for a representative participant with COP crossing COM in the anteroposterior axis.*

Appendix G: Correlation of COP-COM and BMI

Figure 45. Correlation between the mean difference of centre of pressure and centre of mass (COP-COM; cm) in the anteroposterior axis and body mass index (BMI; kg/m^2)

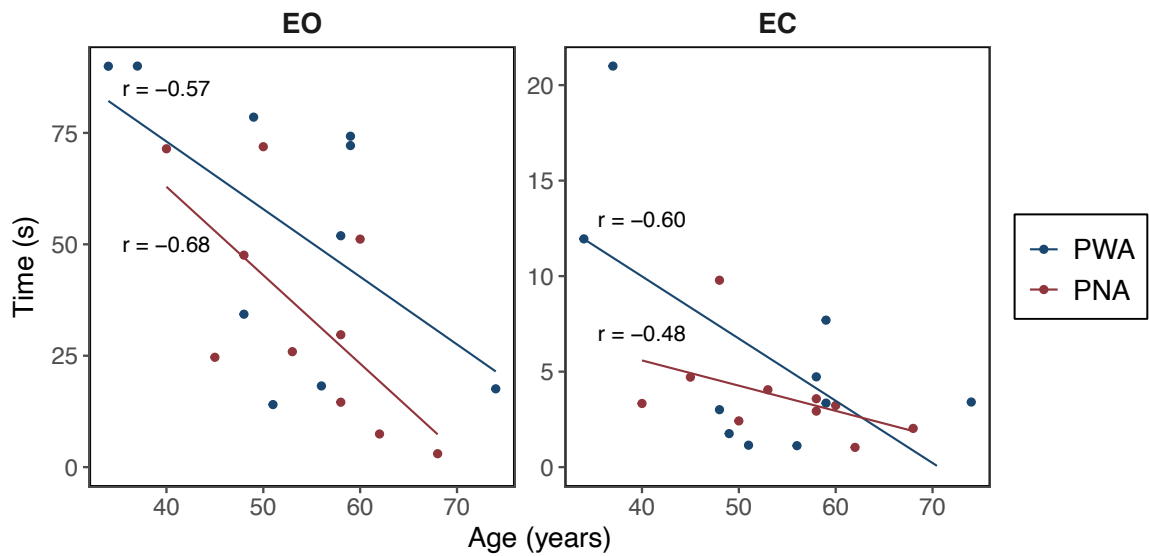**Appendix H: Correlation of Unipedal Stance Time and Age**

Figure 46. Correlation between unipedal stance time (s) and age (years) for PWA and PNA